VOL. 6 NO. 4
WINTER 2017

POWDER METALLURGY REVIEW

HIGH-PERFORMANCE PERMANENT MAGNETS

OPTIMISATION OF IRON-BASED BEARINGS

HIP AT EURO PM2017

www.pm-review.com

Published by Inovar Communications Ltd

The potential of powder metallurgy is only limited by one's imagination…

Hoeganaes Corporation is a world leader in the development and production of metal powders.

Over 65 years, our commitment to innovative technologies spans critical applications from Automotive to Additive Manufacturing.

Hoeganaes Corporation has expanded our global footprint to meet our customers' needs, with powder production facilities in North America, Europe and Asia.

HOEGANAES CORPORATION
www.hoeganaes.com

MOBILE DEVICE APPS NOW AVAILABLE FOR DOWNLOAD

Available on the iPhone App Store | ANDROID APP ON Google play

FOLLOW US ON SOCIAL MEDIA AT:

@HoeganaesCorp

YouTube LinkedIn

Publisher & editorial offices
Inovar Communications Ltd
11 Park Plaza
Battlefield Enterprise Park
Shrewsbury SY1 3AF
United Kingdom

Editor & Publishing Director
Paul Whittaker
Tel: +44 (0)1743 211992
Email: paul@inovar-communications.com

Managing Director
Nick Williams
Tel: +44 (0)1743 211993
Email: nick@inovar-communications.com

Assistant Editor
Emily-Jo Hopson
Tel: +44 (0)1743 211994
Email: emily-jo@inovar-communications.com

Consulting Editor
Dr David Whittaker
Consultant, Wolverhampton, UK

Advertising Sales Director
Jon Craxford
Tel: +44 (0) 207 1939 749
Email: jon@inovar-communications.com

Production
Hugo Ribeiro, Production Manager
Tel: +44 (0)1743 211994
Email: hugo@inovar-communications.com

Submitting news and articles
We welcome contributions from both industry and academia and are always interested to hear about company news, innovative applications for PM, research and more.

Please contact Paul Whittaker, Editor
Email: paul@inovar-communications.com

Subscriptions
Powder Metallurgy Review is published on a quarterly basis. It is available as a free electronic publication or as a paid print subscription. The annual subscription charge is £95.00 including shipping.

Design and production
Inovar Communications Ltd.
ISSN 2050-9693 (Print edition)
ISSN 2050-9707 (Online edition)

This magazine is also available for free download from www.pm-review.com

POWDER METALLURGY REVIEW

Powder Metallurgy: Meeting the needs of future technologies

The development of new technologies, although a threat to some, can offer huge potential to innovative industries with the flexibility to take on the challenge. For the PM industry, one such opportunity lies in the development of fuel cell technology.

As environmental concerns change the way we harvest energy, the technologies we use must be efficient, stable and provide years of service. Researchers at Jülich GmbH and Plansee SE recently reported that a high-temperature solid oxide fuel cell, containing Powder Metallurgy interconnects, successfully completed a ten-year life-cycle test.

The ten-year programme has proved the durability of this technology and the reliability of PM components in demanding applications. Uses for this type of fuel cell include power supply systems for households or small businesses as well as large vehicles such as trucks, trains and ships.

In some cases, limitations in raw material supply can drive the development of alternative materials and technologies. Concerns regarding the supply of rare earth elements to the magnet sector are one example and in this issue of *PM Review*, Dr Sim Narasimhan reports on the development of new materials which could offer alternatives for this important sector.

Paul Whittaker
Editor, *Powder Metallurgy Review*

Cover image
Porous self-lubricating bearings are manufactured by cold pressing, sintering, sizing and oil impregnation

POWDER METALLURGY REVIEW

38

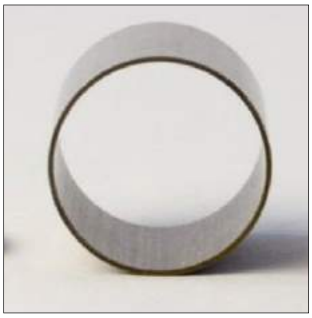

44

50

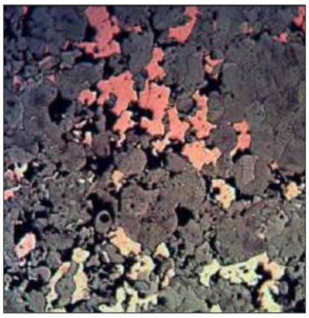

65

69

in this issue

regular features

industry news

To submit news for inclusion in *Powder Metallurgy Review* contact Paul Whittaker, paul@inovar-communications.com

Fuel cell with PM interconnects runs successfully for ten years

A planar solid fuel cell developed at the Jülich GmbH Research Centre, Germany, has been running and producing electricity successfully for ten years. The high-temperature fuel cell, which has been studied throughout as part of a lifetime test, was built using Powder Metallurgy interconnects from Plansee SE, Reutte, Austria.

The lifetime test was launched on August 6, 2007, and is intended to demonstrate the durability of the solid oxide fuel cells developed by Jülich. In order for their operation to be economically efficient, these have to run for between 40,000 and 80,000 hours, or 5 to 10 years. According to Julich, no other fuel cell with ceramic cells has ever run for this long, and short lifetimes have in the past been regarded as the major flaw of this type of fuel cell.

Plansee's interconnects were manufactured from ITM, an iron-based Oxide-Dispersion Strengthened (ODS) alloy with a 26% chrome content and very small amounts of yttrium oxide (Y_2O_3). An ODS alloy of this type can only be manufactured using PM techniques and is reported to offer crucial benefits in terms of SOFC high-temperature fuel cell applications. ITM withstands thermal and redox cycles for longer than other types of ferritic steels.

Over the fuel cell's entire service life to date, the research centre team state that it has exhibited only a very low level of ageing, at approximately 0.6% per 1000 operating hours. A further development to the stack in 2010 provided even better results, reportedly halving ageing over the next 34,500 hours of operation.

Although the Jülich test stack is still being operated in a laboratory environment, it contains all the components that a future commercial product would require. It is operated using hydrogen, which is converted into electrical current in the cell. Other fuels, such as natural gas, can also be converted and, according to other trials, may achieve higher levels of efficiency.

Over the fuel cell's entire service life to-date, the research centre team states that it has exhibited only a very low level of ageing, at approximately 0.6% per 1000 operating hours (Courtesy Plansee)

Applications for this type of fuel cell include stationary power supply systems, such as for households or small businesses, but also for large vehicles such as trucks, trains and ships.

www.plansee.com
www.fz-juelich.de

Höganäs to upgrade and expand its Shanghai metal powder mixing facility

Höganäs AB has begun upgrades to its metal powder mixing facility in Shanghai, China. The company has announced that a state-of-the-art mixing station for advanced metal powder mixes will be opened in 2018.

"Asia, and China in particular, are important markets for Höganäs," stated Fredrik Emilson, Höganäs CEO. "With the upgraded mixing station we can supply our customers in the region with unique, consistent mixes in very short time."

The upgrade of the mixing station in Shanghai aims to increase Höganäs' capacity to both produce tailor made customer mixes and handle large, two ton flex bags. The project will also improve work environment, upgrade existing facilities and equipment and build a new warehouse and quality control lab.

"Höganäs' offering in mixes, especially bonded mixes, has grown immensely year on year in the past six years. Now we are preparing for growth in the years to come," added Terry Chen, Operation & Supply Manager at Höganäs in Shanghai.

The ground-breaking ceremony was held in October. In an opening address, Richard Molin, Operations Manager APAC, stated, "We believe that Höganäs will be an even more attractive company for people in the neighborhood to come and work for. We hope that this important step into the future, with the state-of-the-art facility here in Qing-Pu, will show everyone that Höganäs continues to focus on Asia and especially on China."

www.hoganas.com

Sandvik reports continued growth and appoints new President for Sandvik Materials Technology

Sweden's Sandvik AB has announced the results for its third quarter and the first nine months of 2017. According to the company, it has seen good overall growth for the quarter, with order intake increasing across all business areas. Group-wide revenues increased by 12% compared to Q3 2016, with operating profit rising by 28% compared to Q3 2016.

Sandvik Materials Technology saw order intake increase 9% to 3,045 million SEK (Q3 2016: 2,851 million SEK) and achieved an organic revenue increase of 3%. According to the company's report, business momentum for all segments was strongest in Asia, which reported 14% growth. North America reported growth of 12%, while Europe saw sales growth of 9%.

Despite steady growth, Sandvik Materials Technology has reported an operating loss of -57 million SEK. According to the company, this was primarily due to a negative mix in deliveries, lower profitability in the more standardised tubular business and an adverse impact from changed metal prices, as well as normal seasonal weakness. Changing metal prices reportedly had an adverse impact of -64 million SEK on operating profit. Changing exchange rates were also a factor, having a negative impact of -2% on order intake and revenues across Sandvik Group.

"Order growth in the third quarter was buoyant at 13%," stated Björn Rosengren, President and CEO of Sandvik. "Large orders were received by Sandvik Mining and Rock Technology and Sandvik Materials Technology at a total value of 500 million SEK."

"While the third quarter is seasonally weak for Sandvik Materials Technology, I am nevertheless disappointed with the business area's performance," he continued. "We are working hard to implement the cost initiatives announced earlier that are aimed at gradually restoring profitability from early next year. For the Sandvik Group in general, I am pleased with the performance."

The company also reported that it has appointed Göran Björkman as President of Sandvik Materials Technology and member of the Sandvik Group Executive Management Team. Björkman succeeds Petra Einarsson who is leaving the company to join packaging specialist BillerudKorsnäs as its President and CEO.

"Göran Björkman has with his extensive experience the right capabilities to lead Sandvik Materials Technology going forward. As we all know, this business area is experiencing a challenging situation. I am convinced that Göran Björkman will add the strategic, business oriented focus that the business area now requires," added Rosengren.

Björkman, age 51, has been with the company since 1990 with almost twenty years at the materials technology operations. He previously held the positions of Vice President Production at Sandvik Coromant and Vice President Production Strategy, Sandvik Machining Solutions.

"I want to take the opportunity to express my gratitude to Petra Einarsson for her devoted contributions to Sandvik during almost thirty years and I wish her all the best in her new position as President and CEO for the packaging industry group BillerudKorsnäs," added Rosengren.

www.sandvik.com

Ames Lab receives funding to commercialise gas atomisation design

The US Department of Energy's Ames Laboratory has received $392,000 in funding to commercialise a gas atomisation nozzle design used to produce metal powders for manufacturing. In addition, the laboratory will contribute in-kind matching funds of equal value for the project from private sector partner Ampal, Inc., a part of the United States Metal Powders group of companies.

According to Ames Laboratory, its gas atomisation method efficiently produces metal powders that are customisable, consistently sized and spherical, resulting in a smooth flow, optimal packing and improved quality of produced parts.

The funding is part of the DOE's Office of Technology Transition's Technology Commercialisation Fund (TCF), announced recently by US Secretary of Energy Rick Perry. The funding, totalling $19.7 million, will support fifty four projects across twelve National Laboratories involving more than thirty private sector partners, and is expected to help businesses move promising energy technologies from National Laboratories to the marketplace.

"We'll be working with our industrial partner to adapt our experimental gas atomisation nozzle design to increase efficiency and control in their manufacturing process," stated Emma White, Ames Laboratory metallurgist. "We hope that if we can demonstrate the advantages of our technology with this manufacturer, it will develop interest across the industry."

www.ameslab.gov
www.science.energy.gov
www.usmetalpowders.com

New aluminium alloy update for MPIF Standard 35

The Metal Powder Industries Federation (MPIF) has released an addendum to the 2016 edition of MPIF Standard 35-SP, 'Materials Standards for PM Structural Parts.'

The update includes mechanical property data, elongation and hardness values on two aluminium alloys – AC-2014-32-T8 and AC-2014-38-T8. The updated standard gives a Rockwell hardness of 75 for AC-2014-32-T8 and 83 for the AC-2014-38-T8. Because of their relative high strength in a range of temperatures and their overall mechanical properties, these Al alloys are often used in aerospace applications.

A copy of the standard can be seen online on the MPIF website and will be included in the next published edition of the standard document.

www.mpif.org

AAM showcases PM technology at Shanghai engineering conference

AAM manufactures a range of powertrain components including Powder Metallurgy connecting rods

The SAE-China Congress and Exhibition (SAECCE) and the 19th Asia Pacific Automotive Engineering Congress combine product display and technical discussions into one event attended by China's top automakers and supplier community.

This year American Axle & Manufacturing showcased a portfolio of driveline, metal forming, powertrain and casting technologies focused on increased efficiency and improved performance.

Held in Shanghai, more than 2,000 industry experts and more than 10,000 visitors attended the conference's display area and technical sessions including paper presentations and panel discussions. AAM's display included e-AAMTM Hybrid and Electric Driveline Systems, EcoTrac® disconnecting AWD technology, propshaft, vibration control systems, light and heavy-duty commercial vehicle axles, transmission technology and forged products.

AAM has eight facilities in China which engineer and manufacture driveline, powertrain and metal forming technologies for local customers. AAM continues to grow in China and recently transitioned key driveline system production to be near local customers.

www.aam.com

Alpha Sintered Metals consolidates new acquisitions with company rebrand

Alpha Precision Group (APG), St Mary's, Pennsylvania, USA, has announced the consolidation of its brands – Alpha Sintered Metals (ASM), Precision Compacted Components (PCC) and Precision Made Products (PMP) – to form Alpha Precision Group.

ASM manufactures Powder Metallurgy and metal injection moulded components for the automotive, small engine, commercial vehicle, agricultural equipment and recreational vehicle markets. This year, the company marks its 50th anniversary, with a primary manufacturing focus on products supporting increased fuel economy, improved emissions and enhanced engine performance.

In 2016, O2 Investment Partners and Alpha Sintered Metals formed the holding company, called Alpha Precision Group, to facilitate acquisitions in support of ASM's long-term, strategic growth plan. The subsequent investments in Precision Made Products and Precision Compacted Components provide new technology, expanded capabilities and additional opportunities for ASM in growth markets.

Using PCC's variable cam timing segment, ASM was able to enhance its focus on products supporting increased fuel economy, while PMP's focus on the medical device, aerospace and firearms markets made it possible for ASM's Metal Injection Moulding operations to target the medical device market.

JoAnne Ryan, APG CEO, stated, "The selective integration of the three companies has progressed exceptionally well and reached the point where brand consolidation is appropriate. The single brand identity reflects the full capabilities and strengths of the combined company and presents a unified approach to the market."

Going forward, the group will operate through two primary divisions, APG Sintered Metals and APG Metal Injection Molding. The APG Sintered Metals division will consist of the powder metal operations of Alpha Sintered Metals and Precision Compacted Components. APG Metal Injection Molding will take on the MIM operations of Alpha Sintered Metals and Precision Made Products.

According to APG, the rebranding effort includes the new brand identity, company logo, new building signage and a consolidated website currently under construction.

www.alphaprecisionpm.com

GKN Board removes Kevin Cummings as CEO Designate and appoints Anne Stevens as its Interim CEO

The Board of GKN Group plc has reversed its decision to appoint Kevin Cummings as CEO, which it first announced in September, 2017. According to the company, "the GKN Board has concluded that the next stage of GKN's development is best delivered under alternative leadership." Following the announcement, Cummings left the board and GKN with immediate effect.

Anne Stevens, currently a non-executive director of the board, will assume the role of Interim Chief Executive from January 1, 2018, and remain in the post until a successor is appointed. As previously announced, Nigel Stein will continue as Chief Executive until retiring from the role on December 31, 2017.

Stevens, formerly Chairman, CEO and President of Carpenter Technology Corp, has extensive experience across both the automotive and aerospace industries. Prior to joining Carpenter, she held a number of roles during a sixteen year career at Ford Motor Company, latterly as Chief Operating Officer for the Americas. She was appointed to the GKN Board in July 2016 and is also a non-executive director of Anglo American plc, Lockheed Martin Corporation and XL Group plc.

The appointment of Hans Büthker to the role of Chief Executive GKN Aerospace will be brought forward to take effect immediately, as opposed to on the formerly announced date of January 1, 2018. Büthker will work with the rest of the executive team to develop plans to improve margins and cash flow across the group.

A review of working capital has recently been initiated across GKN's Aerospace plants in North America. While this review is not yet complete, the group stated that it is likely to result in a write-off estimated to be between £80-130 million, much of which built up before 2017.

With the exception of the working capital write-off referred to above, all other financial guidance for the year remains unchanged.

www.gkn.com

Submitting news..

To submit news to *PM Review* please contact Paul Whittaker: paul@inovar-communications.com

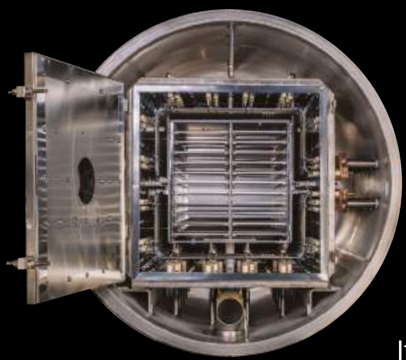

Ceratizit acquires precision tool manufacturer Komet

Ceratizit Group, Luxembourg, has announced the acquisition of Komet Group, based in Besigheim, Germany, a manufacturer of high-precision tools for almost 100 years. The group currently employs 1,500 and is represented by twenty-two global subsidiaries.

"This move lifts the close and long-standing partnership between the two companies to a new level," explained Jacques Lanners, Chairman of the Executive Board, Ceratizit. "It opens up completely new prospects both for our customers and our employees." According to Ceratizit, the Komet brand will now play a pivotal role in the group's cutting tools strategy, from turning and milling to the complete machining of holes.

"The synergies in terms of technical expertise in substrate development, sintering technology, cutting tools technologies and coating are substantial and represent significant added value for our customers," added Lanners.

"The disruptive changes in the market environment pose enormous challenges for Komet," added Dr Christof Bönsch, Komet CEO. "The acquisition by Ceratizit now opens up new opportunities for sustainable growth. The takeover sees the emergence of a new global player with superior technology expertise and broad market access."

"Employees can look forward to a positive and attractive future," Bönsch continued, "because, as a privately owned company, Ceratizit is keen to develop its sites in a sustainable manner. The implementation of the 'Komet 2026' strategy will be continued in order to ensure the safety of the jobs."

In addition to playing a key role in Ceratizit's cutting tools strategy, the company also reportedly offers 'Digital Productivity Solutions' to the group, which could enable it to develop products in line with the demands of Industry 4.0.

According to Ceratizit, this acquisition is part of a continued growth strategy which has enabled it to double sales in the past ten years, while strengthening its position in core markets.

www.ceratizit.com

Höganäs opens permanent Indonesian office

Höganäs AB has announced the opening of a permanent office in Jakarta, Indonesia. The move is said to follow the establishment of several Indonesian plants by large automotive companies.

Margaretha Kho, Sales and Customer Manager at Höganäs as of August 2017, will work from the Jakarta office having previously worked for other European industrial companies in the region.

"Höganäs is an exciting company, with a long history and a lot of experience", stated Kho. "Indonesia is an exciting country with many segments where Höganäs can help develop businesses through technical expertise. I am very much looking forward to being Höganäs's link to the local market."

Ola Litström, Höganäs's Country Manager for Taiwan and South-east Asia, stated, "We have to be in Indonesia on a permanent basis. We need to be part of, and understand, the local culture and the business climate so that we can serve the market in the best way possible."

www.hoganas.com

Kobe Steel reports 'improper conduct' in PM steel powder data

Kobe Steel Ltd, headquartered in Tokyo, Japan, has issued a statement on what it calls 'improper conduct' in the company following the rewriting of inspection data relating to steel powder supplied to one of its customers. The report follows the announcement in early October, 2017, of investigations in response to the discovery of similar issues in the company's Aluminum & Copper Business.

According to Kobe Steel, evidence of "improper rewriting of inspection data of a product outside the compact density agreed with the customer" was identified for "one type of steel powder to one customer". The powder in question was produced at Kobe's Takasago Works, Takaishi, Japan.

Although an investigation being conducted by an external law firm is still not complete, Kobe Steel stated, "As the steel powder outside the specifications is on the high-quality side, the effect on product performance is believed to be low."

The problem is said to have been discovered through "self-inspections and emergency quality audits of the compliance status of contracts executed for products that Kobe Steel shipped over the past one year."

In addition to the matters identified above, the company stated that it has uncovered issues in the production of sputtering target materials at Kobelco Research Institute, Inc.'s Takasago Works site. In this instance, tests agreed with customers were not carried out and inspection data was rewritten with regard to products which fell outside agreed component values.

The investigation by an external law firm is ongoing, as well as a continuing internal investigation on the facts of the stated improper conduct.

www.kobelco.co.jp

Japan metal powder shipments see double-digit growth in first eight months 2017

The Japan Powder Metallurgy Association (JPMA) has reported that iron powder shipments, including exports, reached 74,728 tonnes in the eight months to August 2017, an increase of 14% compared with the same period last year. The trade association also reported that PM-grade copper-base powder shipments increased by 13.4% to 3,307 tonnes.

The growth in powder shipments reflected an 8% increase in domestic car production during the same period, with automakers reporting a total of 5.473 million units produced in the first eight months of 2017.

The JPMA reported that of the 108,514 tonnes of iron powder shipments for PM in Japan in 2016, over 95% went into automotive applications, while the majority of copper-based powders went into PM bearings, with 79% destined for the automotive sector.

www.jpma.gr.jp

North American Höganäs applies to join foreign trade zone program

It has been reported that North American Höganäs has become the first manufacturer to join Pennsylvania's foreign trade zone program. Public notices published by local newspaper *The Tribune-Democrat* confirm that Höganäs has applied for its manufacturing facilities in Cambria, Somerset and Elk counties to be given subzone status.

Established in January 2016, the trade zone program allows participating companies to receive reduced or eliminated duty tariffs on imported material being used to produce other products.

Matthew Smith, Logistics Manager for Höganäs, reportedly stated that the subzone status will allow the company to reduce costs on imported material used to turn scrap metal into specialised iron powder used in manufacturing around the world.

Currently, there are around 400 workers at Höganäs facilities in Hollsopple, St Marys and Bridge Street in Johnstown's Moxham section.

www.hoganas.com

Sumitomo Electric Industries reports growth in hardmetals and structural PM components

Sumitomo Electric Industries Co Ltd (SEI), Itami, Osaka, Japan, reported a buoyant six month period to the end of September 2017, with an 11.2% increase in group sales to Yen 1,459 billion ($12.856 billion) compared with the same period in 2016. Group operating income increased by 39.6% to Yen 65.7 billion ($578.9 million).

SEI's Industrial Materials & Others division is the third largest after its Automotive and Environment & Energy divisions and incorporates the production of cemented carbides (hardmetals), PM parts and bearings, PM magnets, plus W, Mo, heavy metal, thermal management materials, ceramics, plus diamond tools and hardmetals produced at the wholly owned A.L.M.T. subsidiary. The division saw a 23% increase in sales in the first six months to Yen 176.4 billion ($1.554 billion) compared with the same period last year.

Hardmetals (cemented carbide) sales grew by 14.6% to Yen 46.9 billion ($413 million). Sintered PM products increased by 32.6% to Yen 37 billion ($326 million), whilst sales at A.L.M.T. increased by 5.8% to Yen 20 billion ($176 million). SEI forecasts full-year sales for its Industrial Materials & Others division to increase by 11.8%.

www.global-sei.com

Element Six introduces new grade of optimised PCD for automotive industry

Element Six has announced the launch of CTB004, a new grade of polycrystalline diamond (PCD), said to be customised to meet the precision cutting demands of the automotive industry. Reportedly offering high-speed machining advantages, CTB004 delivers optimised workpiece surface finish in both engine and chassis applications.

The new grade, which joins Element Six's existing product CMX850, is targeted at the cutting of aluminium alloys, where a high surface finish is required alongside higher wear resistance. CTB004 has a four-micron fine grain structure delivering a balance between tool performance and resistance to abrasion and chipping.

"Cutting-edge materials that offer considerable advantages to our customers is our constant focus," stated Richard Townsend, Product Manager – PCD at Element Six. "PCD materials provide the end-user with unsurpassed levels of productivity and workpiece quality that meet the demands of very specific applications. The push in the automotive industry to make vehicles lighter and more efficient while retaining durability has meant that aluminium use by the major OEMs has significantly increased."

The CTB004 grade also joins Element Six's Aero-Dianamics™ CFRP workpiece tooling solutions, which allow tool designers to form entirely new PCD geometries with a large variety of profiles.

www.e6.com

Dates announced and Call for Papers issued for India's PM18

The Powder Metallurgy Association of India (PMAI) has issued a Call for Papers for its PM18 International Conference on Powder Metallurgy and Particulate Materials & Exhibition.

The event, scheduled to take place February 21-23, 2018 at the CIDCO Exhibition Centre in Navi Mumbai, India, will once again bring together an all topic technical programme and an international trade exhibition.

The PMAI has requested that abstracts of papers for oral presentation as well as posters should be submitted no later than January 31, 2018. The comprehensive technical programme will include a full range of topics.

www.pmai.in/pm18

PSI celebrates thirty years in gas atomisation technologies

In 2017, Phoenix Scientific Industries Ltd (PSI), Hailsham, East Sussex, UK, celebrates its thirty year anniversary. The company is best known for its activities in gas atomisation equipment for the production of metal powders and, in particular, close-coupled atomisation for very fine powder manufacture.

PSI was founded in 1987 with the goal of developing gas atomised metal powders for the then-emerging Hot Isostatic Pressing (HIP) industry. Since then, the company has continuously developed its technology in response to the evolving application areas for gas atomised metal powders, notably in the Metal Injection Moulding industry and more recently in metal Additive Manufacturing processes.

The company was founded by Bill and Jan Hopkins and backed by Lucius Cary of venture capital company Oxford Technology, and has grown from building small research machines for universities to supplying multi-million dollar production systems for large corporations. Today, the company has installed systems in twenty one countries on seven continents.

A sister company to PSI, Metal Powder and Process Ltd (MPP), was recently formed with the purpose of developing and producing novel powder alloys for demanding applications, placing the company in a strong position to address world demand for new PM applications requiring high purity spherical metal powders.

PSI is also involved in a number of collaborative research projects addressing the need to develop new advanced metal powders and innovative production processes, as well as building a knowledge base on how these powders perform in today's advanced applications.

www.psiltd.co.uk

PSI builds a wide range of systems for atomising metal powders. The Hermiga gas atomiser shown here is from a product range that includes research and pilot systems as well as production capable units

Oerlikon strengthens technology portfolio with multiple acquisitions

Oerlikon, Pfäffikon, Schwyz, Switzerland, has acquired Primateria AB in Sweden and signed an agreement to acquire the assets of DiaPac LLC and Diamond Recovery Services Inc (DRS) in the USA. According to the group, these acquisitions are aimed at adding promising technologies and expertise in the field of advanced materials and surface solutions, to reinforce and expand its business offering.

Primateria is a provider of surface engineering services in Sweden, specialising in pre- and post-treatment solutions for tool optimisation. With this acquisition, Oerlikon expects to strengthen its foothold in the gear cutting market and to provide greater expertise and a broader portfolio of surface treatments to its customers worldwide.

DiaPac LLC is an internationally recognised leader in providing high-performance powder metals, wear-resistant surface coatings and cemented carbides for use in oil & gas, mining, construction, agricultural and manufacturing operations. Diamond Recovery Services (DRS) specialises in providing hard materials and environmentally complementary reclamation services, applied across a broad spectrum of applications.

With these acquisitions, Oerlikon expects to gain strong complementary knowledge for the manufacturing, processing, application and recovery/recycling of advanced materials, especially tungsten carbide. It will also benefit from increased market access in the oil & gas, metal matrix composites and US powder metals industries.

Dr Roland Fischer, Oerlikon Group CEO, stated. "These acquisitions are proof points that we are successfully executing on our strategy for surface solutions and advanced materials. We target very specific companies, which are leaders in their fields, have proven market success with their technologies and services and thereby can bring to Oerlikon excellent value that complements our existing competencies. As we see a growing demand for surface solutions technologies in many of our end markets, we will continue to expand and improve our technology and service offering to meet the needs of our customers today and in the future."

The acquired companies bring to Oerlikon Group a combined 2016 revenue of CHF 10 million and a combined workforce of forty employees. As part of the group, DiaPac, DRS and Primateria are expected to be able to leverage the global market reach, innovation competencies and financial power of Oerlikon to bring their products and services to the next level. The purchase prices were not disclosed.

www.oerlikon.com

Schunk opens new customer centre in Austria

Schunk Group has opened a new customer centre in Bad Goisern, Austria, in an inauguration ceremony attended by company management, the board of directors and the Schunk workforce, as well as representatives from local politics, business and media. The new centre is the result of a reported €4 million investment, and replaces a former site which was active from 1947.

Bad Goisern is home to the group's Automotive Business Unit headquarters, part of Schunk Carbon Technology. At the opening ceremony, Dr Klaus Löcker, Managing Director of Schunk Carbon Technology, stated, "Bad Goisern is becoming increasingly important on the world stage thanks to the inauguration of the headquarters of the Automotive Business Unit. This has allowed us to enhance both the attractiveness of Schunk Carbon Technology as an employer as well as the attractiveness of Bad Goisern as a business location situated in the heart of the Salzkammergut region."

"The investment emphasises Bad Goisern's importance as a centre for the international automotive business of our Carbon Technology Division," added Dr Arno Roth, Schunk Group CEO.

Schunk Carbon Technology Austria reports that it is serving an increasing number of major automotive manufacturers as end customers through close development partnerships, technological exchanges and global collaborations. The customer centre will also accommodate the company's Management and Controlling, Sales, HR and IT Departments.

schunk-carbontechnology.com

Schunk's new Customer Centre in Bad Goisern, Austria (Courtesy Schunk)

PM technology boosts energy savings for industrial furnaces

Sandvik Materials Technology (SMT) reports that Powder Metallurgy materials under its Kanthal brand have been used to boost the productivity of industrial heat treatment furnaces. Efficient heat treatment is a vital step in the production of a wide range of products, from integrated circuits for smartphones to solar cells and most steel- and aluminium-based products. For efficient heat treatment to be possible, industrial ovens have to cope with the extreme heat required for these processes, often up to 1,250°C.

"A common problem is that the construction components within heating systems deform over the course of time," explained Bo Jönsson, technical specialist at Kanthal. "For a material to function properly at high temperatures, two essential properties are required: good form stability and oxidation resistance."

"The types of material traditionally used in the construction of industrial furnaces are often nickel-based, which provides good form stability but limited oxidation-resistance." However, conventionally produced materials – based on iron, chromium and aluminium – have excellent oxidation properties but relatively low form stability.

In May 2017, SMT received the 'Wilhelm Haglund Medal to the Product Developer of the Year' award for the development of two materials able to cope with extreme temperatures, which it called Kanthal APM™ and Kanthal APMT™. "The Kanthal APM and Kanthal APMT materials combine uniquely high oxidation resistance and form stability," Jönsson continued. "The key to successfully developing these properties was the use of Powder Metallurgy to obtain an optimum microstructure in the materials."

An industrial furnace (Courtesy Sandvik)

The Powder Metallurgy technique made it possible for the company to structure the metal with billions of small particles, substantially boosting its strength at high temperatures. The materials are now used in applications such as heating systems for industrial furnaces and other demanding uses.

"One example is furnace rollers for continuous annealing lines made from Kanthal APMT, that eliminates the need for water cooling," Jönsson added. "This provides significant energy savings and environmental benefits. In many cases it has also been possible to reduce maintenance needs and boost productivity as a result of increased process temperatures and fewer shutdowns."

Jönsson stated that he sees significant opportunities for expanding the use of Powder Metallurgy materials. For example, the development of Kanthal APMT has contributed to Sandvik's new involvement in a number of projects relating to a fossil-free energy supply.

"The combustion of bio-based fuels generates corrosive environments that our materials have demonstrated good abilities to resist," he explained. "They could even be of use in the next generation of nuclear power plants. And for large-scale concentrated solar power to be cost-effective, new materials are needed that can handle and store solar energy at higher temperatures."

www.smt.sandvik.com
www.kanthal.com

ORS offers CT Powder Analysis Services using 3D X-ray imaging

Object Research Systems (ORS), Montreal, Canada, is now offering CT Powder Analysis through its Product Testing Services. Using its proprietary software and 3D X-ray imaging, the company provides clients with full volumetric data and analysis of metal powders for R&D and quality assurance purposes.

According to ORS, laser diffraction and other conventional powder testing methods do not provide the same depth of analysis as CT scanning, which can reveal powder characteristics only visible through X-ray. After scanning, a 3D visualisation of the powder can be produced, with the option to add visual details and animation for presentations.

By visualising powder structure in 3D, ORS states that it enables its clients to extract meaningful quantitative descriptions relating to size and spatial distribution, as well as accurate data on sphericity, particle aspect ratio, size and porosity.

The company also offers a Complete Scanning Schedule Plan Analysis, which can be used to determine the variability of powders from, for example, nominally identical batches. This is expected to enable companies to provide better quality control.

www.theobjects.com

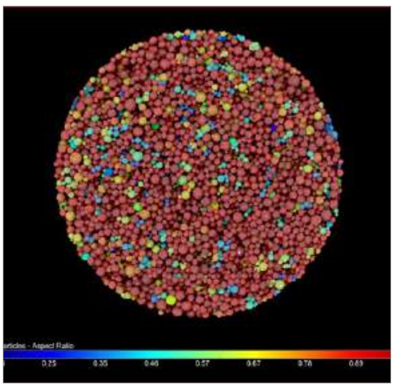

Metal powder as viewed through ORS' 3D imaging software

Leaders in PM industry, science and academia recognised at Euro PM2017

The Euro PM2017 Congress & Exhibition took place in Milan, Italy, October 1-5, 2017. Organised and sponsored by the EPMA, the event attracted over 1000 participants, including delegates, authors and exhibitors from forty-two countries. According to the EPMA, over two-hundred oral and poster presentations were given during the five-day event.

At the opening Plenary Session the EPMA presented its annual Distinguished Service Award and the first EPMA Fellowship Awards, a new award designed to recognise significant contributions to Powder Metallurgy from the scientific and academic community.

EPMA Distinguished Service Award

The award is presented in recognition of individuals who make an outstanding contribution to the European PM industry over a number of years. Recipients are selected by the EPMA Council and this year, the EPMA presented its Distinguished Service Award to Thomas Lambrecht, Dorst Technologies, Germany.

Lambrecht studied Chemical Engineering at Munich Technical University from 1978-1984, after which time he began as Project Engineer at a Munich-based company designing and realising ceramic plants globally. He joined Dorst Technologies in 1995 as a Sales Manager. Since 2000, he has been employed as the company's Managing Director.

EPMA Fellowship Awards

The EPMA's inaugural Fellowship Awards were presented to Professor Doctor Ingenieur Christoph Broeckmann, Professor Alberto Molinaro and Professor Doctor José Manuel Torralba.

Thomas Lambrecht (left) received this year's EPMA Distinguished Service Award

Prof Dr-Ing Christoph Broeckmann (centre) received the EPMA Fellowship Award

Prof Alberto Molinaro (centre) received the EPMA Fellowship Award

Prof Dr-Ing José Manuel Torralba (left) received the EPMA Fellowship Award

Broeckmann began his career at Ruhr-University Bochum, Germany, studying Mechanical Engineering before going on to work at the Institute of Materials Science at Bochum for ten years. Shortly after receiving his PhD for a thesis on the fracture of carbide rich steels, he began work at Köppern GmbH & Co. KG, before being appointed Managing Director at Köppern Entwicklungs GmbH. In 2008, he joined RWTH Aachen University as a professor and, in 2009, was made Head of the Institute for Materials Application in Mechanical Engineering (IWM).

Molinaro gained his PhD in Metallurgical Engineering from the University of Torino, Italy, and teaches as a Professor at the University of Trento. He was made Honoris Causa PhD by the University Carlos III, Madrid, in 2016. He is Chairman of the EPMI, the European Powder Metallurgy Institute of the EPMA. At Euro PM2017, he served as Congress Chair alongside Ing. Matteo Federici. He was Chairman of the 2010 PM World Congress.

Torralba is the Director-General for Universities and Research of Madrid Regional Government. He has published more than 450 scientific papers and supervised twenty-six PhD theses and eighty Diploma theses. He has participated in more than seventy international scientific committees of International Conferences, being Chairman of seven of them and involved in thirty-five competitive projects.

EuroHM Lifetime Service Award

The EPMA's working group for hardmetals presented a special 'Lifetime Service Award in the Hardmetal Industry' to Kenneth J A Brookes, EurIng, FIMMM, CEng, of International Carbide Data.

Brookes, whose sixty-plus-year career began at Tungsten Electric Company in 1951, has published multiple books on hardmetals and consults globally on the hardmetals industry.

www.europm2017.com
www.epma.com

Ford and Zotye establish JV to build electric vehicles in China

Ford and Zotye Auto have formed a JV to build electric cars in China

Ford Motor Company and Zotye Auto have announced plans to invest 5 billion RMB (approximately US $756 million) to manufacture a range of electric vehicles for the Chinese market. Following the signing of a 50:50 joint venture agreement, the two companies will establish Zotye Ford Automobile Co., Ltd.

Zotye Ford plans to build a dedicated product research and development centre as well as its own sales and services network. A new manufacturing plant for the JV will be constructed in Zhejiang Province. The all-electric vehicles produced by the JV will be sold under a new Chinese brand.

"We are delighted to have signed this joint venture agreement with Zotye to form our third joint venture automotive company in China. Subject to regulatory approval, Zotye Ford will introduce a new brand family of small all-electric vehicles," stated Peter Fleet, Ford Group Vice President and President, Ford Asia Pacific. "We will be exploring innovative vehicle connectivity and mobility service solutions for a new generation of young city-dwelling Chinese customers."

Zotye Auto is the market leader in China's all-electric small vehicle segment and sold more than 22,500 all-electric vehicles year-to-date through October 2017, representing a growth of over 14% year-over-year. The JV is said to benefit from Zotye's expertise in designing and commercialising EVs in China and Ford's global product development and technology capabilities.

"This is an important day for Zotye as we partner with Ford to help advance the growth of the Chinese auto industry," stated Ying Jianren, Chairman of Tech-New Group Ltd. and Board Director of Zotye Auto. "We will work closely together to help meet Chinese consumers' growing demand for electric vehicles."

Upon its establishment, the new JV will expand Ford's footprint in China. Ford already operates successful vehicle joint ventures with Changan Ford Automobile Corporation, Ltd. and Jiangling Motors Corporation.

www.ford.com

www.zotyeglobal.com

Centorr Vacuum Industries offers detailed online furnace finder application

Centorr Vacuum Industries has updated its website for custom vacuum and controlled atmosphere furnaces. The new site now provides quick and easy searching of furnaces based on application or furnace type.

Technical data sheets are now also listed for each of the 65 different furnace configurations the company offers in its line of laboratory and production furnaces. The new site includes:

- Furnace Finder feature to quickly select the best equipment for your needs
- A 'Request for Quotation' form to easily gather information for receiving a custom proposal
- Ability to be viewed in over 90 different languages
- Downloads for technical data sheets, articles and company press releases
- Links for spare parts, field service support, used furnaces, and toll lab testing.

www.centorr.com

Mitsubishi Materials Corp reports PM business sales up in first half results

Mitsubishi Materials Corp. (MMC), headquartered in Tokyo, Japan, has reported group sales up 20.3% year-on-year for the six months to September 30, 2017, reaching Yen 725,450 billion ($6.393 billion). The company recorded an operating profit up 33.5% to Yen 39,530 billion ($348 million) in the period.

Sales in the group's Advanced Materials & Tools division – which includes cemented carbide (hardmetal) tools, structural PM parts and PM bearings, high-performance alloy products and superalloys – increased by 7.1% to Yen 78.3 billion ($689.9 million) and operating profit was up 2.1% to Yen 8.6 billion.

The company stated that a combination of aggressive marketing and higher demand in Japan, Europe, USA and Southeast Asia saw increases in sales for cemented carbides, and sintered PM products also benefitted thanks to the launch of new products and increased sales.

www.mmc.co.jp

Submitting news..

To submit news to *PM Review* please contact Paul Whittaker: paul@inovar-communications.com


RENISHAW
apply innovation™
RENISHAW
RenAM 500M

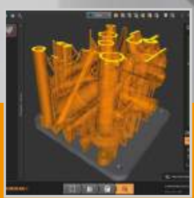


RENISHAW
ULTRASONIC SIEVING
SYSTEM

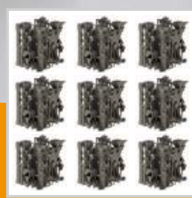

MPIF announces its 2017 Outstanding Technical Paper award

The Metal Powder Industries Federation (MPIF) has announced that the 2017 Howard I Sanderow Outstanding Technical Paper Award has now been selected from presentations made at its POWDERMET2017 conference held in Las Vegas, USA, June 13-16, 2017. The winning paper, titled 'Deformation Processed Al/Al_2Ca Nano-filamentary Composite Conductors', is by Charles Czahor, Trevor Riedemann, Alan Russell and Iver Anderson, FAPMI, Ames Laboratory, Iowa State University, USA.

The Howard I Sanderow Outstanding Technical Paper Award (renamed in 2009), was established in 1993 to recognise authors of manuscripts for excellence in scientific and technical written communications from those papers presented and submitted for publication from the annual technical conference organised by the MPIF and APMI International. Its aim is to enhance the quality of technology transfer in PM literature by increasing the professional level of papers submitted for the annual technical conference and to enhance and promote the science and technology which is fundamental to Powder Metallurgy products, processes, and materials.

Paper excellence is measured using a system of four quality standards: (1) the paper is scientifically or technically new, innovative, or is a constructive review; (2) has clear presentation in writing, organisation, graphics, format and has professional integrity; (3) has clear industrial application; and (4) has long-term value.

The authors will be officially recognised during the Industry Luncheon to be held during POWDERMET2018 in San Antonio, USA, June 17–20, 2018.

The paper is available for download on the MPIF website. It is also included in *Advances in Powder Metallurgy & Particulate Materials – 2017*.

www.mpif.org

Magna forms joint venture for electric-drive powertrain production in China

Global automotive supplier Magna International Inc., Aurora, Ontario, Canada, as entered into a joint venture agreement with SAIC Motor subsidiary Huayu Automotive Systems Co., Ltd. (HASCO), Shanghai, China. The JV will initially be focused on the production of Magna's electric-drive powertrain system for the Chinese market.

Both partners report that they will give the JV full support to develop localised core competencies in terms of market development, R&D, advanced manufacturing and key parts supply such as gearboxes, inverter components and e-motors. Magna brings to the JV ten years of experience as a developer and manufacturer of electrified powertrains including e-motors, gearboxes, inverters and control software.

"The new-energy vehicle (NEV) market will continue to grow at a rapid speed in China," stated Chen Zhixin, President of SAIC Motor and Vice Chairman of HASCO. "With this trend, SAIC Motor is developing the New Four Modernisation strategy focusing on car electrification, connectivity, intelligence and sharing economy. The establishment of the JV, a strong combination of HASCO and Magna's strength to initiate cooperation in NEV electrified powertrain systems, has been a milestone for HASCO to develop its core competencies in the field of key new-energy-related components, as well as a critical measure to strengthen the New Four Modernisation strategy for SAIC."

"China is the number-one growth market in the world, and they have been clear about their intended leadership in bringing hybrid and electric vehicles to market," added Don Walker, Magna CEO. "Combining strengths with HASCO helps position Magna and the joint venture for future growth and success."

In 2009, Magna announced a vehicle-development partnership with Ford Motor Company to introduce a zero-emission lithium-ion battery electric vehicle (BEV) – the Ford Focus BEV, which entered the market in 2011. Magna was responsible for providing the electric motor and electronic control module, and also played a role in engineering the vehicle to integrate the electric propulsion system and other new systems into the vehicle architecture.

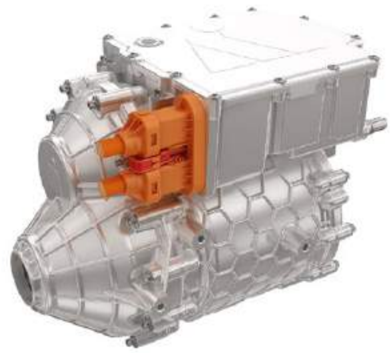

Magna's electric-drive powertrain system will now be produced for the Chinese market (Courtesy Magna International)

Since 2012, Magna has also supplied Volvo with the electrified rear axle drive system (eRAD) featured on the Volvo V60 and S60 plug-in hybrid models. Magna's eRAD system complements a traditional gas- or diesel-engine front-wheel-drive powertrain with an independent electric powertrain to power the rear wheels and offers multiple hybrid driving modes while adding four-wheel-drive capability.

www.magna.com

First plant in Europe to produce aviation-grade titanium by recycling

A new plant in Saint-Georges-de-Mons, France, will be the first in Europe to produce aviation-grade titanium by recycling. The EcoTitanium project makes alloys from titanium solid scrap and chips collected from the major aircraft makers and their subcontractors, and is said to provide Europe with a titanium supply source which is independent of the major global producers.

The €48 million project has three shareholders: UKAD (43.5%), a joint venture by Aubert & Duval and UKTMP International, ADEME (41.3%) under the Investissements d'Avenir programme and Crédit Agricole Centre France (15.2%) through its investment subsidiary CACF Développement. The EcoTitanium site was inaugurated during a recent ceremony attended by Benjamin Griveaux, French Secretary of State for Economy and Finance, and Christel Bories, Chairman & CEO of the ERAMET Group.

"The ERAMET Group is proud to support the EcoTitanium project for the creation of a recycling stream that will provide Europe with a titanium supply source which is independent from the major global producers. EcoTitanium is a milestone in ERAMET's constant commitment to environmental and social responsibility, as well as industrial innovation," stated Bories.

At full capacity, EcoTitanium will produce several thousand tons of titanium alloy ingot per year to meet high growth in demand for titanium on aviation markets. Titanium and its alloys provide this industry with valuable properties: lightness (44% lighter than steel), excellent corrosion resistance and advanced mechanical characteristics.

It is said that EcoTitanium's recycling route will prevent the emission of 100,000 tons of CO_2 by consuming four times less power than the conventional, ore-based production supply chain. To support the creation of this environmentally responsible stream in Europe, the European Investment Bank (EIB) granted a €30 million loan for EcoTitanium funding.

Denis Hugelmann, CEO in charge of the Alloys Division, ERAMET and Chairman of EcoTitanium, stated, "I thank our partners UKTMP, Crédit Agricole Centre France, ADEME and the European Investment Bank for their involvement in this pioneering project."

www.eramet.com

Alan Lawley passes away aged 84

Alan Lawley, Emeritus Professor, Drexel University, Philadelphia, USA, passed away on October 17, 2017, at the age of 84. As a long-time friend and supporter of the Powder Metallurgy industry, Lawley made significant contributions to research and development in PM and particulate materials, and guided the professional development of undergraduate and postgraduate students, many of whom work in the industry today.

Lawley received BSc, Physical Metallurgy and PhD, Metallurgy degrees from the University of Birmingham, UK, after which he went on to work at the University of Pennsylvania's School of Metallurgical Engineering as Post-Doctoral Fellow and at the Franklin Institute's Solid State Research Laboratory.

He joined Drexel University in 1968, where he initiated a PM programme, and over the years his PM teachings, research and consulting activities impacted the academic world, industry and national laboratories, as well as federal government and state agencies.

While at Drexel, he was appointed Department Head/ Materials Engineering and made A.W. Grosvenor Professor of Metallurgy. Hoeganaes Corporation, Cinnaminson, New Jersey, USA, endowed a professorship in PM at Drexel where two dedicated PM laboratories were established. Lawley published over 300 articles in archival journals, conference proceedings and books — more than 200 of which embrace PM and particulate materials.

Lawley was named Editor-in-Chief of APMI International's International Journal of Powder Metallurgy in 1985 and served in this capacity until 2015. He was co-chairman of the 1993 International Conference on Powder Metallurgy & Particulate Materials (Nashville, USA), co-chaired the MPIF/APMI PM2008 World Congress (Washington, D.C, USA) and was a long-time member of the MPIF's Technical Board. A recipient of numerous professional and societal awards, Lawley was among the first class of Fellows of APMI International (1998). Additionally, he served on APMI's Panel of Fellows, Awards Committee, and Publications Committee. He received the MPIF Distinguished Service Award in 1991 and the MPIF Kempton H. Roll PM Lifetime Achievement Award in 2012.

GKN launches UK Innovation Centre for state-of-the-art vehicle technologies

GKN plc has opened a new UK Innovation Centre for its automotive division, which will focus on developing state-of-the-art vehicle technologies and systems. The centre, in Abingdon, Oxfordshire, UK, will make use of GKN group's expertise in electrified drivelines through lightweight structures, composite materials and Additive Manufacturing to create a range of new technologies for next-generation vehicles.

Central to GKN's recently-announced Official Partnership with the Panasonic Jaguar Racing Formula E team, the UK Innovation Centre will take the lead on delivering the group's new components and technologies for the Jaguar Formula E electric race car. GKN has already delivered its first parts for the I-TYPE 2 in the form of custom-built fluid ports made from laser-sintered steel.

"Our new UK Innovation Centre will develop an array of next-generation technologies that will deliver significant benefits to electric vehicle, motorsport and off-highway applications," said Phil Swash, GKN Driveline CEO. "For electrified systems in particular, GKN's expertise will help automakers to develop lighter, quieter and more efficient vehicles. No other company can apply aerospace experience to automotive applications in the same way as GKN, unlocking exciting opportunities for Additive Manufacturing and composites."

At the launch of the new centre, GKN displayed a range of its automotive technologies, including its two-speed TorqueShift powertrains. GKN stated that it has developed the only two-speed eTransmission currently in production – for the BMW i8 hybrid supercar – and revealed the world's first fully-electric drive system with two-speed gearing and Twinster torque vectoring technology at the Frankfurt Motor Show – the eTwinsterX.

At the UK Innovation Centre, GKN will work to develop a new 'TorqueShift' system for electric vehicles. The company stated that two-speed systems can deliver more 'miles per kilowatt' than conventional eDrive systems, but GKN is focused on developing a 'dual-clutch feel' experience for electric car drivers.

GKN also displayed a range of electric motors and flywheels. The UK Innovation Centre is now developing a new prototype energy storage unit, which will have a significantly larger capacity at lower cost than its previous-generation flywheel systems. This new flywheel technology has been designed specifically with commercial vehicles and off-highway applications in mind, delivering useful electric-driving capability without the higher cost of a plug-in hybrid or fully-electric system.

www.gkn.com

Jaguar Formula E electric race car on display at the opening of GKN's new UK Innovation Centre (Courtesy GKN plc)

Dr W Brian James receives ASTM Frank W Reinhart Award

Dr W Brian James, Ph.D., retired, has received the Frank W Reinhart Award from the ASTM International Committee On Metal Powders And Metal Powder Products. James, who joined ASTM in 1986, was honoured for his contributions to the standardisation of terminology for the metal powder industry.

According to ASTM International, the award recognises his leadership and commitment to developing consistent and coherent terms for the committee. James has previously received the Award of Merit, the Distinguished Service Award, and two Awards of Appreciation from the committee.

Prior to his retirement, James served as Manager of International Technical Service for Hoeganaes Corporation, as a product development engineer for GKN Technology, as a development engineer for Round Oak Steel Works, among other roles. He holds both a Bachelor's and Doctorate degree in metallurgy from the University of Manchester's Institute of Science and Technology.

In addition to ASTM International, James is a member of the American Powder Metallurgy Institute, the Institute of Materials, Minerals and Mining, the European Powder Metallurgy Association and the American Society for Metals.

www.astm.org

Submitting news..

To submit news to *PM Review* please contact Paul Whittaker: paul@inovar-communications.com

Paper submissions now open for Euro PM2018

The EPMA has issued a Call for Papers for Euro PM2018, the association's annual Powder Metallurgy congress and exhibition, Bilbao, Spain, October 14-18, 2018. According to the EPMA, Euro PM2018 is set to feature a world-class technical programme as well as a 5000m² exhibition, showcasing the latest developments from the global PM Supply Chain.

This year's Euro PM2017 was reportedly attended by over 1000 participants. The Euro PM2018 Congress and Exhibition, along with social events such as the welcome reception and congress dinner, is expected to provide excellent networking opportunities within the PM industry.

The conference programme of plenary, keynote, oral and poster presentations will focus on all aspects of Powder Metallurgy. Abstracts can be submitted on the following topics:

- Additive Manufacturing
- Applications for current and future PM
- Full density and alternative consolidation
- Hardmetals, hard materials and diamond tooling cermets
- Hot Isostatic Pressing
- Modelling and simulation
- Powder Injection Moulding
- Powder manufacturing and processing
- PM functional materials
- PM lightweight and porous materials
- PM magnetic materials
- PM non-ferrous and special materials
- Powder pressing
- Secondary & finishing operations

Euro PM2018 will take place in Bilbao, Spain

- Shaping
- Sintered steels
- Sintering
- Tools for improving PM

All abstracts should be submitted using the EPMA's online submission form by no later than January 24, 2018. Abstracts must be between 100-150 words in length and give sufficient information to allow the Technical Programme Committee to evaluate the proposed presentation.

www.europm2018.com

Powder Piloting Service for powder-based materials and components

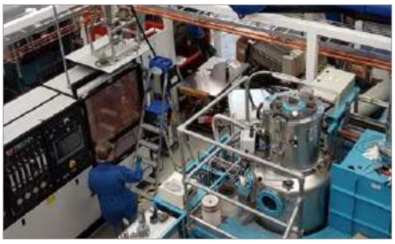

VTT Technical Research Centre of Finland Ltd (VTT), Tampere, Finland, a facility specialising in powder-based materials technology, now offers a Powder Piloting Service for the design and pilot scale processing of powder-based materials and components. The service is said to provide users with an easy way to check the feasibility of ideas and innovations in a confidential setting, without large investments in machinery, and covers the whole production chain from raw material synthesis to component performance testing.

The centre serves clients in the private and public sectors, both domestically and internationally, and has over 75 years' experience supporting client growth with top-level research and science-based results.

The organisation's Powder Piloting Service is focused on the key areas of:

Coatings

- Cost efficient solutions against wear, corrosion and high temperatures
- Tailoring of material properties to fulfil performance criteria for harsh operating environments

Components

- High-performance components using cost-efficient and sustainable manufacturing
- Tailoring of components to meet high demands and standards

Powder based additives

- Graded or locally reinforced structures
- Structures with added functionality such as integrated catalytic or electro-magnetic properties

Circular economy

- Alternative raw materials based solutions
- The utilisation of secondary materials and industrial side-streams

Pilot facilities are available at almost all levels of powder manufacturing, consolidation, post-treatments and characterisation, from gas atomisation and plasma spheroidisation to heat and surface treatments. VTT's equipment includes Additive Manufacturing, Hot Isostatic Pressing (HIP) and Powder Injection Moulding machinery.

www.vtt.fi/powder

EPMA rewards PM theses, keynotes and poster presentations

The EPMA presented Keynote Paper Awards to (L-R) Dr Gian Filippo Bocchini, Dipl-Ing Julia Ureña, Dr Torsten E M Staab and Dr-Ing José Manuel Torralba (on behalf of Prof Dr Luis Llanes)

During the opening Plenary Session of the Euro PM2017 Congress & Exhibition held in Milan, Italy, the EPMA announced the winners of its PM Thesis Competition as well as recipients of the conference Keynote Awards.

Organised and sponsored by the EPMA, the event took place October 1-5, 2017 at the MiCo Convention centre in Milan. According to the EPMA, over two-hundred oral and poster presentations were given during the five-day event.

PM Thesis Competition

Sponsored by Höganäs AB, Sweden, the EPMA Powder Metallurgy Thesis Competition is open to any students studying Powder Metallurgy within the EU in two categories – PhD and Masters.

According to the EPMA, the aim of the competition is to develop interest in and promote Powder Metallurgy among young scientists at European academic institutions and to encourage research. Winners of the awards receive financial prizes and have the opportunity to present their work at the EPMA conference and receive a plaque from the EPMA President.

In 2017, the winners of the PM Thesis Competition were:

- Doctorate category – Dr Bey Vrancken, 'Study of Residual Stresses in Selective Laser Melting', KU Leuven, Belgium
- Masters category – Dipl-Ing Silvia Baselli, 'Shrinkage Kinetics Model of Uniaxial Cold Compacted Green Iron', University of Trento, Italy

Keynote Awards

Four Keynote Paper Awards were given to those papers selected as having the highest merit. Each received an extended thirty-minute slot for their presentation at the beginning of the relevant session during Euro PM2017. Their papers were also published in the journal Powder Metallurgy, which sponsored a €250 prize for each of the selected authors.

- Dipl -Ing Julia Ureña, 'Role of Beta-stabilizer Elements in Microstructure and Mechanical Properties Evolution of PM Modified Ti Surfaces Designed for Biomedical Applications', University Carlos III Of Madrid, Spain
- Dr Torsten E M Staab, 'Sintering Iron And Steel: Are There Indications For Defect-Activated Sintering?', Fraunhofer ISC Wuerzburg, Germany
- Prof Dr Luis Llanes, 'Implementation of Advanced Characterization Techniques for Assessment of Grinding Effects on the Surface Integrity of WC-Co Cemented Carbides', Universitat Politecnica Catalunya, Spain
- Dr Gian Filippo Bocchini, 'Can Industrial Standards Disregard Thermodynamics And Material Science?', PM Consultant, Italy

Peter Brewin Poster Award

The EPMA's Peter Brewin Poster Award was introduced in 2014 to recognise the contribution made by poster authors to the EPMA's annual Euro PM Congress.

This year's Poster Award was presented during a special poster session on Monday October 2. The winner was announced as:

- Dipl-Ing Wolfgang Limberg, 'Enhancement of Fatigue-properties of MIM-processed Ti-6Al-4V by Addition of Yttrium and Characterisation by In Situ X-ray Scattering"', Hemholtz-Zentrum Geesthacht, Germany

www.epma.com

Prof Kim Vanmeensel (left) collected the PM Thesis Competition Doctorate award on behalf of Dr Bey Vrancken

Dipl-Ing Silvia Baselli (left) received the PM Thesis Competition Masters award

Enhanced die wall lubrication compaction process achieves high density chain sprockets for Hitachi

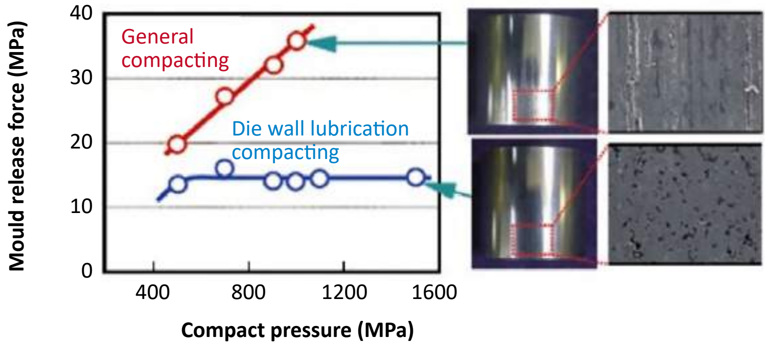

Fig. 1 Comparison of mould release using conventional compaction and die wall lubrication compaction using the newly developed liquid lubricant (Hitachi Chemical Technical Report No. 59)

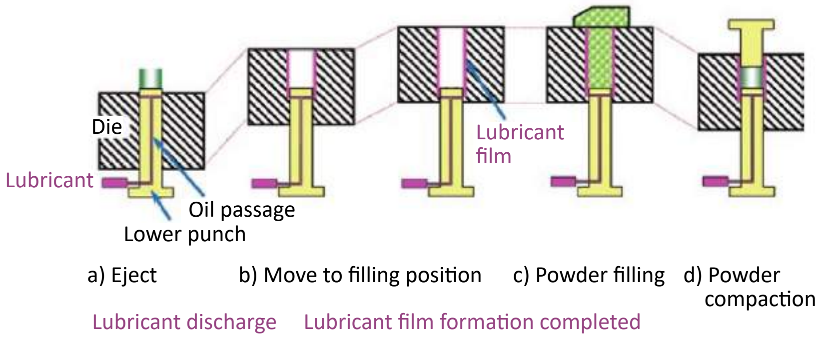

Fig. 2 Production sequence in die wall lubrication compaction using the new liquid lubricant film (Hitachi Chemical Technical Report No. 59)

Sintered steel chain sprockets are extensively used in automotive engine valve mechanisms. Their design and high density in the teeth provides for a combination of high contact fatigue strength at the tooth surfaces and a significant reduction in engine noise during operation of silent chains even at high revolutions.

Hitachi Chemical Co. Ltd of Tokyo, Japan, has been producing silent chain sprockets for a number of years using the tooth flank form rolling process to achieve the required high density (7.5 g/cm^3) by removing residual porosity on the surface layer of the sprocket's teeth. However, increasing competition from other manufacturing methods and the need to reduce costs and improve productivity has resulted in the company developing a new, alternative manufacturing process to achieve high density and fatigue strength in the chain sprockets.

Writing in *Hitachi Chemical Technical Report*, No. 59, 2017, Satoshi Onodera stated that the company has developed a modified die wall lubrication compaction process where the chain sprockets can be compacted to the desired high density by: (a) reducing the volume of pressing lubricant normally added to steel powder in conventional die compaction, and (b) using a die which is uniformly coated with a liquid lubricating film.

This involved developing a new lubricant containing mineral oil added to a solid lubricant and an extreme pressure agent to provide the excellent mould release capability during die wall lubrication compaction at pressures ranging from 400-1500 MPa. As can be seen in Fig. 1, the mould release pressure in die wall lubrication compaction is significantly lower using the newly developed liquid lubricating film. At a compaction pressure of 1000 MPa the mould release force required is reduced by 50% compared with conventional powder compaction.

Fig. 2 shows a schematic of the various steps in the newly developed die wall lubrication system where the application of the liquid lubricating film is completed for each compacting cycle. As can be seen in the figure, lubricant is supplied through the interior of the die and is also applied to the internal wall and sides of each die element during the compaction sequence from mould release position to the powder filling position.

Onodera stated that this system allows for the compaction of high density PM parts at much greater compacting speeds. Fig. 3 shows a high density sintered sprocket for silent chain made by the enhanced die wall lubrication compacting process using the new liquid coating. This PM component has a number of weight reducing holes requiring the use of multi-stage punch forming, and the technology developed has ensured that a uniform lubricant film is applied over all tooling surfaces.

www.hitachi-chem.co.jp

Fig. 3 High density sintered sprocket produced using the newly developed liquid lubricant film in die wall lubrication compaction (Hitachi Chemical Technical Report No. 59)

PM Summer School 2018 heads to Vienna

The European Powder Metallurgy Association (EPMA) has announced that its next Powder Metallurgy Summer School will take place in Vienna, Austria, July 2-6 2018. The popular course is open to young scientists, designers and engineers looking to gain a broader knowledge and understanding of the Powder Metallurgy process and applications.

The five-day residential event consists of a range of lectures given by PM experts drawn from both industry and academia. Topics to be covered will include the manufacture of metal powders, powder compaction, MIM, modelling, sintering, Hot Isostatic Pressing and Additive Manufacturing. Participants will be able to discuss and solve problems as well as get hands-on experience of various PM processes.

The Summer School is designed for young graduate designers, engineers and scientists from disciplines such as materials science, design, engineering, manufacturing or metallurgy. Graduates under 35 and who have obtained their degree from a European institution are eligible to apply. Registration to the Summer School is expected to open in early 2018.

www.epma.com/pm-summer-schools

Organisers report success of Spanish and Iberoamerican PM conferences

The Universidad de Castilla-La Mancha, Universidad Politécnica de Cataluña and the Institute of Ceramics and Glass have reported a successful 6th Spanish National Powder Metallurgy Conference and 1st Iberoamerican Powder Metallurgy Conference.

The conferences took place in Ciudad Real, Spain, June 7-9, 2017, and reportedly brought together more than 140 researchers from eleven countries. According to the organisers, around twenty PM companies attended the conferences' 'industrial session', as well as a number of industry associations.

In addition to plenary presentations from Dr Frank Petzoldt, Dr Elena Gordo, Dr Sebastián Díaz de la Torre and Dr Paolo Colombo, the conferences saw eighty presentations given across fourteen sessions. A further twenty-four short presentations were given during a poster session. During these sessions, attendees from both academic and industrial fields presented their latest activities and innovations.

An exhibition titled 'Particles in your Life' ran alongside the conference schedule, developed in order to make PM technology accessible to younger people through a series of guided visits from high school students.

www.vicnp.es

Kymera International formed from rebranding of powder businesses

Kymera International, the name by which ACuPowder, ECKA Granules and SCM Metal Products are collectively known, recently underwent a rebrand to help unify the three companies under a single name. Barton White, Kymera CEO, talked to *PM Review* about the origin of and reasoning behind the rebrand.

"We did not want to lose the extremely well-recognised names of ACuPowder, ECKA and SCM that for years had been synonymous with providing high-quality materials; however, we also felt that it was time for all to become one," explained White. "The goal was to remove any ambiguity in the market as to the relationship between the three brands and also eliminate the internal 'we/they' by becoming 'we'! After weighing all of the positives and negatives it was decided to move forward with the rebranding but also work to preserve the current brand names."

"Our goal was to pick a name that actually had a meaning that fit with our desire to combine the three brands," stated White. "The name would have to be unique enough that it could be copyrighted and also have a domain name that was not taken. We also needed to be sure that the chosen name and logo would not be offensive to people across different cultures… not easy!"

The Chimera of Greek mythology is a creature composed of vital parts from three different animals – a lion's head, a ram's body and a serpent's tail. According to White, this made it a perfect fit for the organisation: "The combination of the three animals makes the hybrid creature more powerful than its individual pieces."

"The problem was that there were many companies either directly named Chimera or where the spelling was very close, and so we decided that it was not unique enough. So we played with the name to make it more unique, as well as easier to pronounce." Kymera was the final result, and a logo – depicting a lion, a ram and a serpent – was designed to match.

ACuPowder, ECKA Granules and SCM Metal Products' plant locations will all now run in conjunction with Kymera International. For the foreseeable future, however, Kymera International will have no legal status and all of the Group's companies will continue to use their respective product labelling and banking for invoicing and payments.

"Over time we expect that people will become more familiar with Kymera International and that it will develop its own excellent brand identity," stated White.

www.kymerainternational.com

Refractory metals for particle producing targets at CERN

Intense and high-energy proton beams are impacted onto fixed targets made of refractory metals to produce secondary beams across the CERN accelerator complex. The interaction of a proton beam with the atoms and nuclei of these target materials produces extremely high and fast depositions of energy with a subsequent rapid rise of temperature, thermal and mechanical load.

In a paper presented at the 2017 Plansee Seminar, held in Reutte, Austria, May 29-June 2, 2017, Claudio Torregrosa and colleagues of the Engineering (EN) Department, Sources Targets and Interactions (STI) Group at the CERN accelerator complex in Geneva, Switzerland, reported on the upgrades to existing target facilities underway at CERN, as well as the design of new target devices using refractory metals. Torregrosa stated that the design of new target devices will require significant R&D activities on the behaviour of the different refractory metals of interest exposed to realistic material operational conditions. The target devices include the Antiproton Decelerator Target (AD-Target), the Beam Dump Facility (BDF) and the n_TOF neutron production spallation target facility. The authors stated that the AD-Target is the only antiproton production target currently in operation in the world. Its current design, shown in Fig. 1, dates from the late 1980s and consists of a water-cooled Ti-alloy (grade 5) assembly. Inside this assembly, a graphite matrix contains the target core, which comprises a 3 mm diameter, 55 mm length iridium rod. A new design of the target is being pursued at CERN for future operations which, among other changes, may include the selection of a different target core material and geometry configuration.

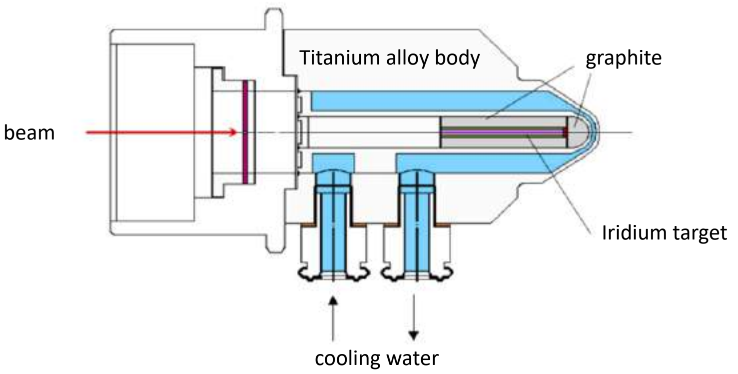

Fig.1 Schematic of the water-cooled antiproton design used from 1987 to the present day. The target core on which the primary proton beam is impacted is a 3 mm diameter rod, 55 mm length, made of iridium (From paper by C Torregrosa, et al., as published in the Proceedings of the 19th Plansee Seminar)

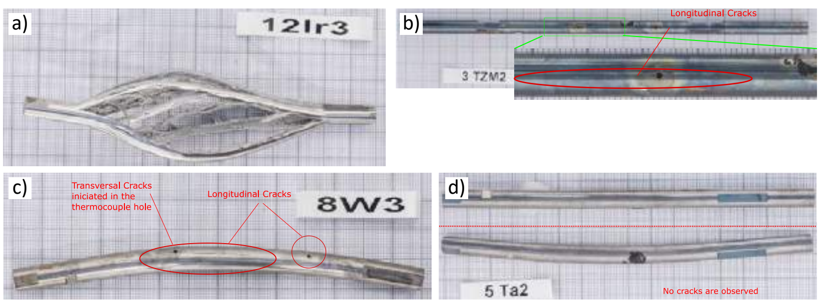

Fig. 2 Effect of some refractory metals exposed to direct impact of proton beams during the HRMT27 experiment. (a) Iridium (b) TZM (c) tungsten (d) tantalum. All the targets except Ta present a leigh degree of internal and external cracking (From paper by C Torregrosa, et al., as published in the Proceedings of the 19th Plansee Seminar)

Antiproton production is said to require a very compact target in order to be as close as possible to a punctual source and to reduce antiproton reabsorption in the material surrounding the core. Iridium is the current core material as it is the second most stable and densest element, although other refractory metals such as tantalum are strong candidates in the new design. The potential material should be as dense as possible, have a very high melting point (above 2000°C) and possess a high resistance to tensile pressures and spalling, even at high temperatures. Fig. 2 shows the results of some refractory metals (Ir, TZM, W and Ta) exposed to direct impact of proton beams during the HRMT27 experiment. All the targets except Ta showed a high degree of internal and external cracking.

The Beam Dump Facility target is a production target for the Search of Hidden Particles (SHiP) experiment currently in the design phase. The proposed target core design comprises several blocks of pure tungsten and TZM (an Mo alloy containing 0.5% Ti, 0.08% Zr, 0.02% C) having a square cross-section of 30 x 30 cm^2 and variable thicknesses, for a total effective target length of around 130 cm (Fig. 3). TZM is chosen because of its higher strength, better creep resistance and higher recrystallisation temperature compared to pure Mo. Due to the high temperatures generated by the beam power delivered on the target, a high-speed water-cooling system flowing around the TZM and W blocks is foreseen in the design. However, the high-speed water in contact with the pure tungsten and TZM blocks could induce undesired corrosion-erosion effects, and the target core blocks are therefore clad with Ta and Ta-W alloys using Hot Isostatic Pressing (HIP). Ta and Ta-W alloys were selected as the cladding material due to its high corrosion resistance and its convenience as high-Z material with short interaction length.

The current n_TOF facility consists of a proton-driven pulsed neutron source, coupled to two flight paths; Experimental Area 1 and 2, respectively 200 m (EAR1) and 20 m (EAR2) long. The facility is designed to study neutron-nucleus interactions for neutron kinetic energies ranging from a few meV to several GeV, determined by time-of-flight (hence the name n_TOF). The conducted studies are important in many research fields (astrophysics, nuclear research and technology, accelerator driven systems, etc). The current target comprises a water-cooled lead cylinder (Ø 60 cm x 40 cm) presently subject to erosion/corrosion phenomena and contamination of its water circuit with spallation products. In addition, in order to avoid water boiling, the average proton beam intensity on the target has been limited.

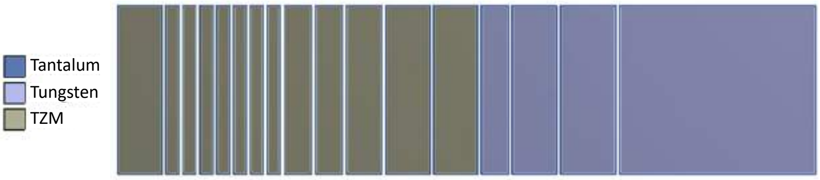

Fig. 3 Schematic drawing of the BDF target design. The target consists of 13 TZM blocks and 4 W blocks, all Ta-clad. (From paper by C. Torregrosa, et al. as published in the Proceedings of the 19th Plansee Seminar)

The existing n_TOF facility will undergo an important consolidation during the CERN Long Shutdown 2 (LS2). One of the possible new target envisaged consists of a HIPed Ta-clad tungsten core in a massive lead block. The new target is expected to improve reliability, avoid the above mentioned issues, and optimise physics performance for both experimental areas. The Ta-W core would be placed directly on the beam axis, undertaking the most critical part of the beam load due to its better thermomechanical behaviour, while the lead enclosure would have to be subject only to the remaining energy. In addition, a more efficient cooling can be obtained on the inner W core thanks to the use of HIPing to create a better thermal conductance at the interface between Ta and W.

Author email:
Claudio.torregrosa@cern.ch

The above paper is published in the Proceedings of the 19th Plansee Seminar, International Conference on Refractory Metals and Hard Materials, May 29-June 2.
www.plansee-seminar.com

Tungsten fibre-reinforced tungsten targeted for fusion reactors

Tungsten, which has the highest melting point of all elements, is considered the main candidate material for the first wall of the plasma vessel in fusion reactors. This is because of its reliable resistance to the harsh operating conditions in the long duty-cycles in these reactors caused by transient heat loading, thermal fatigue, neutron irradiation and erosion. However, whilst tungsten meets the demands of high strength, plasma compatibility due to its low hydrogen retention, low erosion rates and acceptable activation under neutron radiation, the metal has low toughness when handled or operated below the ductile-to-brittle transition temperature. This is stated to range from 400-700K depending on the specific processing history of the material.

Bruno Jasper (Forschungszentrum Jülich GmbH) and research colleagues at the Max-Planck-Institut für Plasmaphysik and the Technical University München, reported in a paper presented at the 2017 Plansee Seminar held in Reutte, Austria, May 29-June 2, on research carried out within the framework of the EUROfusion Consortium, whereby the inherently brittle tungsten is reinforced with W-fibres to increase its toughness. The Wf/W samples are processed by Hot Isostatic Pressing (HIPing), which was introduced as an alternative processing route for Wf/W composites to conventional chemical vapour deposition (CVD) technology since HIP enables the manufacturing of large-sized parts in short processing times.

The authors stated that tungsten fibre-reinforced tungsten (Wf/W) enables extrinsic toughening of inherently brittle tungsten materials by the introduction of energy dissipation mechanisms similar to ceramic matrix composites. These mechanisms, for example the pull-out of the fibres or crack deflection at the tailored fibre-matrix, lead to a reduction of stress peaks at crack tips and thus significantly improve the resistance of tungsten against crack propagation.

In their work on HIPing of Wf/W samples, the researchers used two W powders having a mean particle size of d_{50} = 8.7 µm and d_{50} = 8.8 µm respectively. The W powders were die compacted at 110 MPa and 185 MPa to produce tablets having a diameter of 19 mm and height in the range 4-5 mm, with green densities of approximately 51.5% and 58%. Four pellets of the same green density were filled into a tantalum (Ta) capsule with a single tungsten fibre (wire) placed between adjacent tablets. The capsules were closed with a Ta lid and sealed by electron beam welding under vacuum. The W fibres used had a diameter of 150 µm and were produced by hot drawing. The fibres were coated with an Er_2O_3 interface, using reactive magnetron sputtering with coating thickness adjusted to 1, 2 and 3 µm, and had been cut to 10 mm lengths. The encapsulated materials were densified by Hot Isostatic Pressing (HIP) at a constant pressure of 200 MPa, while varying the sintering

Fig. 1 Processing steps of single-fibre Wf/W composites using hot isostatic pressing (From paper by B Jasper, et al. as published in the Proceedings of the 19th Plansee Seminar)

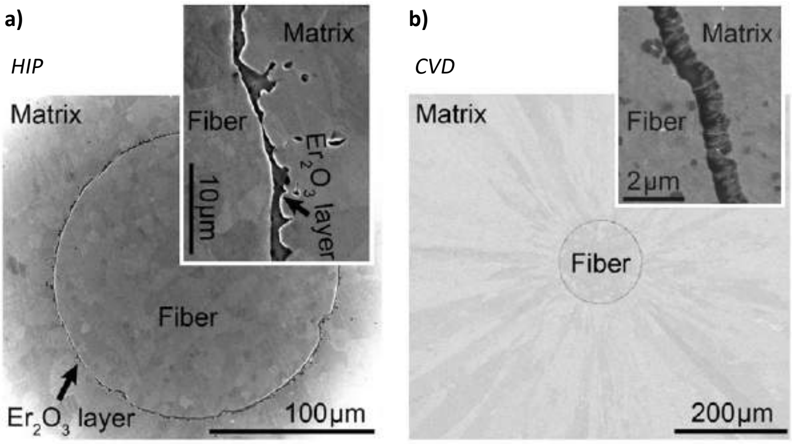

Fig. 2 Microstructure of Wf/W composites with a 1 µm thick Er_2O_3 interlayer produced by (a) hot isostatic pressing, (HIP at 1600 °C, 200 MPa, 3 h) and (b) Chemical vapour deposition, CVD (From paper by B Jasper, et al., as published in the Proceedings of the 19th Plansee Seminar)

temperature between 1300-1900°C. The dwell time of 4 hr at maximum temperature was kept constant in all HIP runs.

The authors reported that temperatures in the range of 1500-1600°C were found to be required to achieve densities higher than 98% of the theoretical density at a pressure of 200 MPa. Higher temperatures would slightly improve the densification but lead to unacceptably high grain growth of the fibre and matrix, which decreases the mechanical strength of the Wf/W composite. A maximum density of 99.5% TD was reportedly achieved at 1700°C. Fig. 1 shows the processing stages of Wf/W samples by HIPing.

Tests were carried out to compare the HIPed Wf/W samples with Wf/W samples prepared by established CVD technology. Analysis of the matrix showed a dense W bulk, a deformed fibre and a deformed but still intact interface layer. Special emphasis was placed on push-out tests of single-fibre HIP samples, where a load is applied via a small indenter on the fibre, to test the debonding and frictional properties of the Er_2O_3 interface region enabling the energy dissipation mechanisms. The authors reported that, while the fibre push-out of the CVD samples behaves as predicted in the shear-lag model, the HIPed Wf/W samples showed a superposition of effects, which they stated impede sound conclusions regarding interface parameters of the system. To clarify the pronounced differences between the push-out behaviour of HIPed and CVD samples, a deeper investigation of the fibre matrix-interface region and its evolution will be required. However, irrespective of this result, their study provides optimised HIP processing parameters enabling the manufacturing of larger sized Wf/W composite parts to further qualify this material for the desired application.

Author email:
B.jasper@fz-juelich.de

The above paper is published in the Proceedings of the 19th Plansee Seminar, International Conference on Refractory Metals and Hard Materials, May 29-June 2. Further details from www.plansee-seminar.com

High-performance permanent magnets: The influence of rare earths and the development of alternative materials

Rare earth permanent magnets have, for the past forty years dominated the higher performance magnetic devices market. However, the availability of raw materials globally is proving a risk to market stability for this important class of magnet. Material scientists have the opportunity to address this issue and the use of elements such as nitrogen, nanostructured materials and metastable materials, is now being explored. Dr Sim Narasimhan reviews the developments and the challenges facing these alternative materials.

Permanent magnets are vital components in a wide variety of products. From mobile phones to computer hard drives to electric vehicles, they can be found in almost every aspect of modern life (Fig. 1). Applications include devices which use the attractive and repulsive forces of magnets, such as door latches, magnetic levitation, torque couplers and magnetic separators. They are also used in devices that convert mechanical to electrical energy, such as magnetos and alternators, as well as devices that convert electrical to mechanical energy such as DC motors, loudspeakers, meters and disk drives. Magnets can also be used for focusing electron beams and in magnetic resonance imaging units. As demand for greener energy grows, with electric and hybrid vehicles becoming more mainstream, the need for more powerful magnets continues.

Permanent magnets are a class of magnets in which a magnetic flux remains, in contrast to an electromagnet for example, which only behaves like a magnet when an electric current is flowing through it. A good permanent magnet should produce a high magnetic field with a low mass, and should be stable against the influences which could demagnetise it. The desirable properties of such magnets are typically stated in terms of

Fig. 1 Examples of the various applications for permanent magnets

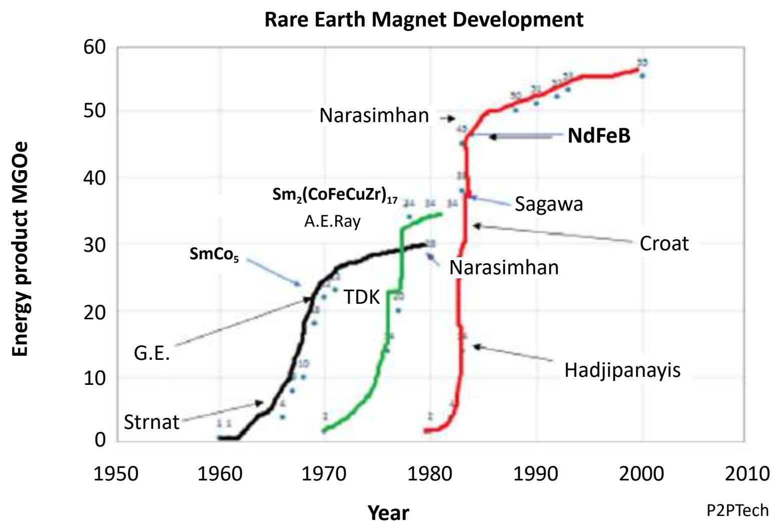

Fig. 2 Evolution of rare earth magnets 1MGOe= 8 kJ/m³

the remanence and coercivity of the magnet materials. Common permanent magnets are ferrites, alnicos and rare earth (Re) magnets ($ReCo_5$, $Re_2Cobalt_{17}$ type, NdFeB). Processing of these magnets is predominantly by the Powder Metallurgy route, except for alnicos which are commonly produced by sand casting.

Of these, rare earth magnets have a very high 'energy product' - a term that defines the volume of the magnet necessary for the maximum performance of a device. The higher the energy product, the smaller the magnet necessary. This energy efficiency is key in allowing the miniaturisation of products, and is one of the main advantages of rare earth magnets. Ferrite magnets, on the other hand, are often seen as the 'workhorse' magnet as they are cheaper and suited to many applications where miniaturisation is not the primary focus.

Rare earths

Rare earths consist of fifteen elements referred to as inner transition elements. Yttrium and scandium have similar properties to rare earths and, hence, are often counted along with rare earths. In nature, they occur together with varying proportions in different ore bodies. The first seven elements (lanthanum, cerium, praseodymium, neodymium, samarium, europium and short-lived promethium) are called light rare earths and they occur in monazite and bastnaesite ores in predominant quantities. Gadolinium, terbium, dysprosium, holmium, erbium, thulium, ytterbium and lutetium are called heavy rare earths and occur in xenotime and other ore bodies. The dispersion of rare earths globally is shown in Table 1. Heavy rare earths Dy, Tb and Gd, which are predominant in Chinese earth ores, are used in small quantities in NdFeB magnets for improved thermal stability.

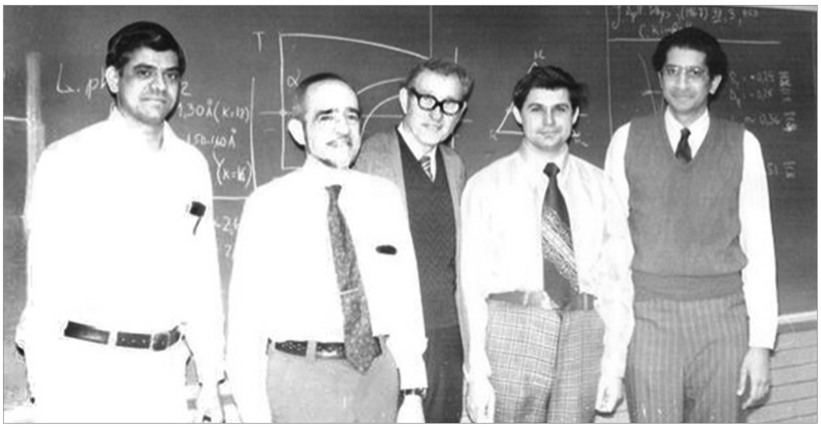

Fig. 3 Professor William Wallace (centre) and colleagues are credited with the discovery of rare-earth permanent magnets (author left)

The development of rare earth magnets

The evolution of rare earth permanent magnets can be seen in Fig. 2. This figure highlights the improvements made in energy product and identifies a number of key researchers notable for advancing the materials' development.

Prior to 1960, rare earths were used primarily in the steel industry for deoxidation and grain refining purposes. It was Professor William (Ed) Wallace (Fig. 3) and his team at the University of Pittsburgh, Pennsylvania, USA, who began exploration of the usage of rare earths in other areas. This group combined rare earth metals with cobalt, nickel and other elements and identified the crystal structure and magnetic properties of a number of intermetallics [1].

In late 1960, under an Airforce Materials Laboratory Contract, Professor Strnat at the University of Dayton, Ohio, USA, identified YCo_5 and later $SmCo_5$ to have potential to be processed into magnets [2]. J J Becker and Benzand Martin of GE R&D centre demonstrated processing details for the production of permanent magnets with R (R = Rare earth) Co_5 [3]. Crucible Steel Corporation in Pittsburgh, USA, under an Airforce Materials Research grant, developed a low-oxygen process where the entire crushing, milling, compaction and sintering were all done in a low oxygen atmosphere to

RARE EARTH CONTENTS OF MAJOR AND POTENTIAL SOURCE MINERALS[1,2] (Percentage of total rare-earth oxide)						
Rare earth	Bastnäsite		Monazite			
	Mountain Pass, CA, United States[3]	Bayan Obo, Inner Mongolia, China[4]	North Capel, Western Australia[5]	North Stradbroke Island, Queensland, Australia[6]	Green Cove Springs, FL, United States[7]	Nangang, Guangdong, China[8]
Yttrium	0.10	trace	2.40	2.50	3.20	2.40
Lanthanum	33.20	23.00	23.90	21.50	17.50	23.00
Cerium	49.10	50.00	46.00	45.80	43.70	42.70
Praseodymium	4.34	6.20	5.00	5.30	5.00	4.10
Neodymium	12.00	18.50	17.40	18.60	17.50	17.00
Samarium	0.80	0.80	2.53	3.10	4.90	3.00
Europium	0.10	0.20	0.053	0.80	0.16	0.10
Gadolinium	0.20	0.70	1.49	1.80	6.60	2.00
Terbium	trace	0.10	0.035	0.30	0.26	0.70
Dysprosium	trace	0.10	0.70	0.60	0.90	0.80
Holmium	trace	trace	0.053	0.10	0.11	0.12
Erbium	trace	trace	0.20	0.20	trace	0.30
Thulium	trace	trace	trace	trace	trace	trace
Ytterbium	trace	trace	0.10	0.10	0.21	2.40
Lutetium	trace	trace	trace	0.01	trace	0.14
Total	100	100	100	100	100	100
	Monazite (continued)		Xenotime		Rare earth laterite	
	Eastern coast, Brazil[9]	Mount Weld, Australia[10]	Lahat, Perak, Malaysia[3]	Southeast Guangdong, China[11]	Xunwu, Jiangxi Province, China[12]	Longnan, Jiangxi Province, China[12]
Yttrium	1.40	trace	61.00	59.30	8.00	65.00
Lanthanum	24.00	26.00	1.24	1.20	43.40	1.82
Cerium	47.00	51.00	3.13	3.00	2.40	0.40
Praseodymium	4.50	4.00	0.50	0.60	9.00	0.70
Neodymium	18.50	15.00	1.60	3.50	31.70	3.00
Samarium	3.00	1.80	1.10	2.20	3.90	2.80
Europium	0.10	0.40	trace	0.20	0.50	0.10
Gadolinium	1.00	1.00	3.50	5.00	3.00	6.90
Terbium	0.10	0.10	0.90	1.20	trace	1.30
Dysprosium	0.40	0.20	8.30	9.10	trace	6.70
Holmium	trace	0.10	2.00	2.60	trace	1.60
Erbium	0.10	0.20	6.40	5.60	trace	4.90
Thulium	trace	trace	1.10	1.30	trace	0.70
Ytterbium	0.02	0.10	6.80	6.00	0.30	2.50
Lutetium	not determined	trace	1.00	1.80	0.10	0.40
Total	100	100	100	100	100	100

[1] Data are rounded to no more than three significant digits; may not add to totals shown
[2] This table is in atomic numerical order
[3] Johnson, G.W., and Sisneros, T.E., 1981, Analysis of rare-earth elements in ore concentrate samples using direct current plasma spectrometry—Proceedings of the 15th Rare Earth Research Conference, Rolla, MO, June 15–18, 1981: New York, NY, Plenum Press, v. 3, p. 525–529
[4] Zang, Zhang Bao, Lu, Ke Yi, King, Kue Chu, Wei, Wei Cheng, and Wang, Wen Cheng, 1982, Rare-earth industry in China: Hydrometallurgy, v. 9, no. 2, p. 205–210
[5] Westralian Sands Ltd., 1979, Product specifications, effective January 1980: Capel, Australia, Westralian Sands Ltd. brochure, 8 p.
[6] Analysis from Consolidated Rutile Ltd.
[7] Analysis from RGC Minerals (USA), Green Cove Springs, FL.
[8] Xi, Zhang, 1986, The present status of Nd-Fe-B magnets in China—Proceedings of the Impact of Neodymium-Iron-Boron Materials on Permanent Magnet Users and Producers Conference, Clearwater, FL, March 2–4, 1986: Clearwater, FL, Gorham International Inc., 5 p.
[9] Krumholz, Pavel, 1991, Brazilian practice for monazite treatment: Symposium on Rare Metals, Sendai, Japan, December 12–13, 1991, Proceedings, p. 78–82.
[10] Kingsnorth, Dudley, 1992, Mount Weld—A new source of light rare earths—Proceedings of the TMS and Australasian Institute of Mining and Metallurgy Rare Earth Symposium, San Diego, CA, March 1–5, 1992: Sydney, Australia, Lynas Gold NL, 8 p.
[11] Nakamura, Shigeo, 1988, China and rare metals—Rare earth: Industrial Rare Metals, no. 94, May, p. 23–28.
[12] Introduction to Jiangxi rare-earths and applied products, 1985, Jiangxi Province brochure, 42 p.

Table 1 Dispersion of rare earths in various ore bodies, globally (Indian, Kerala Monazite beach sand is the second largest reserve for rare earths) avoid formation of rare earth oxides which can diminish the potential of achieving maximum energy product. $SmCo_5$ was processed by the low oxygen technique to BH_{max}. 25-28 MGOe (199-223 kJ/m^3) [4].

Applications for RCo_5 rapidly increased, but problems lingered regarding the availability of samarium for high volume applications in the automotive sector. For mischmetal (MM), which consists of cerium 46-55 wt.%, lanthanum 20-30 wt.%, praseodymium 4-7 wt.%, neodymium 13-20 wt.%, availability was significantly greater than for samarium. However, cerium levels must be reduced in mischmetal, as cerium in $MMCo_5$ lowers the curie temperature.

At Crucible Materials Corporation, Kalathur Narasimhan, the author of this article, and his team developed a tailored mischmetal with a reduced cerium content through the electrolysis of mixed rare earth chlorides [5]. The tailored MM magnets were processed to 15 MGOe (119 kJ/m^3). This was acceptable to General Motors for a variety of automotive applications.

However, just when GM was ready to launch rare earth magnets in the automotive sector in late 1970, cobalt prices increased twenty-fold, and supply of cobalt from Zaire was becoming restricted. GM therefore wanted cobalt-free magnets. As always, inconvenience was the mother of invention, and cobalt-free magnet development was initiated by the US Naval Research Laboratory in late 1970. Kollomorgen Corporation's George Hadjipanayis, Kalathur Narasimhan of Crucible Materials Corporation, Norman Koon of the Naval Research Laboratory, Professor Hans Staudenmaier of NC State University, C D Graham of the University of Pennsylvania and Prof. Lawless of the University of Virginia were all involved in developing cobalt-free magnets under Navy research grants.

New materials were identified that were cobalt-free [6]. At the same time, John Croat and others at GM Research were developing the melt spun process for cobalt-free magnets [7]. Sagawa of Sumitomo Electric Corporation was also active in this area, and announced that cobalt-free NdFeB could be processed by a conventional press and sinter approach to 38 MGOe (302 kJ/m^3), using a process similar to that developed for rare earth cobalt magnets [8]. In 1983, using a low oxygen process, Narasimhan processed NdFeB to 45-46 MGOe (358-366 kJ/m^3) [9], the highest energy product ever reported at that time. Commercial production was limited to about 38 MGOe (302 kJ/m^3). In the ensuing twenty years, ongoing development has resulted in commercial magnets that are now produced at up to 55 MGOe (438 kJ/m^3).

The permanent magnet market

The permanent magnet market is growing at a significant pace, mainly driven by a rise in the demand for rare earth permanent magnets. Rare earth magnets are replacing the majority of alnico magnets and, to a large extent, ferrites, due to the higher energy products of this material. Table 2 compares ferrite magnets with alnico and neodymium magnets in speaker applications. As is clear, miniaturisation of devices can be made possible using powerful neodymium magnets, as was exemplified in the success of earlier Sony Walkman-type devices, earphones and hearing aids. Further applications for permanent magnets can be seen in Table 3, and a selection of automotive examples can be seen in Fig. 4 and Table 4.

The sales volume of ferrite magnets is around 80% of permanent

Unit properties	Ferrite	Alnico	Neodymium-iron
Br (Gauss)	3950 (0.39 T)	12700 (1.27 T)	14200 (1.42 T)
H_c (Oe)	2400 (191 kA/m)	640 (50.9 kA/m)	12500 (994.7 kA/m)
H_{ci} (Oe)	2450 (195 kA/m)	645 (51.3 kA/m)	17000 (1352.8 kA/m)
B_d (Gauss)	2700 (0.27 T)	10400 (1.04 T)	7000 (0.7 T)
H_d (Oe)	1150 (91.73 kA/m)	530 (42.2 kA/m)	7000 (557 kA/m)
B_dxH_d (MGOe)	3.6 (28.62 kJ/m^3)	5.5 (43.8 kJ/m^3)	49.0 (389.9 kJ/m^3)
Density (g/cm^3)	4.9	7.3	7.4
Magnet length	1	1150/530 = 2.17	1150/7000 = 0.16
Cross sectional area	1	2700/10400 = 0.26	2700/7000 = 0.38
Volume	1 x 1 = 1	0.56 of Ferrite	0.0608 (94% less than ferrite)
Weight	1 x 4.9 = 4.9	4.08	0.44 (89% less than ferrite)

Table 2 This comparison of the properties of ferrite, alnico and neodymium magnets in speaker applications clearly demonstrates the advantages of rare earth magnets in applications such as earphones

Device	Type
Motors: Industrial, automotive and consumer products	Constant speed drives, traction, fractional horsepower servo motors, robotics, machine tool axes and spindles, material handling, aerospace actuators, hand tools, antenna tracking, transport accessories, starters, stepper motor, cell phone vibration motors
Audio frequency transducers	Speakers, microphones
MMR tomography (MRI)	Full body stationary, portable units
Bearings	Pumps, flywheels, space craft stabilisation, anti-vibration mountings
Separation	Magnetic separation units
Microwave	Travelling wave tubes, telecommunication
Computers	Disk Drive motors, Spindle motors, printer motors
Wind power	Direct drive motors, energy storage systems
Military	Weapons guidance systems, robots, rail guns,
Switches	Electromagnetic relays, circuit breakers

Table 3 Typical applications of permanent magnets

magnet usage and in revenue terms around 20%. The total market for permanent magnets was reported to be $18 billion in 2015, with neodymium magnets sales of $12 billion. It is anticipated that, by 2025, sales of neodymium magnets alone will reach $17 billion.

The projected growth of both rare earth cobalt and neodymium-iron-boron magnet usage for the foreseeable future is expected to be around 5-6% compounded, with neodymium magnets dominating the growth. The major factors responsible for the growth are the increased demand for energy efficiency, miniaturisation, electric vehicles and the growing need for electromagnetic actuation in place of mechanical.

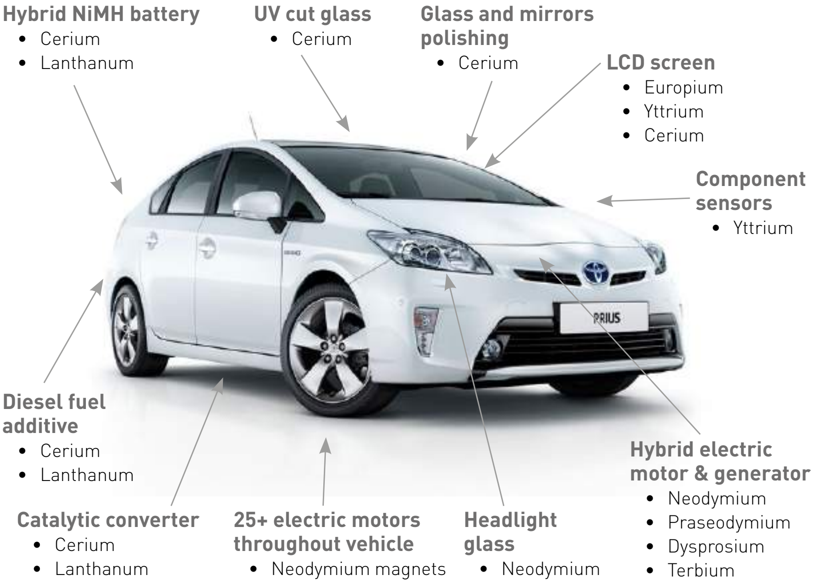

Fig. 4 Rare earth usage in a typical hybrid vehicle. Electric and hybrid cars can contain more than twice as much rare earth metal as a standard car

Manufacturing process for magnets

A typical hysteresis loop for permanent magnets is shown in Fig. 5. The energy product (B_d x H_d) defines the volume of the magnet necessary to provide flux in an operating device. In order to manufacture rare earth magnets, a powder metallurgical process is employed. The concept is to produce close to single domain particles, which can subsequently be oriented in a magnetic field, compacted and sintered.

Magnet use in automotive applications		
Door lock actuator	Brake assist	Oil pump
Window lift motor	Transmission control	Air conditioner
Mirror tilt motor	Anti-lock brakes	Electric braking
Starter motor	Suspension	Differential control
Radiator fan	Fuel pump	Wiper motor
Cruise control actuator	Seat recline	Entertainment
Air pump actuator	Seat supports	Sunroof
Steering control motor	Heater blower	Traction motor
Water pump motor		

Table 4 Examples of magnet usage in automobiles

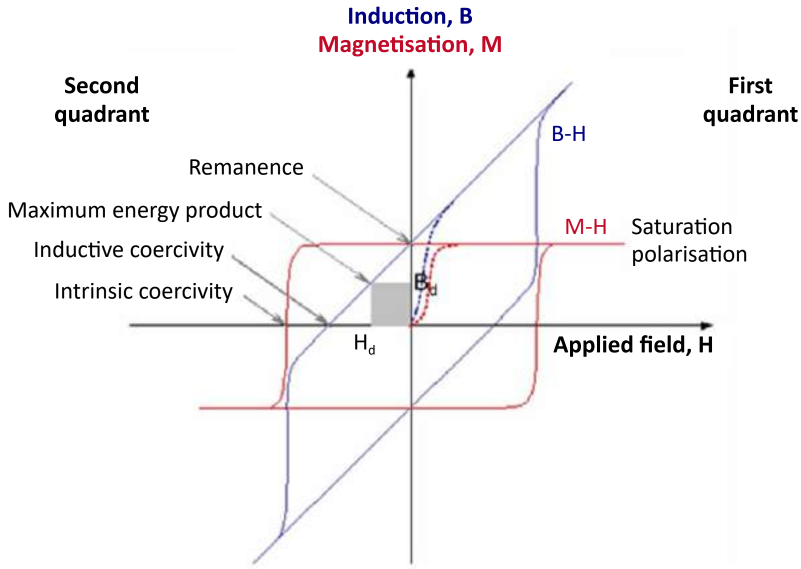

Fig. 5 Typical hysteresis loop for permanent magnets. MvsH loop shows the intrinsic properties and BvsH loop is used by application engineers

Casting
Raw materials, Nd, Fe, B (mostly as ferroboron) are melted in an inert atmosphere in an induction furnace and cast on to a chill plate or atomised with argon (Fig. 6). Care should be taken, as the fines generated in the process can ignite. In the case of neodymium iron boron, it can also be rapidly solidified to form amorphous flakes. These are nano-sized grains and can be used by crushing and mixing with polymer to make bonded magnets with an energy product of 6-12 MGOe. They can also be hot formed to obtain very high energy products, up to 32 MGOe, by the magnaquench process.

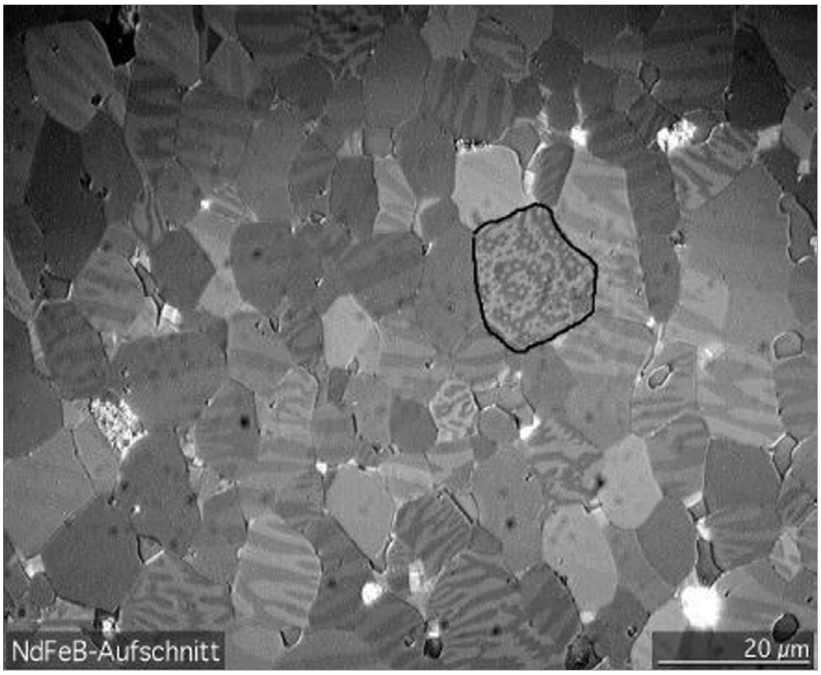

Fig. 6 Multi-domain cast NdFeB alloy. The domains are visualised using the Magneto Optic Kerr effect

Production of single domain particles
The press and sinter permanent magnet processing route requires the cast alloy to be crushed and ground to close to single domain size. The single domain diameter of NdFeB is 0.2-0.6 µm, $SmCo_5$ is 0.8 µm and Sm_2Co_{17} is 0.5 µm. At this size it is very difficult to handle the powder as it is extremely pyrophoric, so instead the cast alloy (Fig. 6) is crushed and jet milled to around 2-3 µm grain size with a few domains (Fig. 7).

Compaction
The crushed powder is then compacted in a die under a magnetic field, which allows each of the grains to orient towards the magnetic field to maximise induction (Fig. 8).

Sintering
The green compact is sintered in vacuum at a temperature of 1040-1160°C, depending on the composition of the alloy. Often, it is customary to mix rare earth lean alloy with rare earth rich alloy to achieve the correct stoichiometry of $Nd_2Fe_{14}B$.

After sintering, an ageing step at about 900°C is included. Ageing allows the formation of the grain boundary rare earth rich phase, which helps to control the coercivity of the magnet

Finishing and magnetisation
To meet dimensional tolerances, magnets are often machined or ground to the final shape. It is also essential in the case of NdFeB that they are coated to prevent corrosion and Ni, Ni-Cu-Ni or polymer coatings are usually employed.

When magnets are first produced they are generally not magnetic, and need to be magnetised in order to reach the required properties. For a number of reasons, it is often preferable to magnetise the magnets in the final assembly of the product or device. Magnets can be extremely powerful and careful handling is necessary to avoid chipping them or injuring operators. Special magnetising fixtures are required to magnetise them and a pulse field of 60 KOe is generally applied.

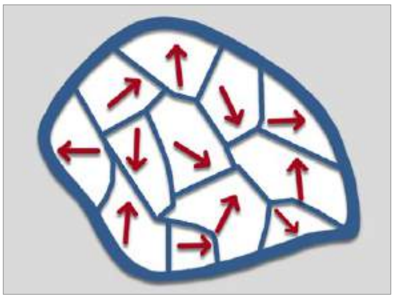

Fig. 7 Domain structure in a single grain of crushed powder

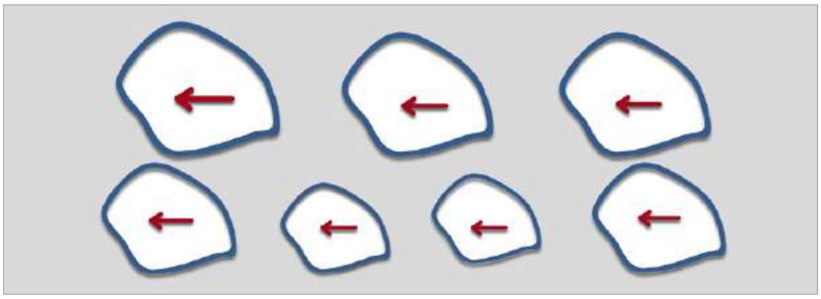

Fig. 8 Orientation of grains before compaction

Magnetising of magnets before assembly is also possible and depends on the final application, however care must be taken when transporting or handling. $SmCo_5$ and 2:17 magnets are made in a similar way as above.

Low oxygen process

In this process the entire crushing, milling and compaction stages are carried out under an inert atmosphere. Pressed compacts are transferred in a closed container that attaches to the sintering furnace. The highest energy products, as well as highly stable magnets, can be made by this process, which the author developed at Crucible Materials Corporation with a US Airforce grant.

Global supply of rare earth magnets

Although developed in the USA and Japan, the supply chain for rare earth magnets began shifting towards China in early 2000. According to the United States Congressional Research Service, China now produces 97% of rare earth ores, 97% of rare earth oxides, 89% of rare earth alloys, 75% of neodymium iron boron magnets and 60% of samarium cobalt magnets (Fig. 9).

The supply chain consists of mining, separation, refining, alloying and manufacturing devices and magnets. With an abundance of rare earths, China can control raw material prices at will and, in recent years, has implemented a quota on their export. This dominance is a cause for concern for many governments and the numerous industries that rely on a steady supply of these materials.

Extensive research is now underway to mitigate raw material supply issues. Discussed below are some of the current activities in the development of new magnets as well as work to reduce the amount of rare earth used in magnets.

Alternatives to reduce rare earth usage

Magnetic materials useful for the permanent magnet industry are shown in Table 5. This table also lists the origin of coercive force in these magnetic materials which may provide a clue to finding newer materials. Generally, higher anisotropy is seen in non-cubic systems. However, cubic systems such as alnicos, which exhibit shape anisotropy, may offer some possibilities.

Fe, Co, Ni and Mn are critical elements for magnets. Listed in Table 6 are magnetic moments of these and the rare-earth elements. Rare earth elements (R) can be combined with cobalt to form RCo_5 and R_2Co_{17} intermetallics. Light rare earths containing RCo_5 achieve very good magnetic properties, except for $NdCo_5$. The heavy rare earths (Gd and above) magnetic moments couple anti-parallel with cobalt moments and reduce the maximum induction that can be achieved. RCo_5 has a $CaCu_5$ crystal

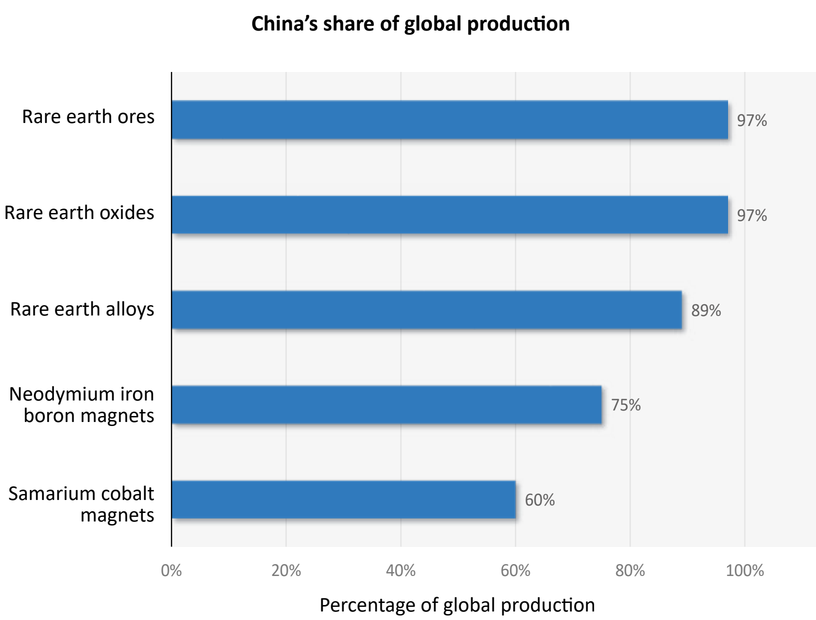

Fig. 9 China's share of global rare earth production and magnet manufacture (Rare Earth Elements in National Defense: Background, Oversight Issues, and Options for Congress; USA ; Congressional Research Service, December 2013)

Coercive force origin	Alloy	B_R Tesla	H_C kA/m	$(BH)_{max}$ kJ/ m³	Theoretical $(BH)_{max}$ kJ/m³
Superstructure alloys	Pt-Fe	0.58	124.8	23.8	
	Pt-Ni	Low Curie temp			
	Pt-Co	0.64	397.5	75.6	
Crystalline anisotropy metallic magnets	Mn-Bi	0.43	270	34.18	118
	Mn-Al	0.572	139	28.6	75.5
	Mn-Al-C	0.52 - 0.62	159 - 206	45.3	127
	$Re\text{-}Co_5$	0.88 - 0.94	700 - 715	151 - 175	238
	$Re\text{-}Co_5$ (Low Oxygen Process)	1.00 - 1.06	715 - 795	199 - 223	238 - 222
	$Re_2\text{-}Co_{17}$	1.04 - 1.12	763 - 779	215 - 262	286 - 477
	Nd-Fe-B	1.07 - 1.47	795 - 922	207 - 422	508
Crystalline anisotropy ceramic magnets	Barium Ferrite	0.38 - 0.40	159 - 318	27 - 30.2	44.5
	Strontium Ferrite	0.41 - 0.43	230 - 198	31.8 - 33.3	44.5
Exchange anisotropy magnets	Co-CoO	Low temp			
	Fe-Co Ferrite	0.62	124	32	56
Steels	Fe-W-C	0.9	20	7.55	
Precipitation alloys; shape anisotropy	AlNiCo Fe-Al-Ni-Co	1.05	48	71	
	Fe-Al-Ni-Co-Ti-Cb-Cu	1.35	59	69	
Cold deformation alloys	Fe-Co-V	1.10	24	13.5	

Table 5 Magnetic properties and the origin of coercive force in well-known permanent magnets [10]

Element	3d /4f electrons	Magnetic moment µB/ atom	Element	3d /4f electrons	Magnetic moment µB/ atom
Mn	5 (3d)	3.6	Sm	5 (4f)	0.85
Fe	6 (3d)	2.6	Gd	7 (4f)	7.94
Co	7 (3d)	1.6	Tb	8 (4f)	9.72
Ni	8 (3d)	0.6	Dy	9 (4f)	10.65
La	0 (4f)	0	Ho	10 (4f)	10.6
Ce	1 (4f)	2.54	Er	11 (4f)	9.58
Pr	2 (4f)	3.58	Tm	12 (4f)	7.56
Nd	3 (4f)	3.62	Yb	13 (4f)	4.54

Table 6 Magnetic moments of common magnetic elements

structure, shown in Fig. 10. Cobalt in hexagonal array has rare earth in the middle. In the case of $SmCo_5$, Sm provides an enhanced crystalline electric field to force the magnetic moments to the easy axis of the magnetisation c-axis, $SmCo_5$ has an anisotropy field of 350 kOe (anisotropy field is the field required to saturate the magnetic material in the hard direction, a measure of how much coercive force can be generated). The hexagonal array of cobalt, by itself, provides the anistropy, as evidenced by the high anistropy field seen in YCo_5 of about 129 KOe [2]. Yttrium is a non-magnetic element, so the anistropy field seen in YCo_5 is mainly from the cobalt sublattice. Exploring other materials that could place cobalt atoms in a similar configuration will be useful.

Nanomagnetic material development

A number of researchers are developing rare earth-free or reduced-rare earth systems using nanocomposite technologies. Research at the University of Delaware by Hadjipanyis's group, Sellmeyer at the University of Nebraska, Iver Anderson's group at the Ames laboratory and others are exploring nanotechnologies to find alternative material systems.

Two areas have been the centre of focus: exchange-coupled spring magnets [12] and exchange-biased magnets (discussed later). The idea behind exchange-coupled spring magnets is to use a non-rare earth soft magnetic phase with a high saturation magnetisation exchange couple with high anisotropy rare earth magnetic phase, resulting in higher saturation and a reasonable coercive force. This would reduce the amount of rare earth in the final magnet.

An excellent review of nanocomposite magnets is given by Lewis and Villacorte [12]. Simply mixing a high saturation induction soft ferromagnetic phase with a hard magnetic phase will result in a hysteresis loop such as in Fig. 11. However, if the soft magnetic phase is of a size less than or equal to twice the domain wall width of the hard phase, exchange coupling takes place and the hysteresis loop will be square and produce a useful permanent magnet, Fig. 12. Increased induction from the soft phase will result in higher energy product magnets. These are sandwich structures with a bulk high anisotropy ferromagnet (HAF) with a nanophase coating of soft ferromagnetic phase (SF).

In exchange-coupled nanocomposite magnetic materials, the nano soft magnetic phase size must be less than twice the domain wall thickness of the hard magnetic phase [13, 14]. This will prevent the formation of reversed domains in the soft magnetic phase and maintain the high coercivity of the hard magnetic phase. Domain wall thicknesses in NdFeB, $SmCo_5$ and Sm_2Co_{17} are 5.2 nanometres, 5.1 nanometres and

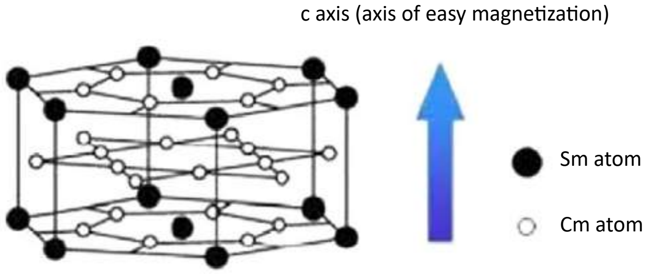

Fig. 10 Searching for similar hexagonal array of cobalt atoms in intermetallic compound will be a worthwhile effort

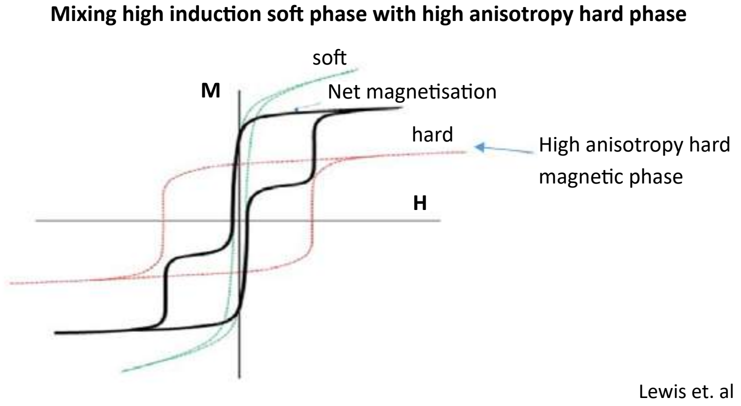

Fig. 11 Mixing of soft phase with hard magnetic phase will produce net magnetisation that is not useful for permanent magnet applications [12]

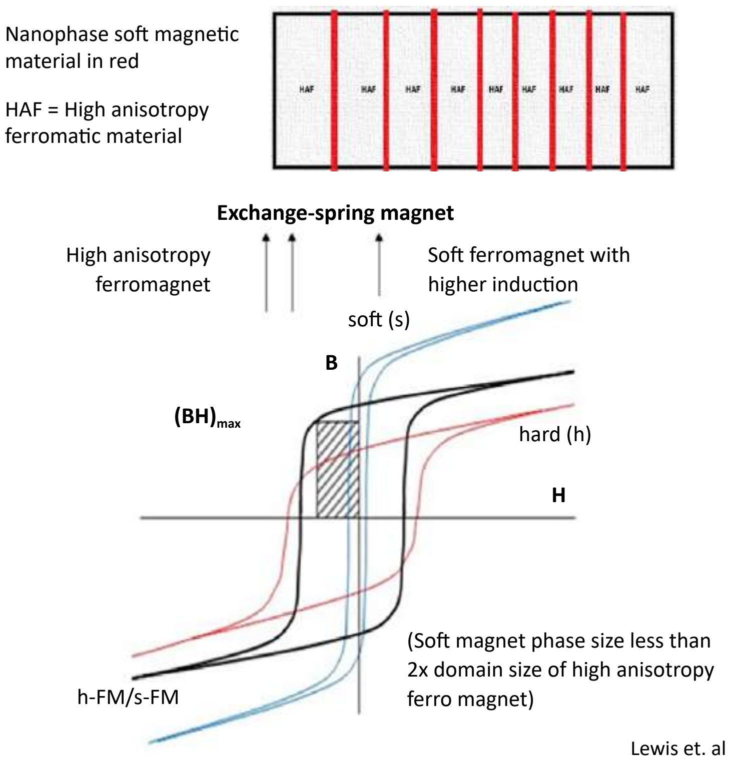

Fig. 12 Exchange scheme in spring magnet coupling at the interface of soft magnet with high saturation magnetisation and high anisotropy ferromagnet [12]

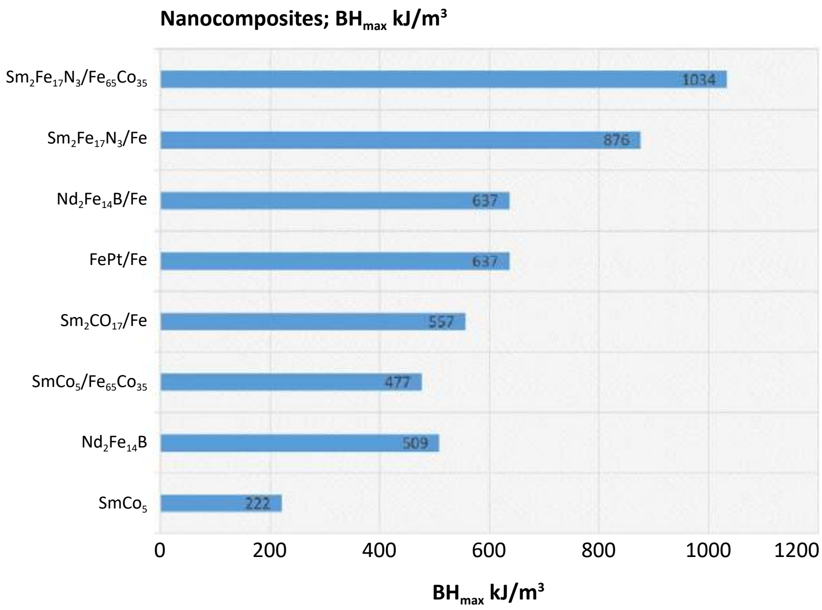

Fig. 13 Nanocomposite sandwiched theoretical magnetic performance

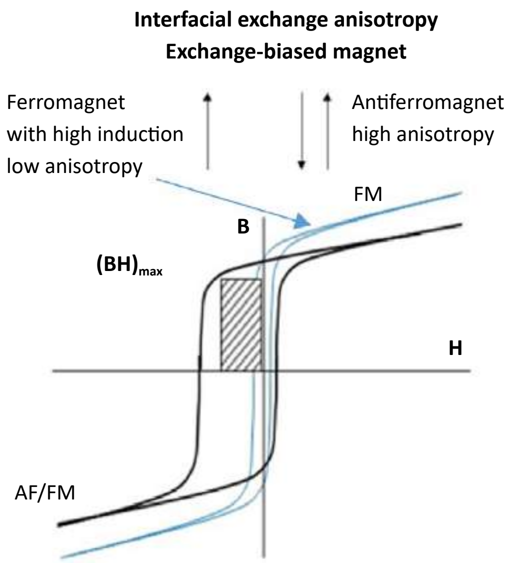

Fig. 14 Exchange-biased magnets scheme [12]

10 nanometres respectively [12]. Nano soft phase must be less than double this domain wall thickness for them to be effective.

Successful fabrication of an exchange-coupled spring permanent magnet with an energy product of 20 MGOe was achieved in the nano-composite equiatomic FePt and Fe_3Pt nanoparticles, a promising result for future research in this area [15].

Shota *et al.* report that $Fe_{40}Co_{22}Pt_{38}$ thin film magnets of 20 nanometres had an intrinsic coercive force of 2.5 T, a saturation magnetisation of 1. 78 T and an energy product of 510 kJ/ m^3 (64 MGOe) [16]; Neu *et al.* report SmCo/Fe sandwich layers produced 39 MGoe (310 kJ/m^3) [17] in a research project supported and managed by the Air Force Research Laboratory and Office of Naval Research, funded by the Defense Advanced Research Projects Agency, at the University of Dayton [18], suggest that rare earth usage can be reduced using nanocomposite Nd-Fe-B magnets. They report that the rare earth content in the nano-composite magnets can be 15-50 at% lower than that in conventional melt-spun and sintered Nd-Fe-B magnets. The new magnets which are nanocomposites of NdFeB/α Fe will have lower cost, higher magnetic performance and better corrosion resistance, because of the significantly reduced rare earth content. The new magnets will also have improved fracture toughness because of the fine nano-grain structure and the existence of a relatively soft α-Fe phase. If α-Co Fe with higher saturation induction is used, $Nd_2Fe_{14}B$/α CoFe nanocom-posites with a Br of 1.4-1.6 T and coercivity of 1.0-1.8 T and energy product of 320-480 kJ/m^3 can be achieved [19].

Work at the University of Nebraska, Lincoln, USA, by Balasu-bramanian *et al.* is interesting, developing 20 MGOe in ZrCo mate-rials [20].

Since Fe-Co alloys have a maximum saturation induction at 35% cobalt, nanocomposites made with $Fe_{65}Co_{35}$ tend to have a high energy product. Ajay Misra reported theoretical energy products in Nano sandwiches shown in Fig. 13 [21].

The problem remains in making practical usable magnets out of these nanocomposites. A number of possibilities are being explored.

Exchange-biased Magnets

In this case, if an antiferromagnet with high anisotropy is coupled with a higher saturation magnetisation soft phase, then the anisotropy of the antiferromagnet prevents the rotation of magnetic moment in the soft phase, resulting in a good permanent magnet. Meiklejohn and Bean demonstrated this in the mid-1950s, when the effect was called interfacial exchange anisotropy [22, 23]. A schematic of the exchange-biased magnet is shown in Fig. 14.

A possibility exists to exploit this exchange-biased coupling scheme in alnicos. Alnico magnets have been the workhorse for magnet applications, along with ferrite magnets, up until the advent of rare earth magnets. Alnico magnets are nano-scale composite magnets. The

Fe Al Co undergoes spinodal decomposition at about 850°C into two BCC phases, ferromagnetic Fe-Co phase and the weakly magnetic NiAl phase. Fe-Co particles are ellipsoidal (Fig. 15) and of single domain nano-size, giving the coercive force from shape anisotropy. If the matrix phase in alnico (NiAl) is replaced with an antiferromagnetic phase with high anisotropy, the interface of ferromgantic phase and the antiferromagnetic phase could make interfacial exchange-coupled permanent magnets with enhanced coercive force. The advantage of alnico magnets is the ease of processing, which consists mainly of casting and heat treating. However, much further research in this area is necessary.

Fig. 15 Spinodal decomposition in a magnetic field in alnico showing Fe-Co BCC elongated single domain particles, magnification 50000X [23]

Other magnetic materials

MnBi has good magneto-crystalline anisotropy, with an anisotropy constant of 1.6×10^6 J/m^3 [24, 25], and a saturation induction of 0.84 T and coercivity that increases with increasing temperature and reaches nearly 26 KOe at 250°C, making it useful in motors that operate at about 150°C. If a nanomagnetic soft phase is embedded in a MnBi matrix, it should be possible to increase induction. Research in these areas is reported to be ongoing.

In the iron-nitrogen system $Fe_{16}N_2$ is claimed to have an energy product three times that of Nd-Fe-B magnets. Saturation induction is claimed to be about 2.4-3.4 T [26] and such a value would be the highest reported. The difficulty is that this phase, which is tetragonal, is difficult to produce due to a narrow range of stability. Further addition of other alloying elements to stabilise the structure would be a worthwhile effort and research continues in this area.

Looking to the future

It is highly unlikely that we will stop making or using rare earth magnets, as rare earths are important for many industries besides the magnet industry. The challenge is that separation plants for extracting rare earths from ores are expensive. Many of the attempts have been for achieving economies of scale by building huge extraction plants for separation of rare earths. Of course, these scale economies may not be relevant when a guaranteed supply of rare earths is seen as a case of national security. Many small-scale industries, setting up extraction plants, may actually be a better economic model.

The development of new extraction methods should also be encouraged. Since the rare earth elements are chemically similar, separation of individual elements is a tedious process. Innovation in this area would be useful.

Research into the use of combinations of rare earths, for example mischmetal-Fe-B, didymium (Nd, Pr)-Fe-B, some of which do not favour an easy axis of magnetisation currently, should be explored. This would reduce the cost of separation of the individual elements.

Research into developing materials that will generate cobalt in a hexagonal symmetry, such as $SmCo_5$, should be explored.

The iron-nitrogen system needs to be developed further by involving material scientists to explore advanced solidification techniques and other methods of alloying nitrogen with iron. Ternary systems may provide ease of forming the difficult phase $Fe_{16}N_2$.

Alnico-type magnets also need to be revisited, with a focus on increasing the magnetic moment from the Fe-Co phase and exploiting exchange coupling between Fe-Co and antiferromagnetic matrix phase. MnBi offers a good opportunity for developing exchange-coupled magnets with soft nanomagnetic phase.

In general, material scientists should be encouraged to participate with physicists, who are driving the exploration of new opportunities.

Author

Dr Kalathur 'Sim' Narasimhan
P2P Technologies
GKN Engineering Fellow; FASM; FAPMI; FIPMI: IEEE Senior member

Email: Sim.Narasimhan@outlook.com

References

[1] Wallace W E, Rare earth Intermetallic, Academic Press (1973)
[2] Hoffer G and Strnat K, IEEE Transactions on Magnetics, MAG-21966,487; Strnat K, Hoffer G,

Olson J, Ostertag W, and Becker J J, *Journal of Applied Physics* 1967; 38, 1001

[3] Benz, M G, LaForce R P and Martin, D L, A. I. P. Conf Proceedings 18,1173,1974

[4] Narasimhan, K S V L, Fifth International workshop on rare earth cobalt permanent magnets and their applications, Roanoke, VA, (1981)

[5] Wells M G H and Narasimhan K S V L, *Goldschmidt informiert* 2/79/ Nr48.P15

[6] Hadjipanayis G C, Cornelison S G, Sellmeyer D J, Magn J, *Mat 21*,101, (1980); Hadjipanayis G C, Wollins S H, Hazelton R and Lawless K R, *Journal of Applied Physics* 55, 2073, (1984)

[7] Croat J J, Herbst J F, Lee R W, Pinkerton F E; *Applied Physics* lett. 44,148,1984: *Journal of Applied Physics* ;55,2078,1984

[8] Sagawa M, Fujimura S, Yamamoto H, Matsuura Y and Hiraga K, *IEEE Trans. Magn.* 1984; 20, 1584

[9] Narasimhan K S V L, MMPA Conference Atlanta, Jan 1984; *Journal of Applied Physics* 57, 4085, 1985.

[10] Narasimhan K S V L, NdFeB and other permanent magnets, Soft and Hard Magnetic materials Symposium, ASM Materials Week, October 1986, edited by Salsgiver J A, Narasimhan K S V L, Rastogi P K, ASM article 8617-012.

[11] Rare earth sources globally. Gambogi J, USGS (United States Geological Survey) *Minerals Yearbook* 2011, Volume 1.

[12] Lewis L H and Jiménez-Villacorta F, *Metall. Mater. Trans.* A 2013; 44 (Suppl.) 2-20; Advanced Permanent Magnetic Materials; Chapter 7, Nano Magnetism 2014; central press

[13] Skomski R and Coey J M D, *Phys. Rev.* B 1993; 48, 15812–15816

[14] Skomski R, Manchanda P, Kumar B, Balamurugan A, Kashyap and Sellmyer D J, *IEEE Trans.Magnetics*, Vol 49, No7, July2013

[15] Zeng H, Li J, Liu J P, Wang Z L and Sun S, Nature 2002; 420, 395

[16] Shota P K, Liu, R.skomski Y, Manchanda P, Zhang R, Fangohr H, Franchin M, Hadjipnayis G, Kashyap A and Sellmeyer, *Journal of Applied Physics* , Vol 111, PP07E345-1-3,2012

[17] Neu V, Sawatzki, S Kopte, M Mickel, C and Schultz L; *IEEE Trans. Magn.* Vol 48, No11, PP3599-3602, Nov 2012

[18] University of Dayton research institute (UDRI) bulletin

[19] McCallum R W, Lewis L H, Skomski R, Kramer M J and Anderson I E, *Ann. Rev. Mater. Res.* 2014; 44, 10.1-10-27.

[20] Balasubramanian B, Das B, Skomski R., Zhang W Y and Sellmeyer D J, *Adv. Mater.* 2013; 25, 6090

[21] Misra A, 8th Annual CAFÉ Electric aircraft symposium; April 25-26, Santa Rosa, California, 2014.

[22] Meiklejohn W H and Bean C P, New Magnetic Anisotropy, *Phys. Rev.* 1956; 102, 1413.

[23] Meiklejohn W H and Bean C P, New Magnetic Anisotropy" *Phys. Rev.* 1957; 105, 904.

[24] De Vos K J, Alnico permanent magnet alloy, *Magnetism and Metallurgy*, Academic Press 1969; Vol 1., pp473-512

[25] Cui W-B, Takahashi Y K, Hono K, *Adv. Mater.* 2012; 24. 6530

[26] Williams H J, Sherwood R C and Boothby O L, *Journal of Applied Physics* 28 (1957) 445-447. 19

[27] Cui J, Choi J P, Li G, Polikarpov E, *Journal of Applied Physics* (2014) 115(17)

[28] Wang, Jian-Ping; Ji, Nian; Liu, Xiaoqi; Xu, Yunhao; Sanchez-Hanke, C, Origin of giant magnetization in $Fe_{16}N_2$ thin films, American Physical society , APS March meeting 2010, March 15-19,2010, Abstract #T33.003

Optimising iron-based PM self-lubricating bearings: The influence of graphite

Sintered self-lubricating bearings are typically made from bronze alloys, however, for less demanding applications, iron-copper combinations offer a low-cost alternative. As a relatively high level of final porosity is required, a careful design of base powders and processing is necessary to achieve desirable properties in both the green and sintered states. In this experimental study, Matteo Zanon of Pometon SpA presents existing and newly developed iron-copper PM solutions to address issues arising from the addition of graphite, with a special focus on the influence of natural graphite granulometry.

Porous sintered self-lubricating bearings are a classic product of the Powder Metallurgy industry, with widespread applications in the electrical motors of home appliances and many other machines [1]. Millions of these components are manufactured every year by cold pressing, sintering, sizing and oil impregnation (Fig. 1).

A typical material used for their production is bronze with 10% tin, which allows for optimal behaviour in terms of load-velocity combination (the so-called 'PV value'), but iron-copper and iron-bronze materials are also well established, cost-effective formulations [2]. The shaft-bearing tribological system can be best described by its Stribeck curve. When the shaft starts turning, direct contact between the two surfaces causes attrition and wear, since the rotation speed is insufficient to trigger hydrodynamic lubrication. As the shaft gathers speed, oil is drawn by capillary action towards the bearing-shaft interface. A stable lubricant film sets in between shaft and bearing, which prevents direct surface contact and renders friction coefficients as low as 0.03; an oil dispenser might also be implemented to extend the bearing's service life [1].

The main oil reservoir is the bearing's porosity, which is typically around 15-25%. This in turn affects the green strength requirements of the pressed powder; given that dimensional change is normally limited to below 1%, for both preci-

Fig. 1 Millions of porous self-lubricating bearings are manufactured each year by cold pressing, sintering, sizing and oil impregnation

$$K = \frac{F}{as^2}\,(D_{est} - S)$$

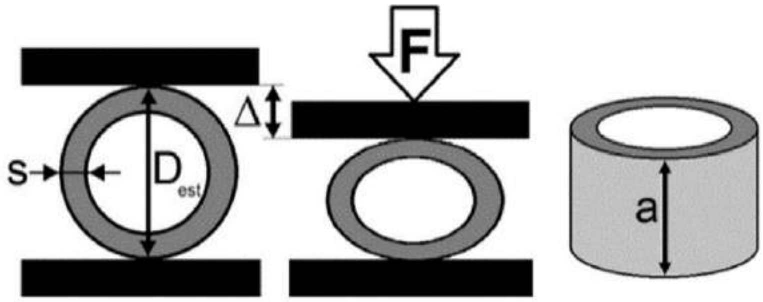

Fig. 2 Calculation of green (K_v) and sinter (K_s) radial crushing strength

sion and metallurgical reasons, this means a green density around 5.80–6.20 g/cm^3. The particles must then achieve a sufficient number of contact points in order to confer mechanical strength to the pressed component. This can be obtained by using irregular particles, which for iron-based materials typically means sponge iron. This type of iron powder, produced via a direct reduction of iron ore, has a highly irregular surface and internal particle porosity, which give very high green strength and also contribute to capillary oil flow. To the contrary, typical water atomised powder has more regular particle shape and a very low level of internal porosity and is thus generally considered suitable only if mixed with sponge iron.

Graphite additions are widely employed as a solid lubricant for the initial dry friction phase. Carbon dissolves easily in iron, with well-known hardening and strengthening effects. This means that less free graphite will remain available for lubrication, resulting in a higher mechanical strength but also higher wear on sizing dies. Carbon diffusion rate can be altered by choosing graphite type and granulometry, but interactions with sintering conditions and also the base material must be taken into account.

In this work, a full characterisation of the die-filling, compaction, mechanical and microstructural properties of sintered bearings is given. Newly developed water atomised powders are presented, along with sponge-based materials and standard water atomised powder as references. Composition and green density correspond to the widely used material DIN B 22. Three different graphite types were used in order to control the extent of carbon diffusion and to study its interaction with base powder properties.

Evaluation of iron-based premixes

Nine different iron-based premixes were prepared in the laboratory using three different types of industrially produced iron powders, combined with three different natural graphites. One base iron is a sponge grade 'Sponge I' normally employed for bearings; the other two are based on newly developed water atomised iron powders 'WA 1' [3] and traditional water atomised iron powder 'Fersint'. Copper was introduced into iron powder by a diffusion bonding process, at a level of 20 wt.%. After milling,1.80% medium-coarse natural graphite (D_{90} = 90 µm) and 0.80% amide wax were subsequently admixed and homogenized for 15 minutes in a Y-shaped rotating mixer. Apparent density and flow time were measured using a Hall flowmeter with a 2.5 mm hole (ISO 3923/1 and ISO 4490).

For the evaluation of green properties, TRS bars 30 x 12 x 6 mm were compacted at a constant pressure of 600 MPa and subsequently broken in a 3-point bending test (ISO 3995). Bushes with nominal 20 mm external and 15 mm internal diameters, 10 mm height were compacted at 6.00 ± 0.01 g/cm^3 density and crushed by applying a force along the radial direction. Radial crushing strength is then calculated by applying the following formula (ISO 2739) shown in Fig. 2.

For sintering tests, bushes with 14 mm external and 9 mm internal diameters, 10 mm height were compacted at a constant green density of 6.00 g/cm^3. Sintering was performed in a laboratory belt furnace at a temperature of 880/1020°C for 8 minutes, under a $80N_2$-$20H_2$ atmosphere and normal cooling conditions (cooling rate around 1.0°C/s calculated between 650 and 315°C). After sintering operations, dimensional change (D.C.) was calculated as the percentage variation of final sintered external diameter with respect to die diameter; radial sintered crushing strength was evaluated through the formula described in Fig. 2, while radial deformation "Δ%" was taken as the percentage ratio of radial deformation Δ to Dest. This parameter gives an indication of the maximum deformation that can be imposed during sizing; a higher value is desirable since it means that the material can accommodate larger radial deformation without failure.

	Graphite	Packing properties		TRS bars @ 600 MPa		Bushes @ 6.00 g/cm³
	D90 [µm]	Flow [s/50g]	App. Dens. [g/cm³]	Compressibility [g/cm³]	TRS [MPa]	K_v [MPa]
Sponge I	25	-	2.46	6.82	18.4	14.0
	90	38.0	2.47	6.81	20.1	14.6
	150	35.5	2.38	6.83	21.1	15.6
WA 1	25	-	2.49	6.90	19.3	11.4
	90	39.0	2.51	6.88	20.8	11.8
	150	34.0	2.45	6.90	21.4	13.5
Fersint	25	-	2.86	7.05	12.3	4.4
	90	36.5	2.86	7.03	13.3	4.5
	150	32.0	2.79	7.04	13.6	5.7

Table 1 Packing and green properties of experimental premixes FeCu20 + 1.80% graphite + 0.80% wax

Die filling, compressibility and sintering

Table 1 presents the results on the die-filling and green properties for each premix. The results for Sponge I and WA 1 are very close to each other, while Fersint, as expected, has the highest apparent density with slightly improved flow rate. The finest, 25 µm graphite grade renders the mixes to not be free flowing, while coarser grades markedly improve this important processing property. This is related to both the lower intrinsic flowability of fine powders and to their higher specific surface, which creates a more widespread rheological interaction with the base material.

Moving now to compressibility, we see that water atomised powders as a group outperform the sponge iron counterpart. The highest value is attained by Fersint, followed by WA 1. Graphite granulometry has almost negligible effects. Green strength at constant pressure is definitely lower for Fersint with respect to other products, which all feature similar values. Coarser graphites are slightly beneficial, by interposing among less iron particle contacts. In the manufacturing of bearings, K_v is a key parameter, being green density fixed during the pressing operation, typically around 5.80–6.20 g/cm³. A minimum value is required in order to be able to extract and handle the compacts between the pressing and sintering operations. There is no generally valid threshold value, which depends on wall thickness, component dimensions and manipulation process; it seems that a minimum of 3 MPa is demanded to provide acceptable consistency in industrial practice. Sponge I gives the highest values, followed by WA 1; Fersint performs rather poorly. A coarser graphite is definitely beneficial for this green strength measure, especially for water atomised powders (up to 30%). For sponge iron, it is slightly above 10%.

The sintered properties are shown against graphite type, for each base iron powder, in Figs. 3-8. Dimen-

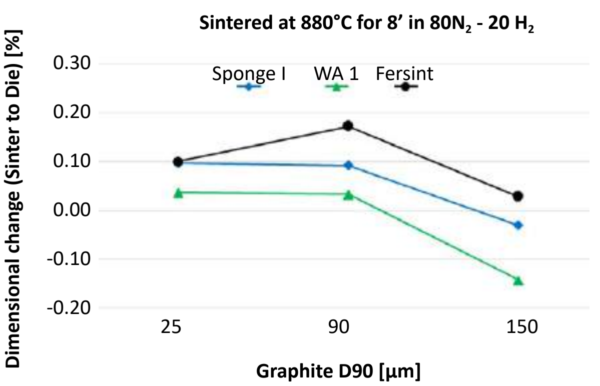

Fig. 3 Dimensional change against graphite granulometry for each iron powder after sintering at 880°C

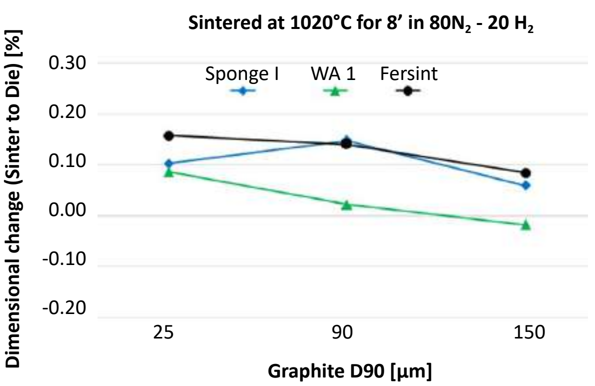

Fig. 4 Dimensional change against graphite granulometry for each iron powder after sintering at 1020°C

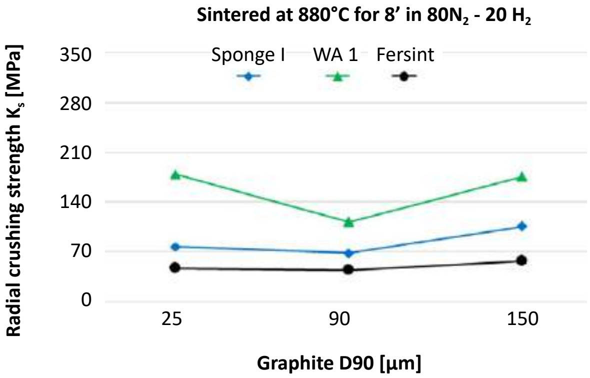

Fig. 5 Radial crushing strength factor K_s against graphite granulometry for each iron powder after sintering at 880°C

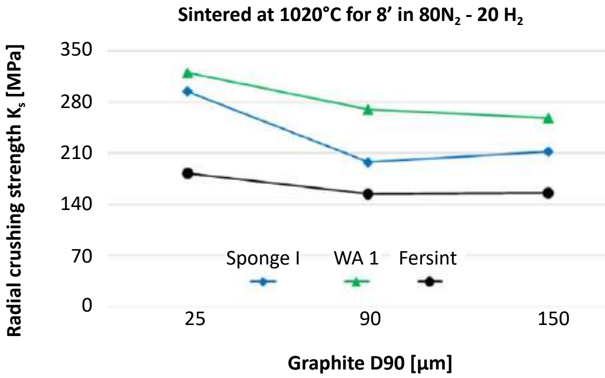

Fig. 6 Radial crushing strength factor K_s against graphite granulometry for each iron powder after sintering at 1020°C

sional change results depend first of all on the base powder, with WA 1 always showing the least growth – or even shrinkage. As documented in [4], for a given base powder, the dimensional behaviour in this temperature range is determined by the degree of carbon diffusion in the austenite phase. The introduced lattice distortion causes an expansion which more than compensates for the natural tendency to shrinkage driven by surface area reduction. Finer graphite granulometry favours deeper carbon diffusion and is thus generally related to higher growth. The 25 µm and 90 µm grades are not very dissimilar, while a noticeable effect is observed with the 150 µm grade at 880°C. Higher temperature enhances both carbon diffusion and surface-free energy reduction (i.e., shrinkage) and its net effect is on average very small, around 0.05% only. The graphite effect is muted, with less variation, especially when comparing the 150 µm grade to the other two. This also means that these materials are insensitive to temperature fluctuations, as far as dimensional properties are concerned.

The mechanical properties are displayed in Figs. 5 and 6. Radial crushing strength, as measured by the K_s factor, is at a maximum for WA 1, especially after 880°C sintering, when evaluated against the other materials. At higher sintering temperature, all mechanical properties increase substantially, being boosted by stronger particle neck formation and carbon microstructural strengthening.

Graphite particle size effect follows a complex pattern, depending on both sintering temperature and base powder. While, at 880°C, a coarser size favours K_s, up to 40% for Sponge I, the reverse is true at 1020°C, in particular for Sponge I (-30% variation). The combination 90 µm graphite – 880°C looks relatively unfavourable, especially for

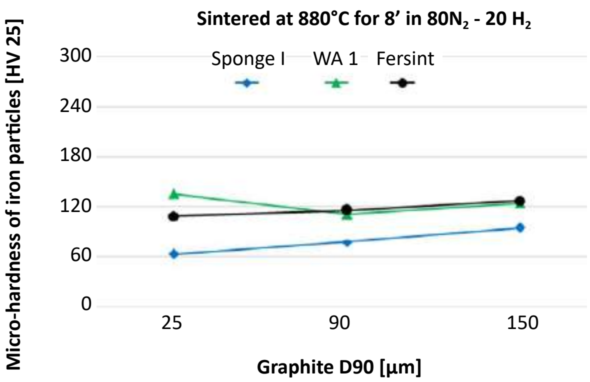

Fig. 7 Micro-hardness measurements against graphite granulometry for each iron powder after sintering at 880°C

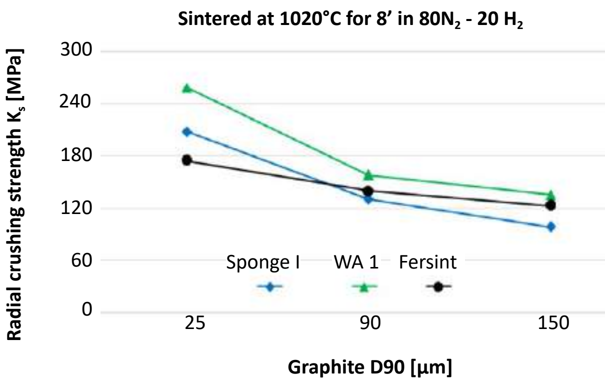

Fig. 8 Micro-hardness measurements against graphite granulometry for each iron powder after sintering at 1020°C

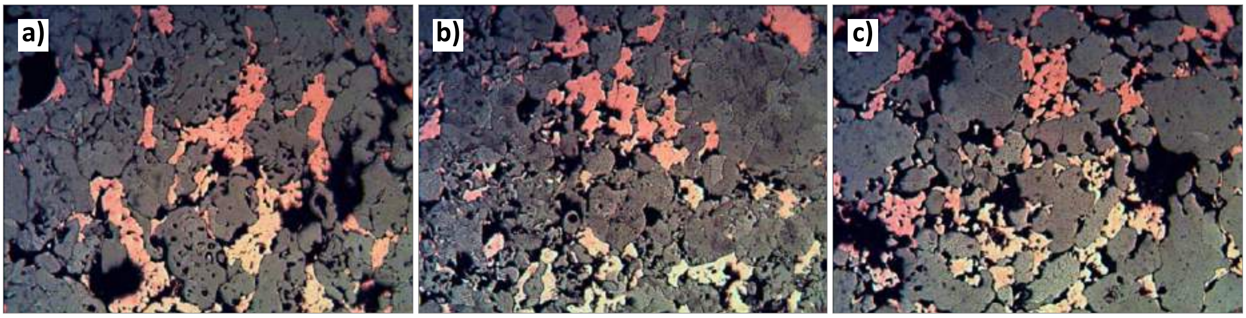

Fig. 9 Microstructures after sintering at 880°C with 25 µm graphite (Nital etched, 400X) a) Sponge I, b) WA 1, c) Fersint

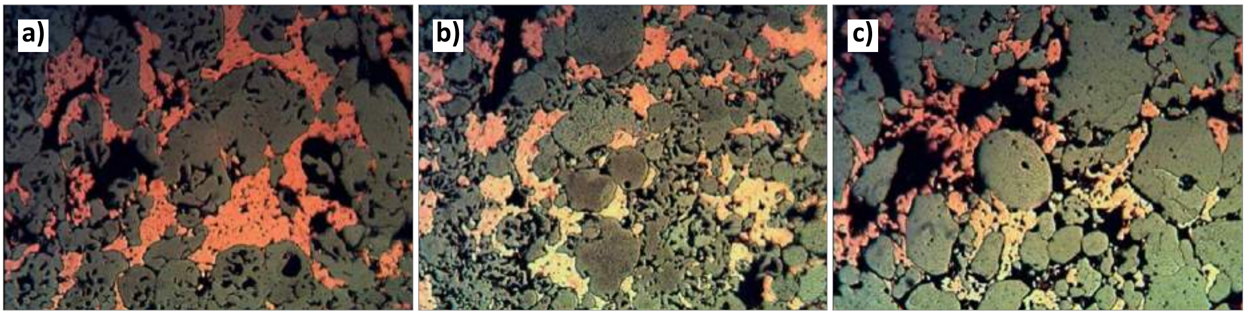

Fig. 10 Microstructures after sintering at 880°C with 150 µm graphite (Nital etched, 400X) a) Sponge I, b) WA 1, c) Fersint

WA 1; the result was confirmed by other experiments, but it is difficult to explain. Water atomised powders are less sensitive to graphite type in this respect.

A trend very similar to that for K_s is followed by radial deformation at fracture "Δ%", rising from an average of 1.4 % to 2.1 % with higher sintering temperature. WA 1 enjoys the best values, while Fersint falls last. This means that the new WA materials generally display higher strength and lower brittleness, which can be related to a higher sintering degree, as reflected by the lower dimensional change with respect to sponge-based materials.

Microscopic behaviour

A deeper understating of the macroscopic behaviour can be acquired by combining micro-hardness measurements with metallographic observations. Comparing Figs. 7 with Fig. 8, it is clear how higher sintering temperature translates into overall improved hardness, although such an increment is strongly related to graphite particle size. The finest grade shows an average increase of around 110 HV, the intermediate of 40 HV and the coarsest remains practically constant. This suggests that the 150 µm grade shows such little reactivity that its diffusion into iron does not change much over this temperature range. At 880°C, low hardness variation is observed with graphite, with a surprising slight increase for coarse particles; at 1020°C, a well-defined tendency can be appreciated, with the finest graphite associated with the highest hardness, as expected in view of its enhanced diffusivity into iron. It is thought that, as atomic carbon diffusion into austenite is still relatively slow at 880°C [4], the graphite particle size is not an important limiting factor. The hardness increase could be due to higher sintering degree, as implied by lower expansion/shrinkage with coarser graphite. At 1020°C, graphite particle size becomes the driver of carbon dissolution and thus hardness. Water atomised grades turn out generally harder than sponge powder, more so at lower sintering temperatures.

"At 1020°C graphite particle size becomes the driver of carbon dissolution and thus hardness..."

Microstructures confirm these comments. Figs. 9 and 10 show the results after low temperature sintering (880°C) for 8 minutes, for the finest and coarsest graphites. The same ferritic microstructure is displayed by iron particles in each material, with no significant difference whatsoever. Some pearlite traces can be seen for WA 1 and also Fersint, which account for the slightly higher hardness observed. Sponge iron particles feature their characteristic internal porosity, which is

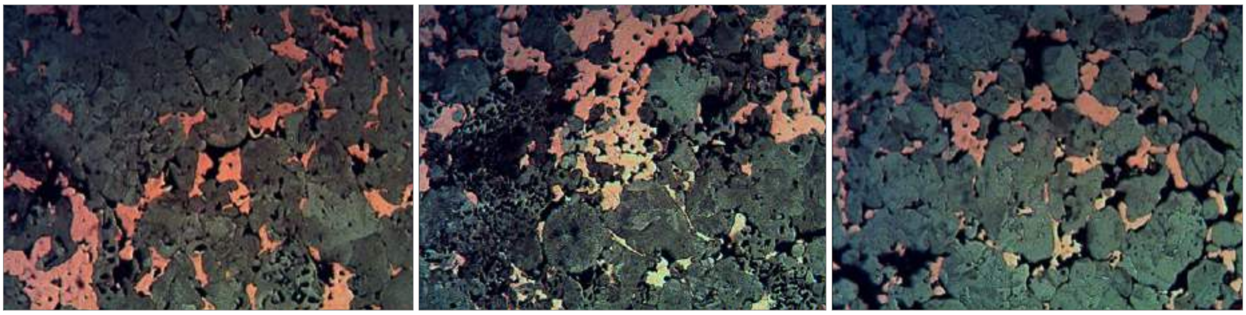

Fig. 11 Microstructures after sintering at 1020°C with 25 µm graphite (Nital etched, 400X) a) Sponge I, b) WA 1, c) Fersint

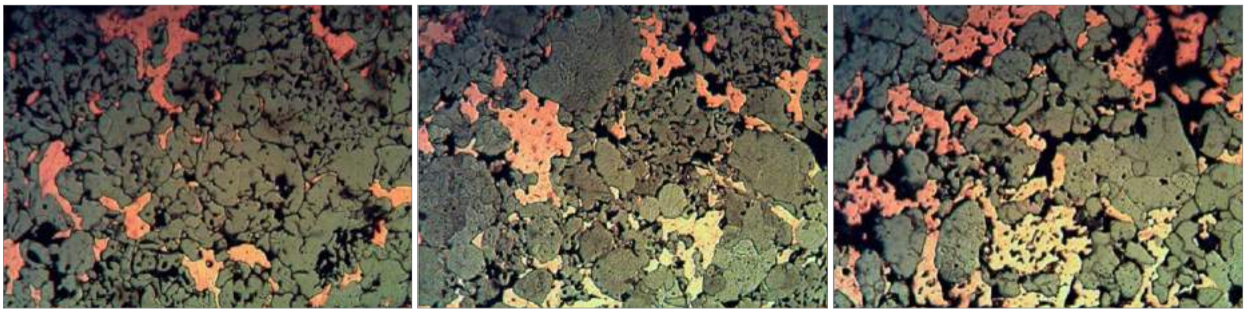

Fig. 12 Microstructures after sintering at 1020°C with 150 µm graphite (Nital etched, 400X) a) Sponge I, b) WA 1, c) Fersint

also present in WA 1, although with a somewhat different distribution. For Fersint, almost only solid particles are present.

Micro-macro relationships

Going to higher sintering temperature, the graphite effect on microstructure becomes evident. At 1020°C, carbon diffusion becomes much more active, with higher hardness and ferritic/pearlitic microstructures as consequences. With 25 µm graphite, extensive pearlite formation takes place in all materials, especially in WA 1. Ferrite instead largely prevails with the 150 µm grade, confirming that carbon diffusion is greatly limited when using such a coarse source. Once again, WA 1 presents the highest pearlite content and hardness. Sponge I looks instead almost 100% ferritic, with no change in hardness with respect to equivalent 880°C sintering.

On average, a systematic ≈ 40 HV increment is reported for WA 1 in comparison with Sponge I. Also Fersint is generally harder, although with one exception. The reasons for this behaviour are not totally clear. It is thought, however, that differences in the amount of silicon, an impurity typically present in sponge powder (around 0.60% in this case) and almost absent (<0.05%) in water atomised powder, could be the main factor. Silicon is well-known to substantially raise the chemical potential of carbon [5], thus reducing its gradient and slowing its diffusion, and to suppress cementite formation [6,7]. Other considerations on physical properties lack consistency when overall experimentation is considered [3].

A plot of radial crushing strength K_s against iron particle hardness for the two sintering conditions is shown in Figs. 13 and 14, with a line connecting the values referring to the same material. The contribution to mechanical properties of iron particle shape, carbon diffusion and neck formation can thus be deduced. K_s-HV slopes are in any case positive, giving a measure of the carbon strengthening effect. Sintering temperature increase confers, on each material, around +100 MPa at a fixed micro-hardness level, thanks to more extensive inter-particle connections. This is the single most important effect in numerical terms. At both temperatures, one can note that the low apparent density materials (Sponge I, WA 1) are positioned at a higher strength level than Fersint, given a fixed micro-hardness. In other words, for sponge and special grade WA 1, hardness can explain more or less their difference in K_s, while standard WA Fersint is intrinsically less resistant. It has been suggested [3] that low apparent density materials already enjoy a higher number of inter-particle contacts after pressing and these become further consolidated during sintering. For relatively low holding temperatures, that do not allow an extensive consolidation, it is logical to expect a strong influence of the green condition. The more rounded shape of Fersint, then, would account not only for a much lower green strength, but also for a K_s difference of around -50 MPa with respect to a low density iron powder with the same hardness.

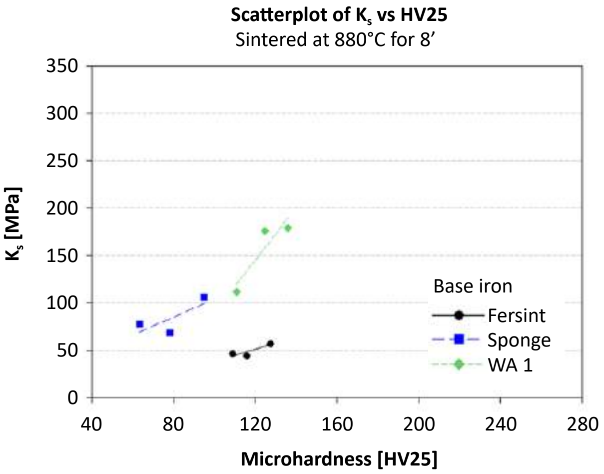

Fig. 13 Chart of K_s against iron micro-hardness K_v for the different materials - Sintering at 880°C

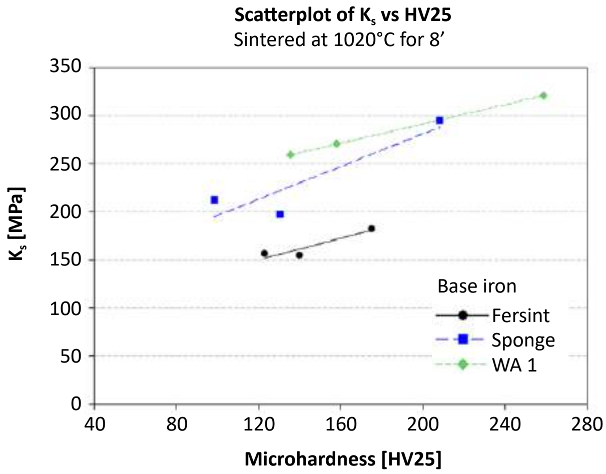

Fig. 14 Chart of K_s against iron micro-hardness K_v for the different materials - Sintering at 1020°C

Conclusions

The die-filling, green and sintered properties of both water atomised and sponge iron-based Fe-Cu premixes for porous bearings were analysed, taking into account their interaction with graphite particle size.

For optimal filling characteristics, a coarse graphite gives clear advantages. Even if apparent density is marginally higher, free-flowing behaviour cannot be achieved when the 25 µm graphite grade is admixed. This explains why fine grades are typically avoided for such mixes. It is notable how the special water atomised-based WA 1 can give an apparent density very close to sponge iron.

Water atomised grades offer better compressibility, while a trade-off exists with green strength. Graphite influence is, in this case, moderate or negligible

A rather complex, temperature-dependent relationship exists between the base iron and graphite granulometry. A coarser graphite will lead to less growth, especially at 880°C, with better dimensional precision. At this sintering temperature, it also yields better mechanical properties, while, at 1020°C, a finer graphite improves carbon dissolution and thus strength. The new WA 1 grade delivers a dimensional change close to 0%, the highest observed radial crushing strength K_s and deformation at failure Δ%.

Micro-hardness and microstructure analysis highlighted how the rate of carbon diffusion is controlled by the base iron, graphite granulometry and sintering temperature. While at low temperature the graphite particle size is of little relevance, at higher temperature it determines the depth of carbon diffusion and thus final hardness.

Different amounts of pearlite were observed, with the highest amount for WA 1 grade and lowest for Sponge I. Dissimilar amounts of chemical impurities, in particular silicon, were proposed to be the main reason behind these differences. In practical terms, this means that, if a lower hardness is targeted in order to reduce the wear on sizing dies, a coarser graphite and/or a lower sintering temperature are to be considered, especially with WA 1. If a very coarse graphite is already being used, these changes were not found to be effective.

Authors

Matteo Zanon[1]
Ilaria Rampin[1]
Alessandro Breda[1]
Francesco Bortolotti[1]
Enrico Tomaello[2]

[1]Pometon S.p.A., Italy
[2]University of Padova, Italy

Email: research@pometon.com

Acknowledgements

A special thanks goes to Dr R Gilardi of Imerys for providing the graphite powder samples.

References

[1] W Pahl, Boccole sinterizzate, AIM course on non-ferrous sintered metals, Milan (I) 15/04/2008

[2] N A Arnold,P/M Bearings, *ASM Handbook* Vol. 7 1992, pp. 705-6

[3] M Zanon & others, Iron-base solutions for bearings, World PM2016 Congress, Hamburg, proceedings, EPMA

[4] K P Jonnalagadda, Influence of graphite type on copper diffusion in Fe-Cu-C alloys, MSc degree thesis, 2012

[5] L S Darken, Trans. *AIME*, Vol. 180 (1949), pp. 430-438

[6] H K D H Bhadeshia, Case study: Design of bainitic steels, 2000, www.msm.cam.ac.uk/phase-trans/2000/C9/C9-8.pdf

[7] C Shade and T Murphy, Microstructure and mechanical properties of PM steels with Silicon and Vanadium, MPIF Congress, Nashville 2012 proceedings

Innovation drives success in the Japan Powder Metallurgy Association's 2017 awards

The winners of this year's Japan Powder Metallurgy Association (JPMA) PM component awards highlight the continuing developments being made to further expand the range of applications for our technology. The number of components recognised for their innovation suggests that there continues to be the potential for new applications in the automotive sector, particularly in the latest generation of highly efficient international combustion engines and automatic gearboxes.

Development Prizes: New Design

Development of a low-cost sintered ravigneaux planetary carrier

A Development Prize was awarded to Toyota Motor Corporation for a ravigneaux planetary carrier for a new high-efficiency automatic transmission. It consists of a PM carrier A, a PM carrier B, a steel sleeve and a steel hub (Fig. 1). The carrier design was optimised for PM to provide a significant reduction in manufacturing costs compared with forging and stamping. The stress to be applied to the ravigneaux carrier was reduced to below the fatigue limit by optimising the shape of the part at the points where stress was concentrated. The average density of this PM carrier is 7.05 g/m^3. For forming of the different height of the legs, green machining was adopted to provide further cost benefits.

The two PM carriers A, B (of composition Fe-2Cu -0.9°C) and a steel sleeve, having an optimal joint design, were brazed during the sintering process. After brazing, the steel hub was welded to the sleeve.

For the purpose of cost reduction, a completely automatic production line from compaction to machining was developed and the number of operators was halved. In order to improve productivity, adjustment of compacting conditions was abolished through the introduction of a filling method to stabilise filling density, and tool changeover time was reduced to less than 160 seconds.

These developments contributed to substantial improvements in cost competitiveness. It is expected

Fig. 1 Toyota Motor Corporation received a Development Prize in the New Design category for its low-cost sintered ravigneaux planetary carrier

Fig. 2 Sumitomo Electric Industries Ltd. received an award for its development of this complex pulley with high-accuracy non-circular gear teeth

Fig. 3 A sprocket drive for a low fuel consumption automatic transmission oil pump

that these technologies will be applied to global production in the future.

Development of a complex shaped pulley with high-accuracy non-circular gear teeth

Sumitomo Electric Industries Ltd. received a prize for a pulley with non-circular - in this case, triangular - gear teeth, which is a part of a VTC in a 3-cylinder engine (Fig. 2). The part was developed to achieve a reduction in vibration.

To deliver the required improvements in function, a complex shape and high dimensional accuracy had to be achieved. High accuracy was required to achieve the extremely tight geometrical tolerances of the non-circular external teeth (the outer diameter, the whole circumference, profile and squareness). In relation to the shape requirements, the female screw holes and oil passing slots had to be formed, taking into account the subsequent assembly. Additionally, production of the pulley had to correspond to the requirements for future globalisation in production.

Uneven density after compaction and deformation due to sintering were identified as factors affecting external teeth accuracy. These were resolved by optimising the sizing conditions. Four oil-passing slots were formed by long and thin side cores in the tool-set; however, this led to the breakage of these side-cores after the compaction of around 500 parts. Therefore, two measures were taken; improvements were made to the side-core design to enhance rigidity, and side-core extraction during green compact ejection was delayed.

Eventually, the mass production of large parts having high accuracy non-circular gear tooth surfaces was achieved by optimising production conditions. It is expected that, in the future, demand for sintered pulleys with non-circular gear teeth for VCTs will expand greatly, particularly in Europe.

Development of a sprocket drive for a low fuel consumption automatic transmission (AT) oil pump

Diamet Corporation was awarded a prize for its development of a sprocket drive for a next-generation fuel consumption AT oil pump (Fig. 3). From a cost point of view, an Fe-Cu-C based sintered sprocket with 6.8g/cm^3 density was used for this unit, instead of a fine-blanked sprocket.

Although induction hardening treatment is often used for gear tooth surface hardening, post-processing is required since dimensional accuracy deteriorates. In order to achieve both mechanical strength and low cost, Diamet has tried to improve the dimensional precision of an as-induction hardened body.

By setting the sizing conditions to minimise residual stress, it was possible to reduce the deformation during induction hardening and to achieve the required parallelism, with a dimensional accuracy of 50 μm, without post-processing.

The next-generation of AT units are expected to see an expansion of production volumes in the future thanks to their superior fuel consumption and further expansion of demand for the sintered parts can therefore be expected.

Development Prizes: New Materials

High wear resistant Fe-sintered alloy slider for high-speed trains

A prize was awarded to Fine Sinter Co Ltd. for the development of a high wear resistant slider for high-speed trains (Fig. 4). The slider, or contact strip, is designed to collect electric currents and transmit them to train vehicles through a pantograph from the trolley wire. The basic requirements for the slider are high wear resistance and a low level of attack on the trolley wire. Among many expendables in railway vehicles, the slider is most frequently replaced and, consequently, represents one of the highest costs in train maintenance. Recently, increases in train running speeds have made it necessary to improve the wear resistance of sliders at high speeds.

The aim of this development was to significantly decrease slider wear and to reduce the level of attack on the trolley wire, through the provision of good lubrication, and to maintain good mechanical properties. In order to increase wear resistance in the high-speed range, while maintaining good lubrication and high mechanical properties, a MnS-containing, free-cutting Fe powder was used as the matrix and a complex mixture of Fe-based and Cr-based hard particles was added. In addition, by avoiding the sulfurisation treatment used in conventional sliders, an improvement of more than 40% on lead-times was achieved without any cost increase.

A wear test at 300 km/h relative running speed found that slider wear was improved by 38% and the level of wear on the trolley wire was equal to or better than that of a conventional slider.

Fig. 4 High wear resistant Fe-sintered alloy sliders for high-speed trains

Fig. 5 Fe-Cu system oil-impregnated sintered bearings with excellent high pressure resistance and wear resistance

Development of an Fe-Cu system oil-impregnated sintered bearing with excellent high pressure resistance and wear resistance

Diamet Corporation won a further award for the development of a bearing that is designed to form part of the armature used in an electronically controlled wiper motor, as a typical application example (Fig. 5).

In order to improve pressure and wear resistance, the company targeted excellent sliding and lubricating performance with higher hardness and strength than conventional Fe-Cu system oil-impregnated sintered bearings.

For better sliding characteristics, the developed bearing material incorporated a large amount of copper (exceeding the solubility limit in iron) and had a microstructure with a large fraction of copper phases. In addition, as a result of optimising the raw material particle size of the copper powder and graphite and the sintering conditions, the material has become an Fe-Cu system composite structure, in which undissolved copper phases and free graphite are dispersed and distributed, resulting in high hardness and high strength. Furthermore, Diamet succeeded in securing the dimensional accuracy of the sizing process by making the dimensional change rate in sintering almost zero (< 0.1%).

The developed bearing material is said to achieve a wear resistance of more than four times that of a conventional bearing, under the electronically controlled wiper motor operating conditions. The material has high hardness and high strength, but also has excellent lubricating properties, sliding performance and dimensional accu-

Fig. 6 A gasoline direct injection mechanism part 'guide, fuel pump lifter'

Fig. 7 Diamet won an award for the development of this thin sprocket produced without a sizing process

racy. Diamet stated that there is no other example of this type of bearing material in the marketplace.

Effort Prizes

Development of a gasoline direct injection mechanism part 'guide, fuel pump lifter'
An effort prize was awarded to Sumitomo Electric Industries Ltd. for the development of a 'Guide, fuel pump lifter' used in a boosting mechanism for gasoline direct injection engines (Fig. 6). In the future, the introduction of this booster mechanism to engines will expand globally, rising to around 150,000 engines per month. Therefore, reducing the cost of each part in this mechanism was actively considered.

Specifically, the cost of the PM guide lifter part was reduced by 30%, compared with that of a cast part, by minimising machining allowance while selecting optimal material and production process for the satisfaction of the required specifications.

The Fe-Cu-C system was chosen as the material on the basis of its performance and price competitiveness. On the basis of the results of endurance tests carried out by the customer, it was determined that the heat treatment process could be omitted. The maximum level of near net shape was realised, by divided upper and lower punches to make holes, which satisfied the weight reduction requirement. The knock hole pitch and the inside diameter of the part were machined due to the high dimensional accuracy requirement.

As a result, the developed PM guide, fuel pump lifter parts were installed in a gasoline direct injection mechanism pump for the first time in Japan.

Development of a thin sprocket without a sizing process
Diamet Corporation gained a further award for the development of a sprocket with a diameter of over 100 mm and a 3.8 mm tooth thickness, for use in a Variable Valve Timing (VVT) system (Fig. 7). The development goals were to hold the same dimensional accuracy as a conventional sprocket and to offer lower cost than a fine-blanked sprocket.

To achieve the cost target, Diamet improved the dimensional accuracy of the sintered compact and eliminated the sizing process by optimising the tooling arrangement, powder feeding conditions and sintering setter shape.

Magnetic flaw detection was also eliminated, through the introduction of a 'touchless' line from compaction to the sintering process.

www.jpma.gr.jp

The JPMA awards archive

The Japan Powder Metallurgy Association's website features information on all of the association's award winning Powder Metallurgy parts dating back to 2004.

www.jpma.gr.jp/en/about/prize.html

Euro PM2017: Hot Isostatic Pressing for enhanced performance and demanding applications

A technical session at the Euro PM2017 congress, held in Milan, Italy, October 1-5, 2017, identified a number of process developments in Hot Isostatic Pressing (HIP) that address the need for high performance components in demanding applications. In this report, Dr David Whittaker reviews three papers from the session which highlight the processing of the superalloy Astroloy, study the influence of isostatic pressure on phase transformations and suggest the use of glass container encapsulation to improve density distribution in stainless steel components.

Investigation of post-HIP interface formation between powder Astroloy and steel capsule

The first paper, from Emilio Bassini, Valeria Vola, Sara Biamino and Daniele Ugues (Politecnico of Torino, Italy), Massimo Lorusso (CSFT, Italy), R Ghisleni (INSTM, Italy), Gianfranco Vallillo (Avio Aero, Italy) and Benjamin Picque (Aubert & Duval, France), focused on interface reactions between Astroloy powder and the steel capsule.

A number of aircraft engine manufacturers are seeking to enhance turbine performance by raising operating temperature. The solution to this objective involves the use of nickel-based superalloys with a high volume fraction of reinforcing particles. The higher the amount of γ' (Ni_3Al), the typical reinforcing system in nickel-based superalloys, the higher will be the thermal stability of components, but the lower will be their forgeability. This technological difficulty can be solved by changing the manufacturing route from casting or forging to a Powder Metallurgy route. In particular, Near Net Shape HIP (NNSHIP) and Net Shape HIP (NSHIP) are outstanding process alternatives.

In the reported study, Astroloy powders were consolidated by Hot

Fig. 1 Euro PM2017 took place in Milan, Italy

Element	Ni	Co	Cr	Mo	Al	Ti	Fe	Zr	N	Mn	C	S
w.%	Bal.	17.8	14.3	5.6	4.6	3.7	0.2	0.05	0.004	-	0.014	<0.002
w.%	-	-	-	-	-	-	bal.	-	-	0.8	0.16	0.040

Table 1 Chemical compositions of the Astroloy powder and steel capsule used during the HIP treatment [1]

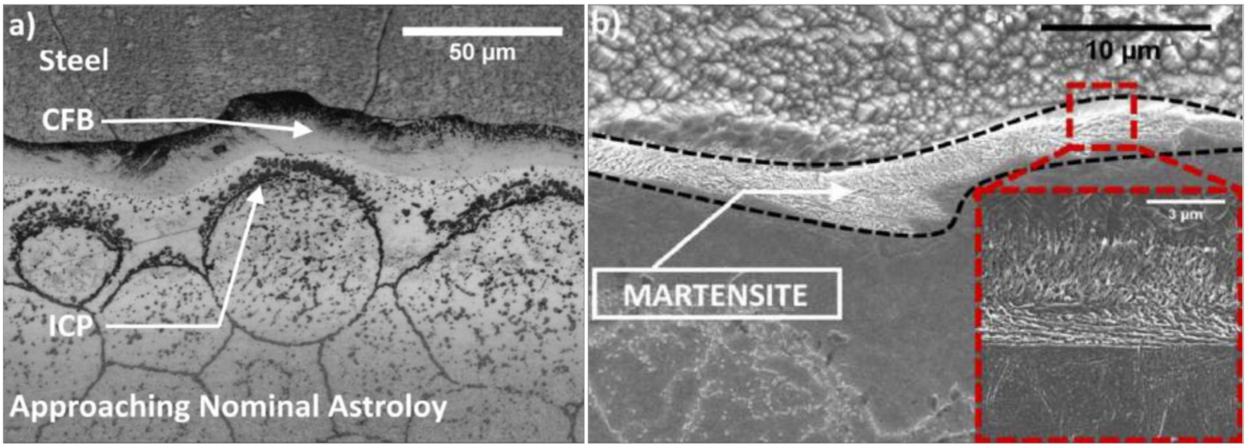

Fig. 2 a) HIP sample after Glyceregia etching observed with optical microscopy; b) FESEM image reveals the presence of martensite above the CFB [1]

Isostatic Pressing and the chemical and microstructural features of the transition region between the capsule and the alloy were investigated in depth. Astroloy is a superalloy that is particularly rich in chromium, cobalt, molybdenum, titanium and aluminium, while the capsule is made of a mild steel (Table 1). The strong chemical compositional difference between these two metals is the root cause of the formation of a complex interface between them during HIP.

The characterisation studies of HIP Astroloy were carried out on coupons measuring 30 x 20 x 10 mm, which were cut from a HIP bar whose original dimensions were 100 x 100 x 1000 mm. The interface between the steel capsule and the HIPed Astroloy was assessed using optical and electron microscopy. SEM was adopted to assess the compositional variations at the interface using secondary and backscattered electrons and EDS probe. The concentration gradient of elements formed at the interface after HIP was evaluated using spot analysis with a distance between two consecutive points of about 5 µm. Thirty spots were acquired for a total depth of 150 µm. Field Emission SEM (FESEM) was also used in order to observe the smallest phases present at the interface. Samples were observed after chemical etching using Glyceregia (HCl 15 ml + Glycerol 10 ml + HNO_3 5 ml).

"Astroloy is a superalloy that is particularly rich in chromium, cobalt, molybdenum, titanium and aluminium..."

Fig. 2a shows the interface after etching with Glyceregia for 15 seconds. This micrograph shows a well-developed prior particle boundary (PPB) network, which can extend up to about 500 µm below the capsule limit. The presence of such a region in the final component would not be acceptable and, therefore, it would have to be eliminated at the end of the HIP process by removal of the final overstock. The interface between steel and Astroloy is defined by the presence of a band made of carbides, the 'intense carbide precipitation zone' or ICP. Between the steel and the carbides, a precipitate free zone appears and is defined as the Carbide Free Band (CFB). Using optical microscopy, a darker band about 10 µm thick appears between the steel and the CFB, but its nature can be assessed only by means of electron microscopy (Fig. 2b) since its microstructure is very fine. In Fig. 2b, a dotted black line was used to separate an upper martensite band from the rest of the CFB. Below the martensite band and the CFB, the ICP appears. This band was considered as the initial point of contact between steel and Astroloy at the start of HIP consolidation and is considered to be the original interface. ICP formation is due to the bonding between carbon (coming from the steel) and the element with highest diffusivity among the carbide-forming elements in Astroloy.

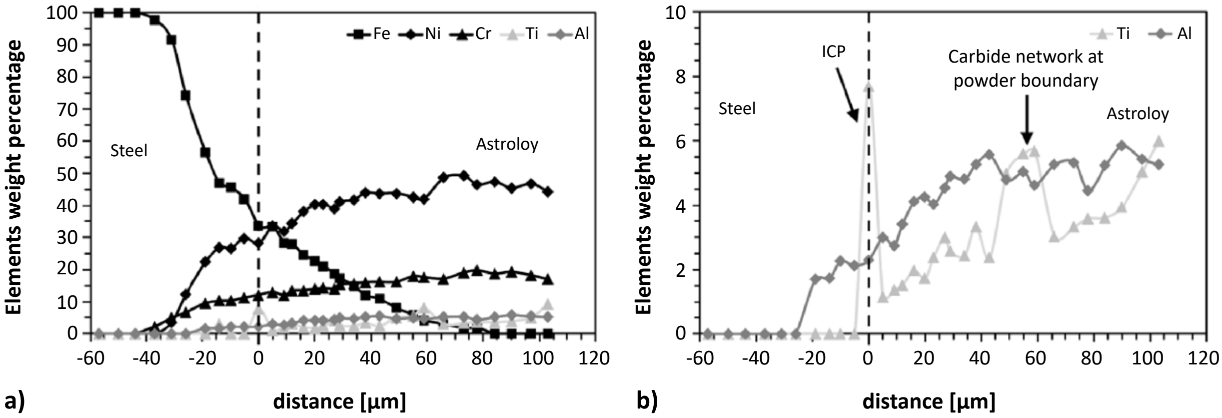

Fig. 3 a) Complete elemental concentration profile across the interface expressed in wt.%; b) detail for Ti and Al content [1]

EDS analysis showed that the ICP is mostly characterised by carbides very rich in Ti which, evidently, is faster to bond with C than is Cr, the other strong carbide forming element present. Thus, Cr is free to form carbides preferably in a deeper layer and at grain boundaries.

Under the ICP, Astroloy spherical powders are still visible. This superficial zone is heated and cooled in a faster way compared to the rest of the material, but reaches the optimal isostatic pressure only after a long transient. For these reasons, the powder in this zone undergoes little permanent deformation and slipping and bonding is mainly due to strong solid-state diffusion. Therefore, powders retain a spherical shape and are surrounded by a semi-continuous network of precipitates, which cannot be broken or dispersed.

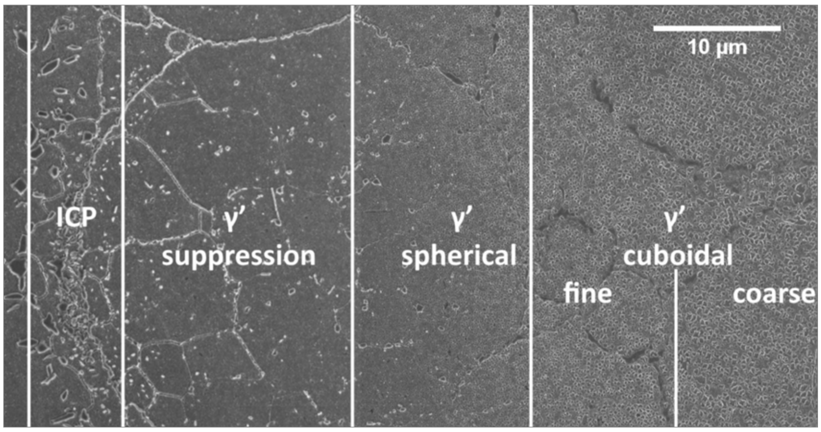

Fig. 4 Evolution of γ' from the ICP zone towards deeper layers [1]

Fig. 3 demonstrates how elements diffuse across the interface after the HIP process due to compositional differences between the steel and the superalloy. These compositional changes not only cause the formation of new phases, but also a modification of the γ' precipitation, which is even suppressed at some critical points. The most important reason for these changes is to be found in the amount of iron, titanium and aluminium (which together with Ni forms Ni_3Al) at the interface. Fig. 3a shows that, in the first 10 µm below the original interface, i.e. below the ICP indicated with a black dashed line, iron content is higher than Ni, making these layers more similar to an iron-nickel superalloy. Layers between 15-40 µm, on the other hand, present a progressively lower amount of iron and a progressive transition from an iron-nickel alloy to a nickel-iron alloy. Only deeper layers can be considered, effectively, to be a nickel-based superalloy. Fig. 3b provides a more detailed evaluation of the diffusion of Ti and Al across the interface, allowing the assessment that, on moving from the ICP to deeper layers of the Astroloy, the amount of Al increases from about 2% up to 5% and this strongly reflects on γ' morphology as shown in Fig. 4.

Fig. 4 shows the γ' evolution across the interface. In the first 10 µm below the ICP, Al content is too low to generate γ' precipitation. Between 20-40 µm, on the other hand, a sharp decrease in iron and a smaller increase in Al allows γ' precipitation, though in a spherical shape, which is typical of a Ni-Fe based superalloy. After a transition zone, the γ' begins to precipitate in cuboidal shape and passes from being very fine to coarser in form. Particle coarsening is due to the fact that, in this region, cooling rate after hipping is lower. This microstructural condition is also observable in the bulk material.

According to these experimental results, Astroloy recovers its nominal composition at around 70 µm below the ICP. However, the fast diffusion taking place at grain boundaries allows PPB network formation over a much deeper layer. These particles are detrimental to fatigue and creep resistance of the alloy and, thus, have to be eliminated. By summing the contributions of volume and

C	Mn	Si	Cr	Ni	Cu	Nb	N	Fe
0.05	0.3	0.4	15.3	4.3	3.4	0.2	~0	bal.

Table 2 Composition of 17-4PH material produced by Carpenter [2]

Hardness, HV	As received HIPed	1038°C heated and quenched	1038°C heated + 482°C annealed
	369		
Heat treated in atmosphere		293	383
Heat treated in HIP		336	428
Difference		+43	+45

Table 3 Hardness measurements for 17-4PH hardened in both the HIP-unit and with traditional hardening with quench in saltwater [2]

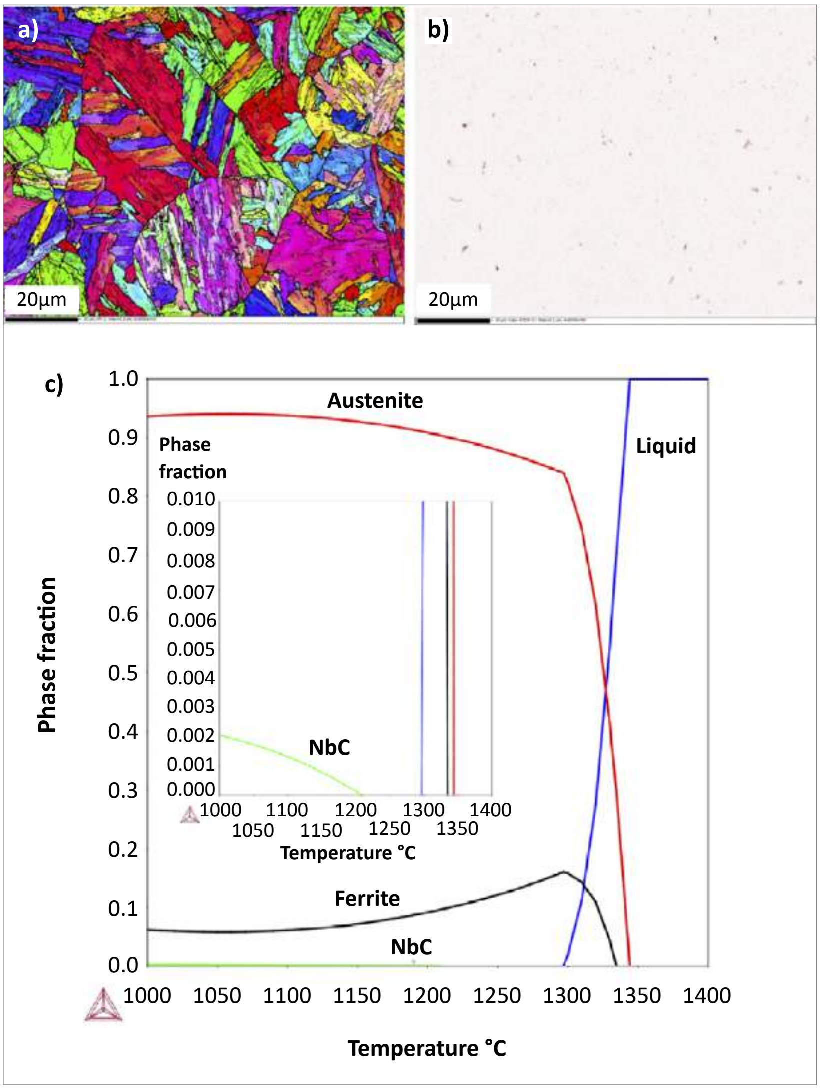

Fig. 5 a) Presenting EBSD map of as-HIPed material; b) Niobium map of the same material (taken at a different location); c) Thermo-Calc calculation of phase stability for 17-4 PH [2]

grain boundary diffusion, a total thickness of 500 µm below the interface can be identified as the final required overstock.

Influence of isostatic pressure on phase transformations in 17-4 PH

Next, a paper from Hans Magnusson and Joacim Hagstrom (Swerea KIMAB AB, Sweden), Mats Persson (Höganäs AB, Sweden), Björn-Olof Bengtsson (Carpenter Powder Products, Sweden), Stefan Sehlstedt (Quintus Technologies, Sweden) and Ingrid Bengtsson (Bodycote Hot Isostatic Pressing, Sweden) examined the influence of isostatic pressure on phase transformations in 17-4 PH stainless steel.

17-4 PH is a martensitic, precipitation hardened stainless steel. It is often used in applications that require good corrosion resistance and high strength. The mechanical properties rely on the precipitation of nanometre-sized copper particles, together with the martensitic transformation. The copper particle precipitation requires ageing at around 482°C (900°F). These particles can quickly overage at higher temperatures and the high-temperature usage of this material is therefore limited.

The reported study investigated how phase transformation is influenced by isostatic pressure. The composition of the 17-4 PH powder, produced by Carpenter, is given in Table 2. This powder was HIPed by Bodycote using a standard cycle for steels; 1000 bar, 1150°C and 2 hours. The HIPed and fully compacted material was then given two different heat treatments: Normal atmosphere, solution treated for 1 hour at 1038°C, quenched in salt water, annealed (aged) for 1 hour at 482°C and then air cooled; High pressure, similar heat treatments were made in the rapid cooling (URQ) HIP unit at Quintus, the material was solution treated for 1 hour at 1038°C, quenched and then annealed (aged) in the same cycle, at a pressure of 1700 bar.

Results from hardness measurements are presented in Table 3. These measurements indicated that

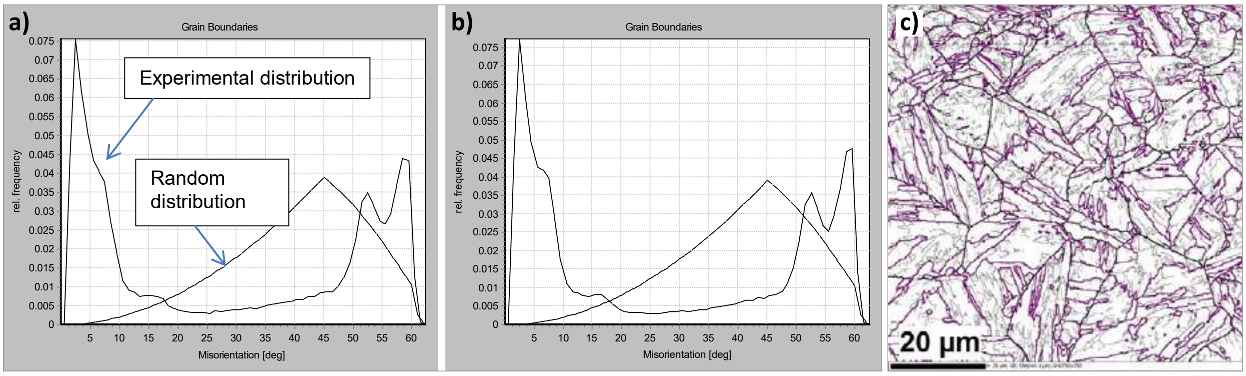

Fig. 6 Misorientation distributions from EBSD evaluations. a) Hardened at 1 atm and quenched in water b) Hardened in the HIP unit c) Example of microstructure for sample hardened in the HIP. Black are prior austenite grains and purple lath-boundaries [2]

hardness increased 40-50 HV for all materials hardened under high isostatic pressure and that hardness increased 90 HV on ageing for all annealed states.

The hardness in the as-received sample was higher than in the quenched state. This could be due to a relatively slow cooling in the conventional HIP unit, compared to the rapid cooling in the controlled HIP-cycle (as quenched) and this cooling rate could have caused precipitation during cooling.

Martensite start temperatures (M_S) were evaluated by dilatometry. M_S was measured as 159°C at 5°C/s cooling rate and 143°C at 100°C/s. The martensite transformation was finished at 45°C. M_S is low, but still sufficiently high to harden when cooling to room temperature.

The as-HIPed material used as the starting condition for the heat treatments is shown in the EBSD image in Fig. 5a, an EDS-map of niobium particles in Fig. 5b and Thermo-Calc calculated (TCFE7) equilibria in Fig. 5c. The EBSD image shows a grain size of 20-80 µm. Niobium-containing particles were seen. These particles are common for this type of steel and are stable up to 1200°C according to Thermo-Calc calculations. Some remaining delta-ferrite was also observed.

A detailed analysis of materials that were given additional heat treatments in both URQ-HIP and normal atmosphere have been made with EBSD. Fig. 6 summarises the misorientation distributions as measured by EBSD for materials hardened by quench in salt water and in the HIP. Misorientations larger than 2° are plotted in Fig. 6. The prior austenite grain sizes and the martensite packet sizes were similar for both materials. The misorientation distributions were also similar, but, if very low angle misorientations were studied, a small increase could be assigned to the HIP-hardened material.

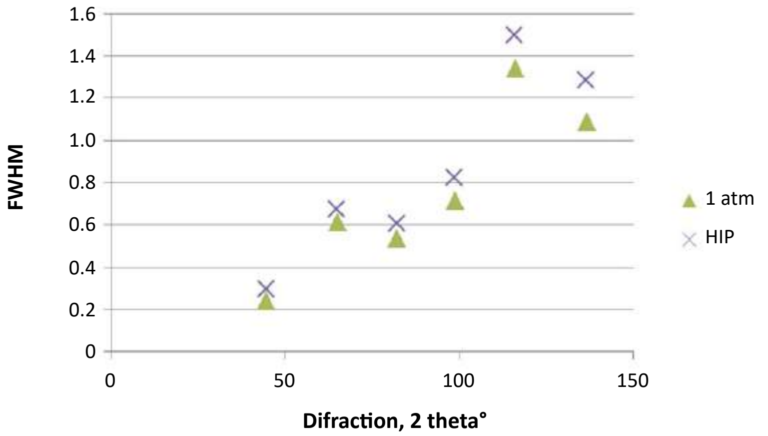

Fig. 7 XRD results for materials hardened in the HIP unit and in salt-water [2]

To assess dislocation density, XRD evaluations were made. The amount of distortion can be evaluated with XRD by measuring the full width at half maximum (FWHM) and these results are presented in Fig. 7 for the hardened materials. It can be seen that the material hardened in HIP has a greater amount of distortion in the crystalline structure and this could be an indication of higher dislocation density and, therefore, harder material.

The authors noted that previous studies have been reported in the literature and these have shown experimentally that isostatic pressure lowers M_S temperature. These previous experiments were carried out in a high-pressure chamber with up to 40 kbar pressure and showed that M_S is lowered by approximately 4°C per kbar pressure. These pressures are much higher than in typical HIP-units, with are often limited to 2 kbar pressure. Phase transformations that result in an increase in volume will not be favoured under hydrostatic pressure. A high hydrostatic pressure will favour those crystalline structures, which have the smallest molar volumes. A phase transformation from austenite to martensite will lead to an expansion of the lattice, requiring an additional driving force for the initiation of the transformation. This will be seen

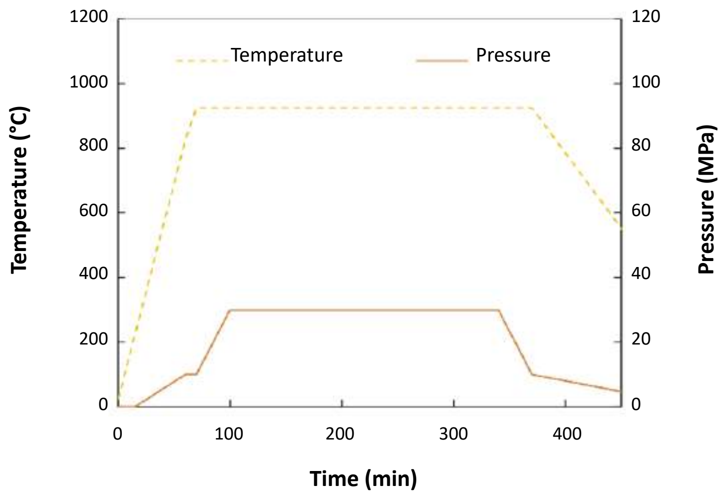

Fig. 8 HIPing temperature and pressure schedule [3]

as a lower M_s temperature at high pressure. As the M_s is lowered by hydrostatic pressure, the resulting martensite upon hardening will be finer and, therefore, of higher hardness.

A study on glass container encapsulation of 316L stainless steel powder during Hot Isostatic Pressing

Finally, a paper from Hosam ElRakayby and KiTae Kim (Pohang University of Science and Technology, Korea) reported on the assessment

Fig. 9 Comparison between experimental data and finite element calculations for the final shape of the 316L stainless steel compact [3]

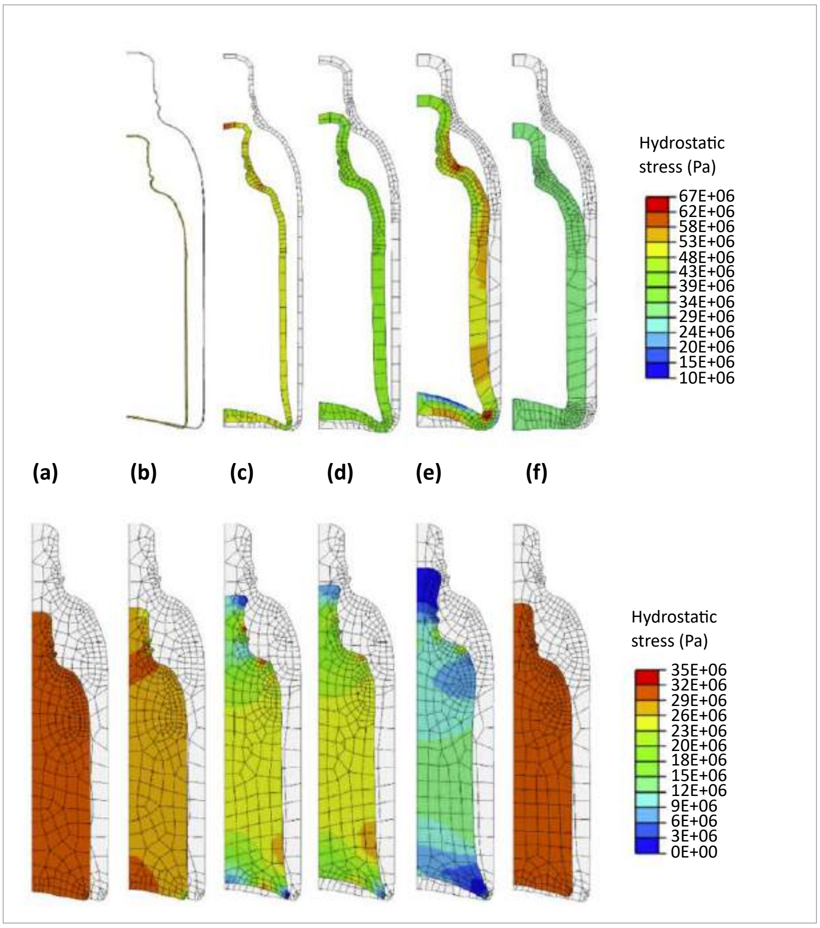

Fig. 10 Finite element calculations for hydrostatic stress distributions for samples HIPed in 304 stainless steel containers with different wall thicknesses, (a) without a container, (b) 0.1 mm, (c) 0.6 mm, (d) 1.24 mm, (e) 2 mm and (f) in a glass container for 240 min under 30 MPa pressure at 925°C [3]

Chemical Composition	Fe	Cr	Ni	Mo	Si	Mn	Cu	P	S	C	O_2
(wt.%)	Balance	15.7	11.3	2.07	0.86	0.09	0.03	0.028	0.002	0.019	0.35

Table 4 Chemical composition of 316L stainless steel powder [3]

of glass container encapsulation, as an alternative to the use of steel capsules, in the HIPing of 316L stainless steel powder. The authors had previously demonstrated that metal containers induce Mises stresses in compacts, due to the rigidity of the container walls. These stresses can cause a nonhomogeneous distribution of relative density over the compact. Metal containers reduce the applied HIPing pressure transmitted to the compacts, but the authors proposed that glass can be used as an encapsulation material to avoid these disadvantages. The reported work studied the effect of glass container encapsulation on densification and deformation behaviour of 316L stainless steel powder and, also, investigated the effect of the glass container on the Mises stress, hydrostatic stress and relative density distributions over the compacts.

Water atomised 316L stainless steel powder, with the composition shown in Table 4, a theoretical density of 7.95 g/cm^3 and an average particle size of 8 µm was used in the study. The powder was filled in commercial borosilicate glass tubes of 46 mm in height, 26 mm in outer diameter and 2 mm in thickness. The container was vibrated to attain an initial relative density of 0.45 and was degassed through the ventilation tube for 4 h at 250°C. The ventilation tube was then sealed under vacuum with an oxy-propane torch.

HIPing was carried out using the conditions shown in Fig. 8, with the samples being supported on Saffil preforms. Numerical modelling of the HIP process was carried out using the finite element analysis program Abaqus – FEA and implementing constitutive equations previously derived by the authors.

Fig. 9 shows a comparison between experimental data and finite element calculations for the final shape change of a 316L stainless steel compact after HIPing in the glass container. Isotropic deformation can be noted, such that the axial shrinkage is almost the same as the radial shrinkage.

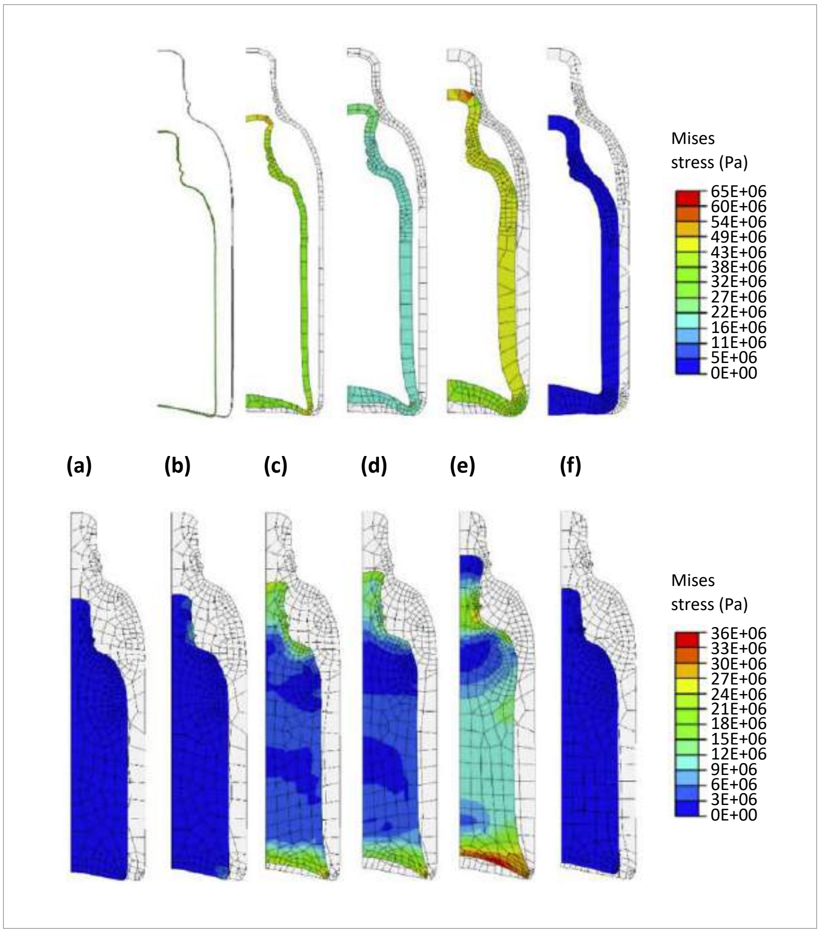

Fig. 11 Finite element calculations for the Mises stress distributions for samples HIPed in 304 stainless steel containers with different wall thicknesses, (a) without a container, (b) 0.1 mm, (c) 0.6 mm, (d) 1.24 mm, (e) 2 mm and (f) in a glass container for 240 min under 30 MPa pressure at 925°C [3]

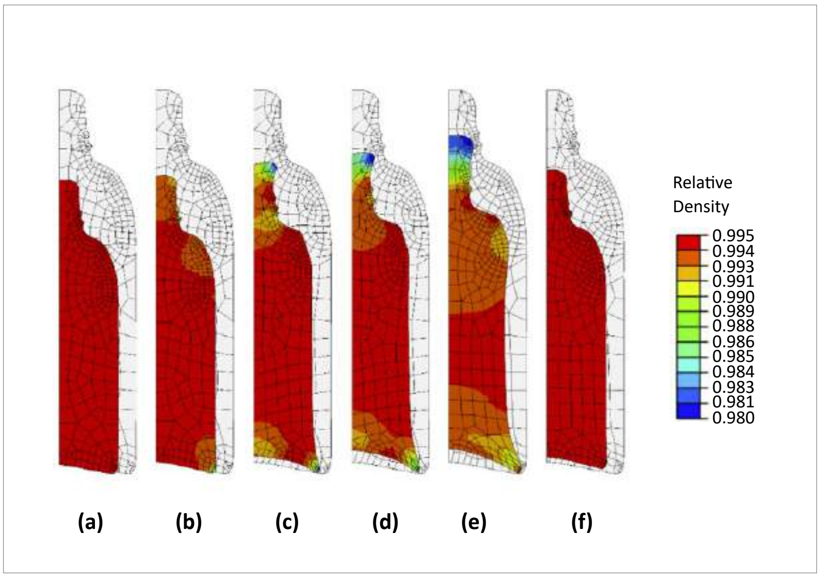

Fig. 12 Finite element calculations for relative density distributions for samples HIPed in 304 stainless steel containers with different wall thicknesses, (a) without a container, (b) 0.1 mm, (c) 0.6 mm, (d) 1.24 mm, (e) 2 mm and (f) in a glass container for 240 min under 30 MPa pressure at 925°C [3]

Fig. 10 shows finite element calculations for hydrostatic stress distributions for samples HIPed in various 304 stainless steel containers with different wall thicknesses, (a) without a container, (b) 0.1 mm, (c) 0.6 mm, (d) 1.24 mm, (e) 2 mm and (f) in a glass container for 240 min under a pressure of 30 MPa at 925°C. Non-uniform distribution of hydrostatic stress in the compacts was observed, due to the rigidity of the metal container. For the compact modelled without a container (a theoretical result), this had a uniform distribution of hydrostatic stress. This uniform distribution of hydrostatic stress can be also noted in the compact HIPed in the glass container.

Figs. 11 and 12 show finite element calculations for the Mises stress distributions and relative density distributions in the samples HIPed with the same container options as in Fig. 10. The Mises stress was induced in the compacts HIPed in metal containers, due to the container wall rigidity, and, therefore, a nonhomogenous distribution of relative density over the compacts was noted. On the other hand, the glass container did not induce Mises stresses in the compacts. It was concluded that the glass containers transmitted all of the applied isostatic pressure to the compacts and the induced Mises stress could be neglected.

From Figs. 10, 11 and 12, it can be noted that the compacts HIPed in glass containers showed homogeneous densification and isotropic deformation behaviour.

References

[1] Investigation of post HIP interface formation between powder Astroloy and steel capsule, Emilio Bassini *et al.*, as presented at Euro PM2017, Milan, Italy, October 1-5, 2017, and published in the proceedings by the European Powder Metallurgy Association

[2] Influence of isostatic pressure on phase transformations in 17-4 PH, Hans Magnusson *et al.*, as presented at Euro PM2017, Milan, Italy, October 1-5, 2017, and published in the proceedings by the European Powder Metallurgy Association

[3] A study on glass container encapsulation of 316L stainless steel powder during Hot Isostatic Pressing, Hosam ElRakayby *et al.*, as presented at Euro PM2017, Milan, Italy, October 1-5, 2017, and published in the proceedings by the European Powder Metallurgy Association

Author

Dr David Whittaker
Tel: +44 1902 338498
Email: whittakerd4@gmail.com

Proceedings

The Euro PM2017 Congress Proceedings are available from the European Powder Metallurgy Association. The proceedings contain oral and poster papers presented at the congress.

www.epma.com

Euro PM2018

The Euro PM2018 Congress & Exhibition will take place in Bilbao Exhibition Centre, Bilbao, Spain, from October 14-18, 2018.

www.europm2018.com

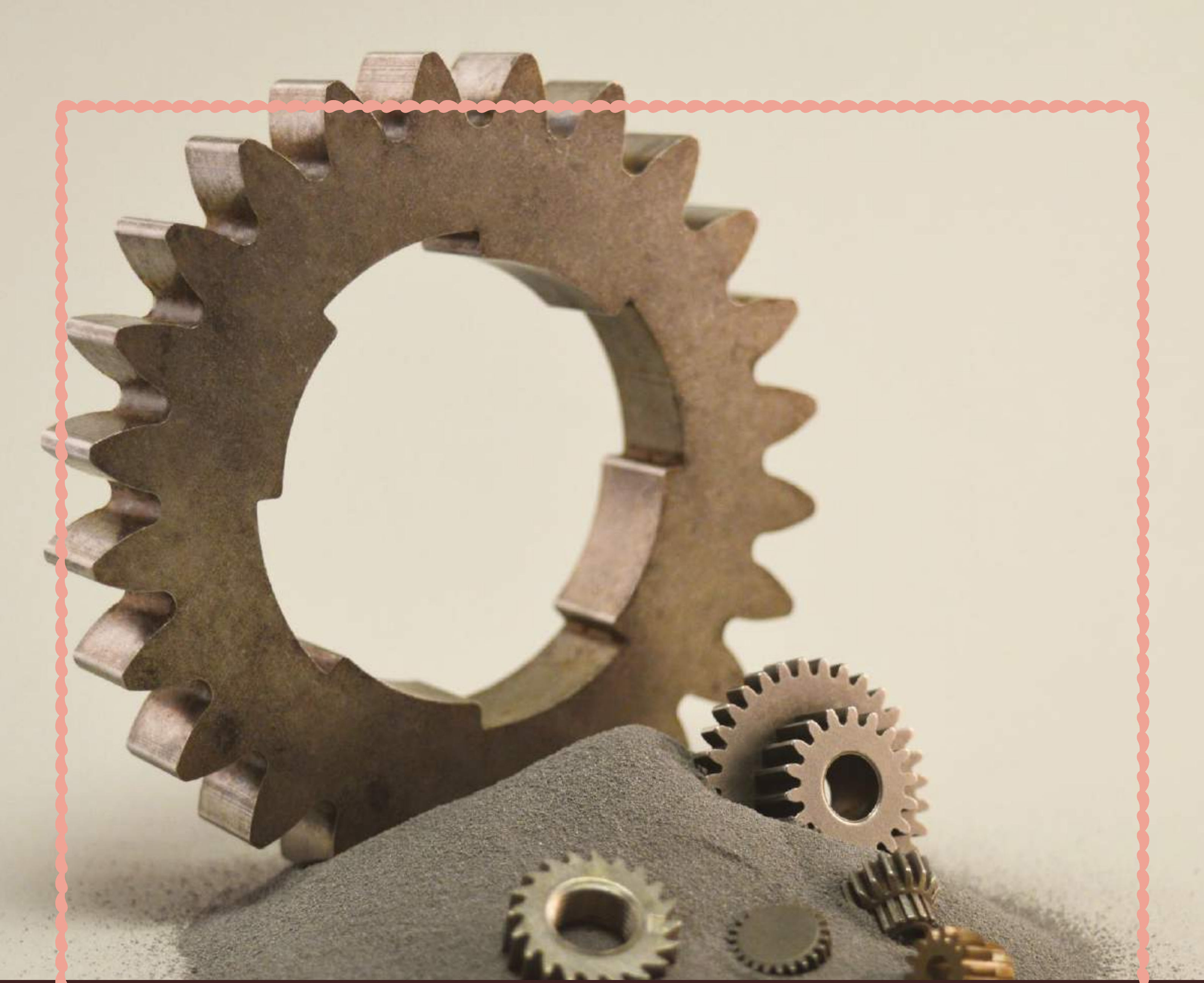

POWDERMET2017: Improved dimensional control in PM iron-copper-carbon materials

Iron-copper-carbon is one of the most widely used materials in Powder Metallurgy component production thanks to its low cost and high mechanical and metallurgical properties. However, there are a number of issues which can result in the need for additional sizing and machining operations. Papers presented at the POWDERMET2017 Conference, Las Vegas, June 13-16, 2017, discussed options to improve dimensional control and limit post processing operations. Dr David Whittaker reviews a selection of these papers.

Iron-copper-carbon materials remain the predominant system for manufacturing Powder Metallurgy parts. However, large pores left behind when the copper addition melts and diffuses into the iron matrix, can lead to variability in dimensional process control, an important issue which can affect PM's major competitive advantage in offering net shape capability. Elemental admixing is the simplest and most common method used to distribute the copper addition into the base iron powder to form a mix before compaction and sintering. However, because the addition particles are free to move, admixed materials are more prone to segregation.

A group of three papers, presented at POWDERMET2017, discussed alternative means of incorporating the copper additions in feedstocks, with a view to eliminating this segregation problem.

Improved precision of iron-copper-carbon materials

In this paper, presented by Sarah Ropar (North American Höganäs, USA) and co-authored by her colleagues Roland Warzel III and Bo Hu, the alternative process of diffusion alloying was studied. Diffusion-alloyed powders involve the annealing of the mix so that the alloying additions partially diffuse into the iron particles and, therefore, eliminate segregation.

Fig. 1 POWDERMET2017 took place at the Bellagio Hotel in Las Vegas, USA

Cu Source	D_{50} (µm)
Cu-165	80
Cu-200	45
D.ACu	*150
D.ACu Improved	*150

*Note: Average PSD for base iron

Table 1 Average particle size distribution (PSD) for the various copper sources [1]

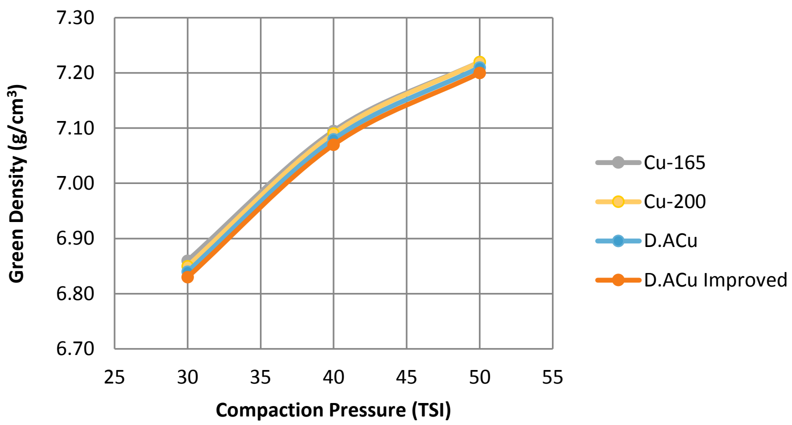

Fig. 2 Compressibility curves for FC-0208 mixes [1]

The MPIF standard material systems used for the reported study were FC-0200 (0% C), FC-0200 (0.2% C), FC-0205 (0.6% C) and FC-0208 (0.8% C). Within each material system, four different sources of copper were selected for evaluation. The copper sources were: elemental Cu-165 (ACuPowder), a conventional PM grade; elemental Cu-200 (ACuPowder), a conventional PM grade with finer particle size than the Cu-165 grade; diffusion-alloyed D.ACu (Höganäs, Sweden), and diffusion-alloyed D.ACu Improved (Höganäs, Sweden). The average particle size distribution for each copper source is shown in Table 1.

The compressibility curves for the FC-0208 mixes are shown in Fig. 2. FC-0208 was chosen as this is the most common material system for PM applications. Compared with the admixed materials with elemental copper, the diffusion-alloyed copper materials provided no significant difference in compressibility. With the diffusion-alloyed copper grades,

MPIF Code	Type of Cu	Sintered C (%)	HRB	TS (MPa)	YS (MPa)	Elongation (%)
FC-0200	Cu-165	0.008	21	228	169	6.5
FC-0200	Cu-200	0.007	22	228	171	6.5
FC-0200	D.ACu	0.007	25	228	174	3.2
FC-0200	D.ACu Improved	0.006	29	234	181	3.2

Table 2 Sintered properties for FC-0200 mixes (0% Sintered C) [1]

MPIF Code	Type of Cu	Sintered C (%)	HRB	TS (MPa)	YS (MPa)	Elongation (%)
FC-0200	Cu-165	0.28	54	331	261	4.3
FC-0200	Cu-200	0.28	54	331	267	4.3
FC-0200	D.ACu	0.29	53	338	272	2.2
FC-0200	D.ACu Improved	0.28	56	352	274	2.2

Table 3 Sintered Properties for FC-0200 mixes (0.2% Sintered C) [1]

MPIF Code	Type of Cu	Sintered C (%)	HRB	TS (MPa)	YS (MPa)	Elongation (%)
FC-0205	Cu-165	0.66	78	483	385	1.1
FC-0205	Cu-200	0.67	76	490	389	3.2
FC-0205	D.ACu	0.67	77	503	394	3.2
FC-0205	D.ACu Improved	0.66	78	510	396	3.2

Table 4 Sintered properties for FC-0205 mixes (0.6% Sintered C) [1]

MPIF Code	Type of Cu	Sintered C (%)	HRB	TS (MPa)	YS (MPa)	Elongation (%)
FC-0208	Cu-165	0.88	84	552	462	1.1
FC-0208	Cu-200	0.88	84	552	468	3.2
FC-0208	D.ACu	0.86	85	572	468	3.2
FC-0208	D.ACu Improved	0.87	85	579	481	3.2

Table 5 Sintered properties for FC-0208 mixes (0.8% Sintered C) [1]

the compressibility of the material containing the D.ACu Improved was comparable to the material with D.ACu.

The measured levels of apparent hardness, yield strength, tensile strength and elongation for each material system after sintering are shown in Tables 2-5. As the sintered carbon level increased, the hardness and strength increased for the iron-copper-carbon materials, regardless of the source of copper. Although the hardness of materials were similar within the same sintered carbon level, the diffusion-alloyed materials consistently showed slightly higher strengths compared with the materials containing the elemental copper. The elongation values for the elemental coppers decreased as the sintered carbon level increased, while the elongations for the diffusion-alloyed materials remained fairly similar.

Fig. 3 shows the relationships between dimensional change and sintered carbon level. All materials showed a growth in dimensional change regardless of the carbon level used. With the carbon level increased from 0.2% C, growth was reduced. Compared with the other material groups, the D.ACu Improved had significantly less growth when no carbon was added (0%) or at the low sintered carbon level (0.2%). Overall, the D.ACu Improved material exhibited less effect on dimensional change from the carbon addition compared with the other material groups.

A dimensional change study was performed in order to assess the dimensional change between each of the materials and to develop an understanding of the consistency of the dimensional change over time. The variation in dimensions was evaluated across all graphite additions, as shown in Fig. 4. The elemental copper (Cu-165 and Cu-200) containing materials showed similar variations in dimensional changes. The diffusion-alloyed materials had less variation compared to the materials with elemental copper. Compared to the D.ACu material, however, the D.ACu Improved material showed significant improvement in reducing the variation in dimensional changes. For the same graphite addition (Fig. 5), the variations for the materials containing the finer elemental copper (Cu-200) were higher compared with the material with coarse elemental copper (Cu-165). Both the D.ACu and D.ACu Improved showed less variation in dimensions, i.e. more consistency in dimensional changes, compared with the admixed material with the elemental copper grades.

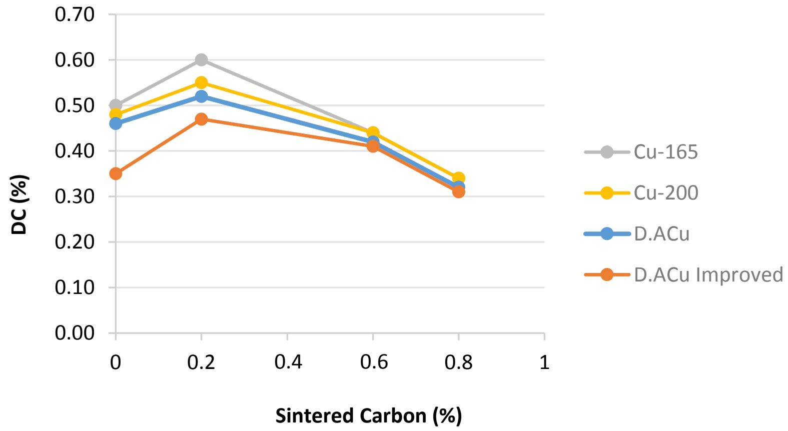

Fig. 3 Dimensional change versus sintered carbon [1]

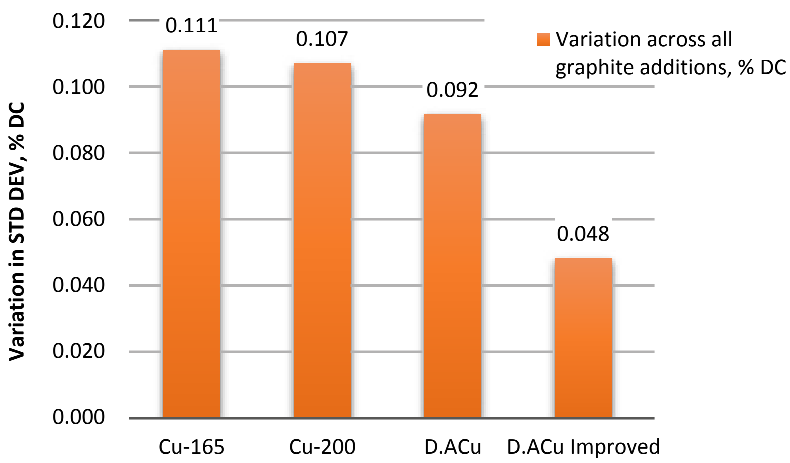

Fig. 4 Variation across all graphite additions [1]

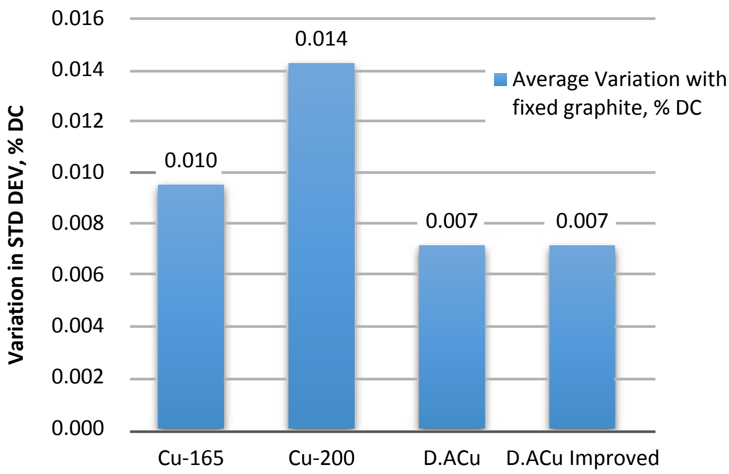

Fig. 5 Variation with fixed graphite levels [1]

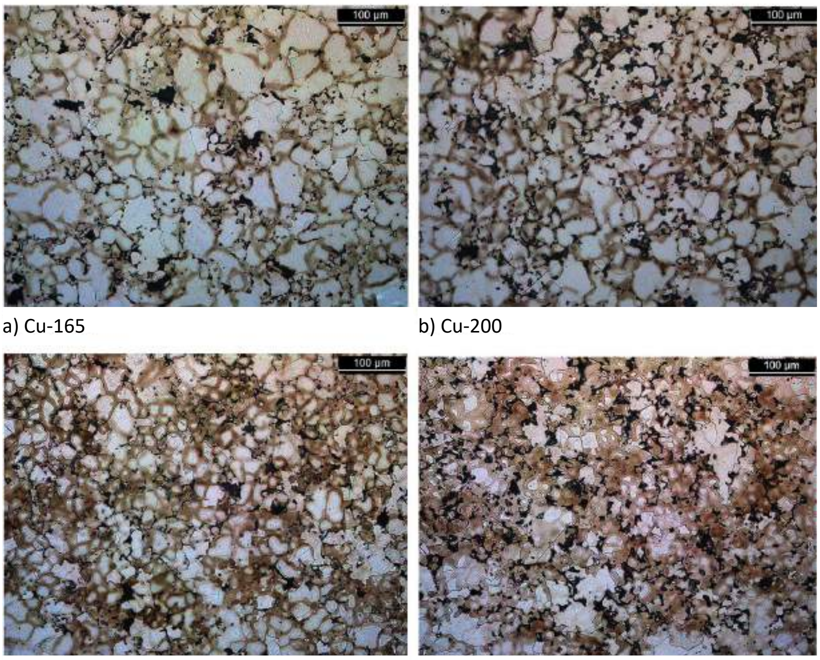

a) Cu-165

b) Cu-200

c) D.ACu

d) D.ACu Improved

Fig. 6 Comparison of copper diffusion between the sintered FC-0200 materials made with admixed and diffusion-bonded copper grades [1]

Metallographic assessments demonstrated that, for the material admixed with Cu-165, large pores were left after coarse copper particles melted and diffused into the iron during sintering. Large pores were also present in the material with Cu-200, although the amount was considerably reduced. However, no large pores were found in the diffusion-bonded materials. The size and distribution of pores in the diffusion-alloyed copper materials was more uniform than in the elemental copper admixed materials.

In relation to the status of copper diffusion in the sintered FC-0200 samples, Fig. 6 shows that, in the elemental copper admixed materials, the diffusion was concentrated around the grain boundaries of iron particles, while the copper in the diffusion-alloyed materials was diffused more into the iron particles. Compared to the D. ACu material, more copper was diffused into the iron matrix in the D.ACu Improved material.

If copper segregation occurs in admixed materials, the large copper particles or agglomerates can cause variation in dimensions or a shift in the properties. When using copper diffusion-bonded material, copper segregation can be eliminated and the diffusion of copper into the iron matrix is more consistent, leading to reduced variation in dimensional changes.

The analysis of the status of copper diffusion in the iron matrix explains why the copper diffusion-bonded materials have less variation in dimensional changes and higher elongation than the elemental copper admixed materials. With more copper diffused into iron particles rather than concentrated at the grain boundaries, the distribution of copper in the iron matrix becomes more homogeneous and makes the matrix more homogenous, resulting in more stable dimensional changes.

Improved diffusion-bonded copper alloy for improved dimensional change and precision of PM steel parts

A second paper, this time submitted by a PM parts maker rather than a powder supplier, also focused on comparisons between elemental admixed copper materials and diffusion alloyed materials. This paper was presented by Cody Kalinoski (Engineered Sintered Components, USA) and was co-authored by his colleagues Heron Rodrigues and Mike Folliard.

The material variants compared in this study all complied with the FC-0208 specification (iron, 2% copper and 0.8% carbon). The breakdown of the alloying additions is shown in Table 6. The five different copper sources comprised a standard and a fine elemental admixed addition and three diffusion alloyed materials: D.ACu and improved D.ACu were based on an atomised base iron powder and were as discussed in the

Acronym	Base Iron	Graphite	Copper	Lubricant
Ele Cu	AHC 100.29	Synthetic	Elemental Copper	Acrawax
D.ACu	AHC 100.29	Synthetic	D.ACu	Acrawax
ID.ACu	AHC 100.29	Synthetic	Improved D.ACu	Acrawax
D.Cu	AHC 100.29	Synthetic	D.Cu	Acrawax
Fine Cu	AHC 100.29	Synthetic	Fine Copper	Acrawax
ID.ACu'	ASC 100.29	Synthetic	Improved D.ACu	Acrawax

Table 6 Breakdown of alloying additions in the various mixes [2]

previous paper; D.Cu, on the other hand, was based on a sponge iron powder.

An outer gerotor was selected as the test component in the reported study. Fig. 7 shows the schematic diagram of the component and the dimensions that were measured. This type of component was selected for the study because it offers a variety of dimensions that can be measured to determine the significance of the variation in the dimensional change from mix to mix. Between the pin diameter, major and minor inner diameter, outer diameter and outer diameter roundness were all measured on this component in the green state and in the as sintered condition. Fig. 7 shows where between the pin diameter (a-e) dimensions were measured. Hardness was also checked in the as-sintered condition.

Test components were compacted to an overall density of 6.8 g/cm^3 and were sintered at 1160°C (2120°F) in an atmosphere of 93% nitrogen and 7% hydrogen and with a normal cooling rate of 0.5°C/s (1°F/s). The total dimensional changes (DC) of all of the mixes used in the study are presented in Fig. 8. Ele Cu and D.Cu had the lowest amount of total dimensional change compared to the other mixes. ID.ACu and ID.ACu' had the highest amount of total DC on the OD compared to the other mixes. D.ACu also had a high total DC relative to Ele Cu and D.Cu. A similar pecking order of these addition types was also revealed in studies of the total DCs for the minor ID and major ID.

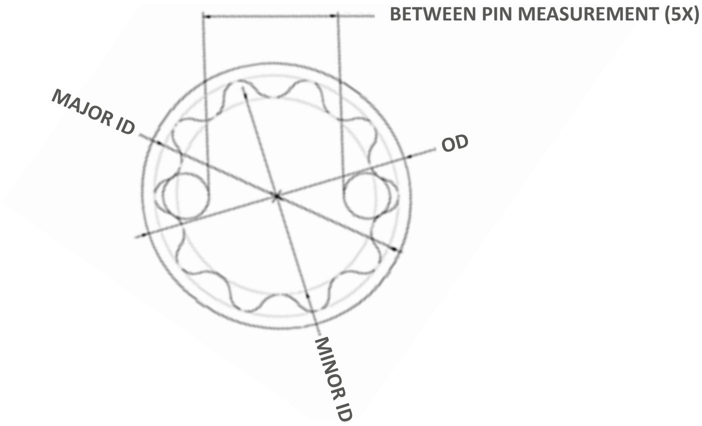

Fig. 7 Production component schematic diagram and measuring locations [2]

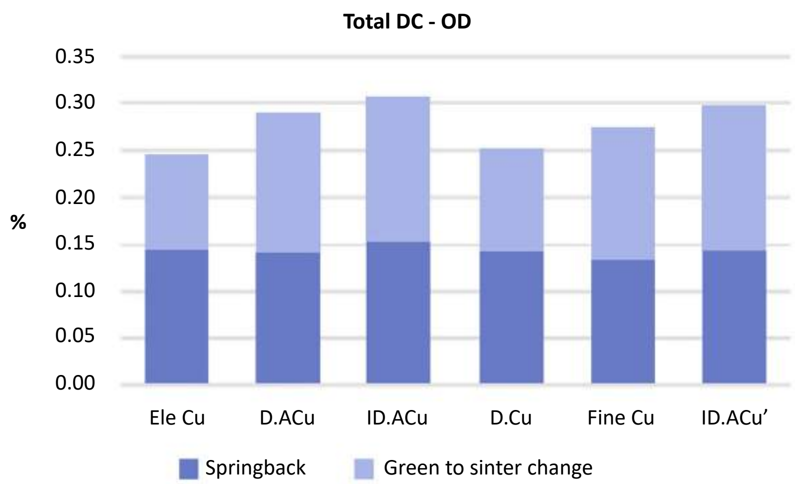

Fig. 8 Total dimensional changes of the OD [2]

In relation to dimensional precision, Fig. 9 shows the standard deviation of the observed dimensional change in the minor ID. Similar observations were also made in relation to the precision of the major ID i.e. the improved D.ACu and the D.Cu alloying variants showed the lowest standard deviation for both the minor and major ID.

Results for the between the pin diameter (BPD) are shown in Fig. 10. In this case, the improved D.ACu had the lowest standard deviation, but the D.Cu had one of the highest standard deviations. The current D.ACu had the second lowest standard deviation.

Fig. 11 shows the standard deviation for the OD and similar observations were made for OD roundness. In both cases, the improved D.ACu

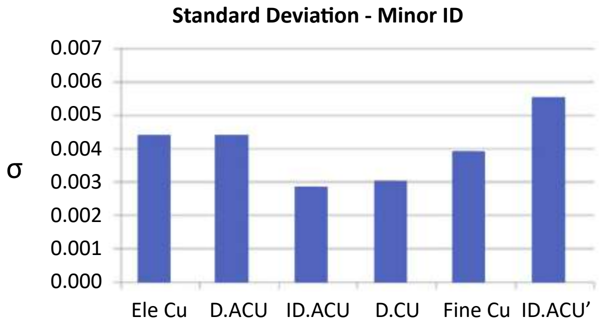

Fig. 9 Standard deviation of the minor ID [2]

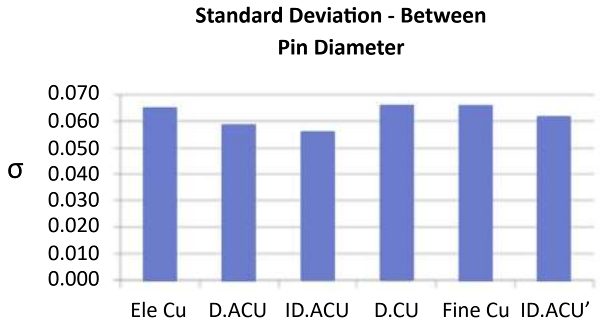

Fig. 10 Standard deviation of the between pin diameter [2]

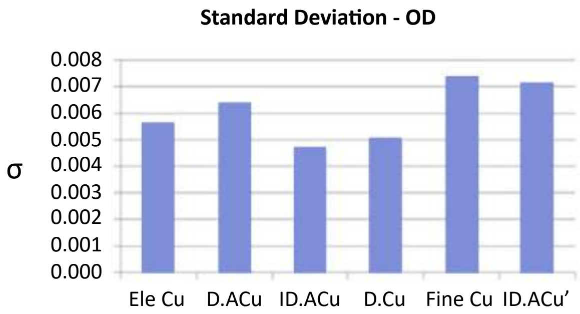

Fig. 11 Standard deviation for the OD [2]

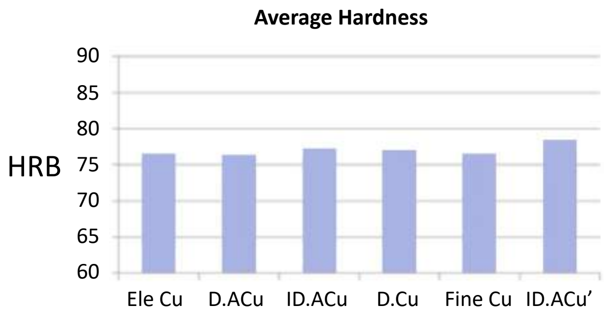

Fig. 12 Hardness of all six material variants after sintering [2]

yielded the lowest standard deviation followed closely by the D.Cu. Fig. 12 shows the results of the as-sintered hardness measurements. The hardness values for all the alloying variants fell between 75 and 80 on the Rockwell B scale (HRB), demonstrating that there was no loss of mechanical properties when using the improved D.ACu vs. currently used materials.

Based on the results of this study, it was observed that the improved D.ACu enhanced the standard deviation (precision) of each characteristic measured on the component. The powders were analysed, by using scanning electron microscopy (SEM) and electron dispersive spectroscopy (EDS), in order to determine why the improved D.ACu produced a lower standard deviation relative to the other materials. The element maps show a difference in copper particle size and copper particle distribution throughout the powder samples. ID.ACu and ID.ACu' have the smallest copper particle size and the best copper particle distribution compared to the other materials.

The authors drew the following overall conclusions from the reported study:

1. Total dimensional change is influenced by copper particle size. The large copper particles will induce swelling during sintering, but only in localised areas of the component. This will lead to an increase in distortion but will inhibit uniform growth. Smaller copper particles will swell the component more uniformly and this in turn leads to more growth.

2. Precision is influenced by the distribution of copper particles throughout the powder. A more uniform distribution of copper particles will lead to less variation from part to part during the sintering process.

3. The alloying method of copper is important in influencing both total dimensional change and precision of a component during compaction and sintering. Low total dimensional change does not translate to better precision.

Production experience with high consistency FC-0208 material made using advanced bonding technology

The final paper reported here focused on the benefits of using bonded pre-mixing, rather than diffusion alloying, as a means of eliminating copper segregation in an FC-0208 material. The paper was presented by Kylan McQuaig (Hoeganaes Corporation, USA) and co-authored by his Hoeganaes colleagues Bridget Reider and Francis Hanejko, as well as Suresh Shah, Gerry Wewer and Gregory Falleur of American Axle & Manufacturing Inc., USA.

Bonded pre-mixing has emerged in recent years as a viable alternative to diffusion alloying and involves the incorporation of an organic binder-lubricant addition, which acts both to chemically bind the alloying additions to the base iron powder and to serve as the pressing lubricant. The development and evaluation of the concept in the context of dimensional stability of Fe-Cu-C materials has been the subject of an extensive collaboration between the two companies and this paper was the latest in a series of publications by the team and reported on a detailed and extensive assessment in a production environment.

In a previous publication, it had been reported that improved sintered DC response of FC-0208 materials was realised by utilising a fine copper addition (-15 µm) in combination with chemical bonding of the premix additives. The fine copper addition showed two benefits. Firstly, proper dispersion of the finer copper eliminates the large voids that result from the melting of 'large' copper particles. Secondly, chemical bonding of the fine premix additives ensures that the premix homogeneity achieved during the premixing operation is maintained through powder transport and, ultimately, delivery into the die cavity. One additional key observation was the concept of sintered difference from standard (DFS) as the metric to evaluate stability of sintered DC from lot-to-lot.

In this reported study, the initial laboratory-based work at Hoeganaes Corporation investigated the effects of copper addition type and premixing alternatives. In this phase of the study, four 500 lb (227 kg) premixes were prepared, as detailed in Table 7. In all premixes, the base iron utilised was Hoeganaes Corporation Ancorsteel 1000C, the carbon addition was 0.72 wt.% natural graphite and the lubricant addition was 0.75 wt.% EBS. Once the laboratory-sized premixes were prepared, they were evaluated for basic powder properties of apparent density and flow, compressibility, sintered dimensional change and sintered TR strength. One additional test performed on each premix was elutriation to measure the potential dusting resistance of each premix. This test uses a steady flow of nitrogen gas that fluidises a column of powder with the objective of segregating the low density or small particle size premix additives. High dusting resistance implies a reduced tendency to segregate during transport and subsequent powder handling during PM part production.

Premixing alternative	Copper type	% Copper type addition
Standard premix	-150 µm	1.70
Standard premix	Diffusion bonded 20% copper master alloy	8.50 (1.70 total copper)
Ancorbonded	-150 µm	1.70
Ancorbonded	-15 µm	1.70

Table 7 Initial pre-mixes evaluating the effects of copper type and pre-mixing alternatives [3]

The production scale testing used the part shown in Fig. 13. This VVT part had three levels with a major sprocket diameter of ~5.3 in (134.6 mm), an inner diameter of 3.307 in (84 mm) and an overall height of ~0.8 in (20 mm). Part mechanical requirements necessitated that the sprocket flange region maintained a sintered density of ~6.9 g/cm^3, while the specification of the major long hub (Fig. 13b) was an overall green density of ~6.8 g/cm^3. The major short hub was formed by a fixed step in the upper punch (Fig. 13a). Compaction was performed on a mechanical press and sintering was carried out nominally at 2050°F (1120°C) for ~25 minutes at temperature in a 95 vol.% nitrogen / 5 vol.% hydrogen atmosphere. All material used in the production testing was an MPIF FC-0208 powder produced via Hoeganaes's proprietary bonded premixing processing. During the course of this production scale study, approximately twenty lots of material were evaluated, representing greater than 800,000 lb (363,000 kg) of supplied material, or approximately six months of actual part production. Additional production testing

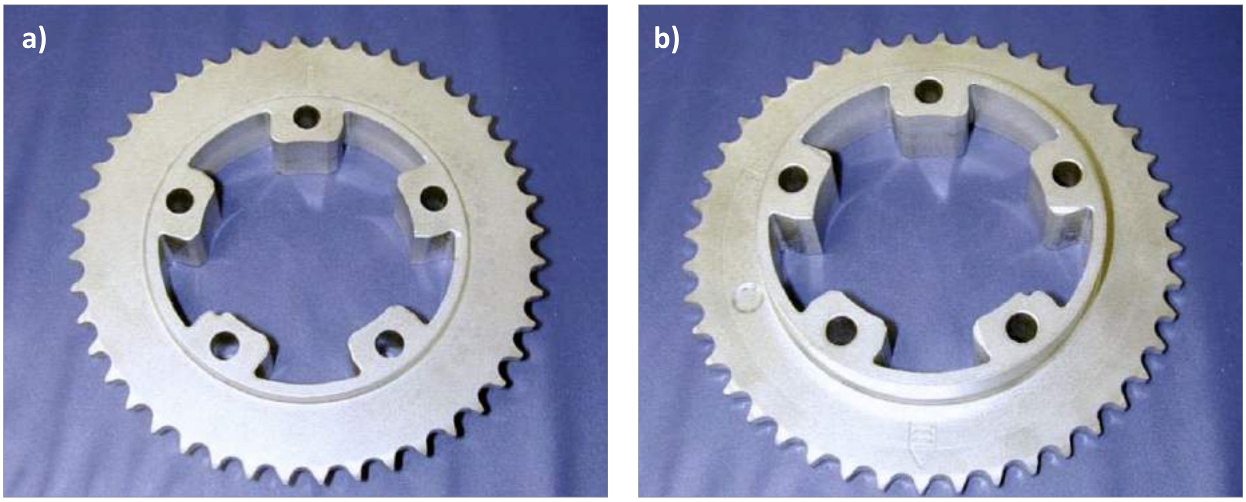

Fig. 13 VVT stator showing major short hub OD (a) and major long hub (b) [3]

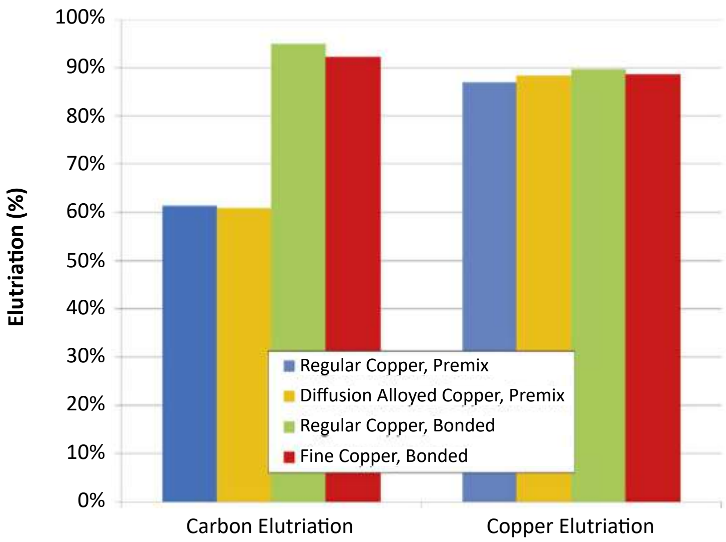

Fig. 14 Elutriation of carbon and copper of the four laboratory premixes [3]

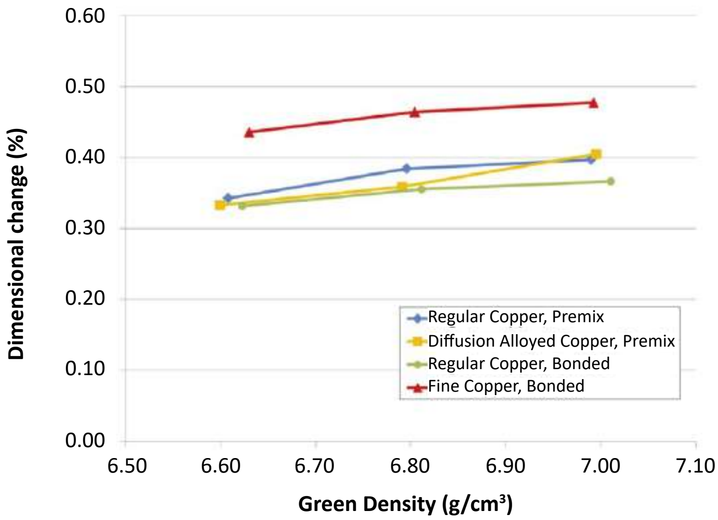

Fig. 15 Dimensional change of various copper additions vs. green density [3]

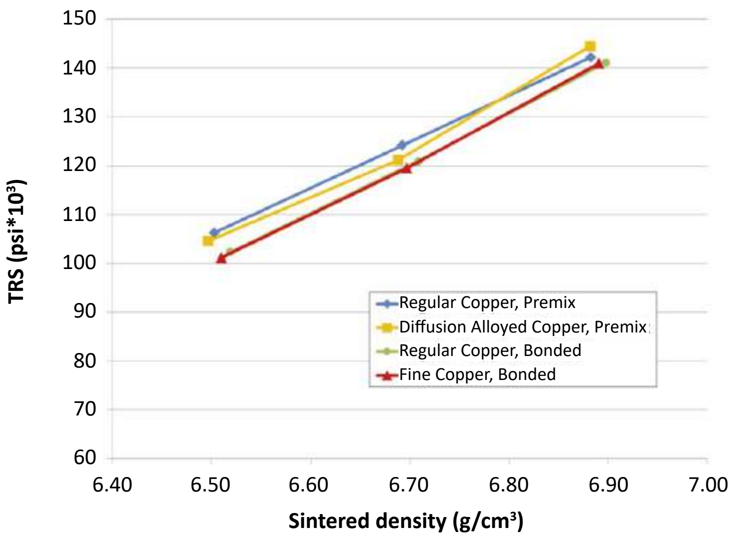

Fig. 16 TRS of various copper types vs. sintered density [3]

assessed the weight uniformity of as-compacted components by measuring thirty consecutive parts for each of two lots twice a day for three days of production.

In the laboratory-scale testing, Table 8 presents the measured apparent density (AD) and flow of the four mixes evaluated. Conventional double cone blending of the standard copper and the diffusion bonded copper addition gave almost identical AD and flow. Chemical bonding of the standard copper increased the AD by approximately 0.1 g/cm^3 with a 10% improvement in flow. Similarly, chemical bonding of the -15 µm copper powder increased the AD to ~3.2 g/cm^3 with additional improvement in the flow. The higher AD lowers the fill required to produce a part and the improved flow opens the opportunity to increase press speed with no degradation of quality.

The elutriation values presented in Fig. 14 demonstrate two trends. Firstly, graphite is more susceptible to dusting than copper. The density of graphite is 2.2 g/cm^3 and the fine particle size of the additive does promote segregation during the processing of the premix and, ultimately, in the PM part. Copper has a density of approximately 8.1 g/ cm^3, nearly the same as iron. This, combined with the relatively coarser particle size distribution of the copper, does minimise the potential for segregation. It should be noted that both carbon and copper variations can result in variations in sintered DC. Therefore, the chemical bonding of the graphite is significant in eliminating this potential source of variation. The diffusion bonding of the copper as an alloying addition is not necessary to eliminate potential sources of variation. Dusting resistance of both the standard copper premix and chemically bonded fine copper show nearly identical copper values after completion of the elutriation testing.

Figs. 15, 16 and 17 present the sintered dimensional change, sintered TR strength and sintered apparent hardness for the four laboratory premixes, respectively. As seen in Fig. 15, the addition of the -15 µm copper powder promotes greater absolute sintered dimensional change. This results from the greater number of iron-copper particle contacts, thus promoting greater initial copper diffusion during the sintering process with the corresponding greater swelling of the iron lattice. This should not be considered a detriment, provided that within-lot and lot-to-lot consistency of the powder is maintained, so as to produce consistent sintering behaviour. Varying the particle size of the copper does not significantly affect the as-sintered strength or as-sintered apparent hardness of the FC-0208 premix.

Metallographic analysis of test samples prepared from each of the four laboratory premixes, in the as-polished and etched conditions, demonstrated that the melting of the relatively coarse copper (-150 µm) resulted in the presence of larger pores, occurring from the melting and subsequent diffusion of the large copper particles, whereas the melting of the -15 µm powder created correspondingly smaller and more rounded porosity. In the iron premixed with the diffusion alloyed copper master alloy additive, the resulting porosity was intermediate between the coarse and fine copper particle size additions.

The significance of the smaller pore sizes, associated with the -15 µm copper premix addition, did not manifest itself in the static strength values shown in Figs. 16 and 17. However, axial fatigue testing of a production premix, utilising the -15 µm copper vs. the standard -150 mesh copper, was performed. Table 9 provides a summary of the axial fatigue testing (R= -1) of specimens compacted to a 7.0 g/cm^3 green density. These data suggest that the inherently smaller porosity of the -15 µm copper resulted in an approximately 10% higher fatigue life for both the 50% and 90% confidence limits.

Additional metallography was performed on a production premix sintered at temperatures of 1037°C, 1065°C, 1081°C and 1085°C. The rationale for this study was to determine how the -15 µm copper diffused into the iron above and below the melting point of copper (1083°C). As expected, at 1037°C, the copper particles were readily apparent and the interfaces between the copper and iron particles were well defined. On raising the sintering temperature to 1065°C, the copper particles were still evident in the microstructure, although it appeared that the interfaces between the copper and iron particles were less defined, possibly indicating some initial diffusion of the fine copper into the iron. At 1081°C, the amount of undiffused copper had decreased significantly and the remaining copper particles were in intimate contact with the iron particles. Lastly, at 1085°C, the copper was almost 100% diffused into the iron with only minor amounts of undiffused copper. This study illustrated the greater

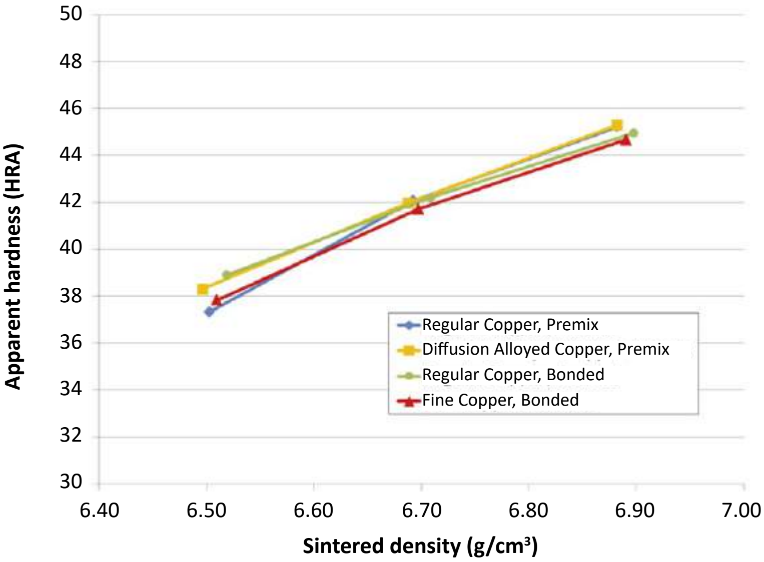

Fig. 17 Apparent hardness of various copper types vs. sintered density [3]

Mix	Apparent Density (g/cm^3)	Flow (s/50g)
Regular Copper, Standard premix	2.95	31
Diffusion Alloyed Copper, Standard premix	2.94	31
Regular Copper, Ancorbonded	3.05	28
Fine Copper, Ancorbonded	3.21	27

Table 8 AD & flow of laboratory prepared premixes [3]

Premix	Sintered Density, g/cm^3	50% Confidence Limit, psi	90% Confidence Limit, psi	Standard Deviation, psi
Production Premix utilising -15 µm Copper	6.93	18,500	16,750	1,290
Laboratory Premix utilising -150 µm Copper	6.91	16,650	15,050	1,170

Table 9 Axial fatigue results [3]

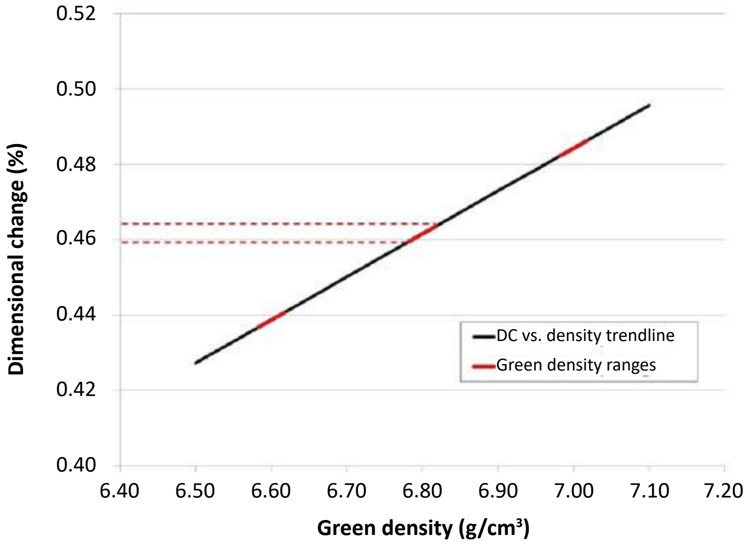

Fig. 18 Dimensional change variation resulting from potential density variations [3]

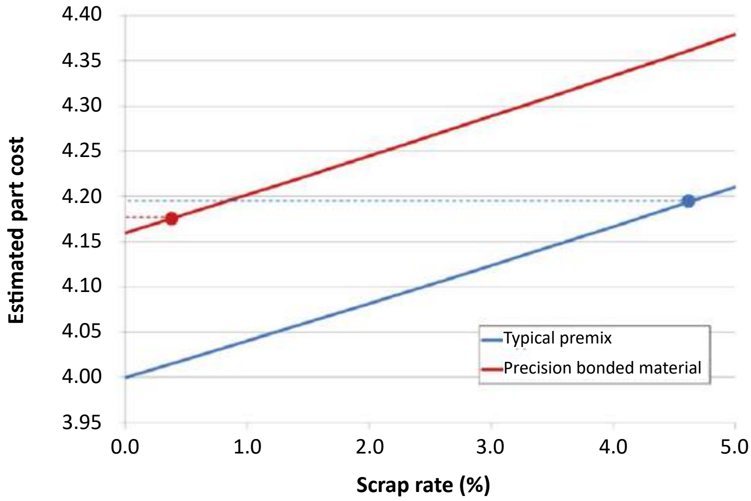

Fig. 19 Cost analysis of various scrap rates with standard and -15 μm copper powder [3]

initial diffusion of the -15 μm copper resulting from the increased number of iron-copper particle contacts. The greater initial diffusion of the -15 μm copper addition is responsible for the higher growth observed in Fig. 15. In addition to better diffusion, because the copper is chemically bonded to the iron, the fine copper will promote reduced segregation in the microstructure.

At the inception of the development work between the two companies, dimensional variations were resulting in unacceptable levels of rejected parts in the VVT stator application. Pareto analysis showed that the major cause for part rejection was an undersized condition on the critical 84 mm diameter dimension. Initially, premix modifications were enacted to produce greater sintered dimensional change. The original premix was a chemically bonded premix using the -150 μm copper additive. To increase the sintered DC, a combination of regular (-150 μm) and fine (-15 μm) copper was utilised, exploiting the trend shown in Fig. 15. Although successful, this approach required lot-to-lot adjustments in the amount of the fine copper addition in order to produce the desired result. The second and final iteration of the premix evaluated the use of fine copper only to effect the dimensional change desired. This iteration was pursued vigorously because it offered the potential to chemically bond the fine copper, therefore preventing potential segregation effects, and also offered the possibility of a slight reduction in the total amount of copper added to achieve the same absolute dimensional change. Outputs from the initial study showed that, with proper selection of a testing standard and utilising chemical bonding with the fine copper, lot-to-lot variation was significantly reduced.

In the newly reported production-scale study, the AD for the twenty lots examined showed a total variation of 0.06 g/cm^3. The significance of this tight control of AD is reduced press adjustment between lots as received for production. Previous work had shown that the chemical bonding gave excellent consistency within lot. Therefore, the need for tooling adjustments is reduced, leading to improved overall productivity.

Absolute dimensional change and dimensional change DFS data were determined at both the premix production facility and at the parts producer. As expected, the absolute DC did vary between the two different sintering locations, but the overall range of absolute DC was identical from the two locations. DFS testing also showed similarity of results from the two locations. Interestingly, the DFS at both locations showed a total variation of just 0.05% over the twenty lots evaluated. Differences existed between the two locations, but the lot-to-lot consistency remained at the same level. Implications for these data are reduced set up time as premix material lots are used in production, an overall lowering of scrap rates because of reduced changeover and greater press and sintering furnace utilisation because fewer changes are required.

Sintered carbon levels were also measured at the two locations and it was observed that the chemical bonding promoted very consistent results in this context. Consistency of sintered carbon is critical in maintaining the restrictive DC necessary for this VVT part.

Table 10 presents the consistency of part weights in production using two lots and over three days of production for each lot. Of significance in these data is the relatively tight control capability. The specification for the part is a green weight range of 530 to 536 g. For each run, the consistency observed was approximately 50% of this given specification range. Equally importantly, over the production cycle for each lot, minimal variation in weight was observed. Table 10 includes a column representing the potential density variation resulting solely from weight variation observed for each measured run. It is worth noting that the calculated density range (6σ) was, at most, 0.04 g/cm^3 for the part. This means that the potential DC variation from the maximum density variation is less than 0.005%, as shown in Fig. 18. This illustrates that DC is not just from potential chemical variations, but can also arise from variations in green density. To maintain the DC control required for a demanding application such as this VVT component, maintaining both rigid chemical control and part density will facilitate the required part performance. The consistency of both material AD and part weight in this study show a capability to maintain tight density control for this application.

A final point, discussed by the authors, related to the cost implications of the additional powder premix processing. The -15 µm powder has a higher cost to produce than the standard -150 µm material. Additionally, the chemical bonding has a higher cost than standard double cone premixing. However, the cost of the premixed powder is only one element of the final part cost. As shown in Fig. 19, using a developed cost model, the cost of sintered part scrap also has a significant effect on total part cost. In the context of this study, at the ~5% scrap rate initially observed with this component, the extra cost of the fine copper and enhanced premixing is completely offset by the reduction in scrap rates. It should also be noted that the data presented in Fig. 19 relate only to part cost without any consideration of factory utilisation and additional press availability that may be realised through the use of the higher consistency, precision bonded material.

Run	Date	Average Weight (g)	Standard Deviation (g)	Corresponding Density Range (6σ, g/cm³)
1	12/22/2016 AM	534.23	0.4159	0.0318
2	12/22/2016 PM	533.06	0.3770	0.0288
3	12/27/2016 AM	532.09	0.3207	0.0245
4	12/27/2016 PM	533.25	0.5273	0.0403
5	12/28/2016 AM	533.98	0.5072	0.0388
6	12/28/2016 PM	533.74	0.4964	0.0379

Table 10 Density variations resulting from weight variations in Fig. 18 [3]

References

[1] Improved precision of iron-copper-carbon materials, Sarah Ropar *et al.*, as presented at POWDERMET2017 International Conference on Powder Metallurgy & Particulate Materials, Las Vegas, USA, June 13-16, 2017, and published in the proceedings by the Metal Powder Industries Federation

[2] Improved diffusion-bonded copper alloy for improved dimensional change and precision of PM steel parts, Cody Kalinoski *et al.*, as presented at POWDERMET2017 International Conference on Powder Metallurgy & Particulate Materials, Las Vegas, USA, June 13-16, 2017, and published in the proceedings by the Metal Powder Industries Federation

[3] Production experience with high consistency FC-0208 material made using advanced bonding technology, Suresh Shah *et al.*, as presented at POWDERMET2017 International Conference on Powder Metallurgy & Particulate Materials, Las Vegas, USA, June 13-16, 2017, and published in the proceedings by the Metal Powder Industries Federation

Author

Dr David Whittaker
Tel: +44 1902 338498
Email: whittakerd4@gmail.com

Proceedings

Advances in Powder Metallurgy & Particulate Materials - 2017, the proceedings of the technical sessions, poster program and special interest programmes (where applicable), is published in digital format by the MPIF. These proceedings are provided to full-conference registrants free of charge or they can be purchased from the MPIF's Publications Department.

www.mpif.org

POWDERMET2018

POWDERMET2018, the International Conference on Powder Metallurgy & Particulate Materials, will take place in San Antonio, Texas, USA, from June 17–20, 2018.

www.powdermet2018.org

industry events

2018

MAPP First International Conference
January 30-31, Sheffield, United Kingdom
mapp.ac.uk/events/mapp-1st-international-conference

SAE 2018 Hybrid & Electric Vehicle Technologies
February 20-22, San Diego, United States
www.sae.org/events/hybridev

METAV 2018
February 20-24, Düsseldorf, Germany
www.metav.com


PM-18 International Conference on Powder Metallurgy + Exhibition
February 21 - 23, Navi Mumbai, India
www.pmai.in/pm18


MIM2018
March 5-7, Irvine, United States
www.mim2018.org


PM China 2018
March 25-27, Shanghai, China
www.cn-pmexpo.com


ceramitec 2018
April 10-13, Munich, Germany
www.ceramitec.com


rapid + TCT
April 23-26, Fort Worth, United States
www.rapid3devent.com


Ceramics Expo
May 1-3, Cleveland, United States
www.ceramicsexpousa.com


Metalloobrabotka
May 14-18, Moscow, Russia
www.metobr-expo.ru/en/

AMPM2018 Additive Manufacturing with Powder Metallurgy Conference
June 17-19, San Antonio, USA
www.ampm2018.org


POWDERMET 2018
June 17-20, San Antonio, USA
www.powdermet2018.org


World PM2018
September 16-20, Beijing, China
www.worldpm2018.com


Euro PM18 Congress & Exhibition
October 14-18, Bilbao, Spain
www.europm2018.com


Pick up your free copy at PM related events worldwide

Powder Metallurgy Review magazine is exhibiting at and/or being distributed at events highlighted with the *Powder Metallurgy Review* cover image

Event listings and Media Partners

If you would like to see your Powder Metallurgy related event listed in this magazine and on our websites, please contact Paul Whittaker:
email: paul@inovar-communications.com

We welcome enquiries regarding media partnerships and are always interested to discuss opportunities to cooperate with event organisers and associations worldwide.

Advertisers' index

Tune up for top performance

Höganäs high precision Fe+Cu+C toolbox for improved operational excellence

Do you want to achieve tighter tolerances and minimise machining work and scrap levels? Höganäs new high precision toolbox for customising Fe+Cu+C mixes enables you to tailor the powder composition to your specific application. Improving dimensional stability and copper distribution, it secures the highest possible raw material utilisation and takes your PM production to formerly unseen levels.

The high precision toolbox

Inspire industry to make more with less.

Höganäs